

Aus der  
Medizinischen Klinik und Poliklinik IV  
Klinikum der Ludwig-Maximilians-Universität München



## **Improving T cell therapy by T cell engineering**

Dissertation  
zum Erwerb des Doctor of Philosophy (Ph.D.)  
an der Medizinischen Fakultät der  
Ludwig-Maximilians-Universität München

vorgelegt von  
Florian Märkl

aus  
Dachau

Jahr  
2024

---

Mit Genehmigung der Medizinischen Fakultät der  
Ludwig-Maximilians-Universität München

Erstes Gutachten: Prof. Dr. Sebastian Kobold  
Zweites Gutachten: Dr. Maike Buchner  
Drittes Gutachten: Prof. Dr. Marion Subklewe  
Viertes Gutachten: Prof. Dr. Irmela Jeremias

Dekan: Prof. Dr. med. Thomas Gudermann

Tag der mündlichen Prüfung: 13.05.2024

## Affidavit



### Affidavit

Märkl, Florian

Surname, first name

Lindwurmstraße 2a

Street

80337 München

Zip code, town, country

I hereby declare, that the submitted thesis entitled:

Improving T cell therapy by T cell engineering

is my own work. I have only used the sources indicated and have not made unauthorised use of services of a third party. Where the work of others has been quoted or reproduced, the source is always given.

I further declare that the dissertation presented here has not been submitted in the same or similar form to any other institution for the purpose of obtaining an academic degree.

Dachau, 20.05.2024

place, date

Florian Märkl

Signature doctoral candidate

## Confirmation of congruency



**Confirmation of congruency between printed and electronic version of  
the doctoral thesis**

Märkl, Florian

\_\_\_\_\_  
Surname, first name

Lindwurmstraße 2a

\_\_\_\_\_  
Street

80337 München

\_\_\_\_\_  
Zip code, town, country

I hereby declare, that the submitted thesis entitled:

Improving T cell therapy by T cell engineering

is congruent with the printed version both in content and format.

Dachau, 20.05.2024

\_\_\_\_\_  
place, date

Florian Märkl

\_\_\_\_\_  
Signature doctoral candidate

## Table of content

<b>Affidavit .....</b>	<b>3</b>
<b>Confirmation of congruency.....</b>	<b>4</b>
<b>Table of content.....</b>	<b>5</b>
<b>List of abbreviations.....</b>	<b>6</b>
<b>List of publications summarized in this thesis.....</b>	<b>8</b>
<b>1. Contribution to the publications .....</b>	<b>9</b>
1.1 Contribution to paper I: Bispecific antibodies redirect synthetic agonistic receptor modified T cells against melanoma .....	9
1.2 Contribution to paper II: Combined tumor-directed recruitment and protection from immune suppression enable CAR T cell efficacy in solid tumors.....	15
<b>2. Introductory summary .....</b>	<b>17</b>
2.1 Tumor immunology.....	17
2.1.1 History .....	17
2.1.2 The immunoediting concept .....	18
2.1.3 Cancer immunotherapy .....	20
2.2 Adoptive T cell therapy.....	21
2.3 Challenges of adoptive cell therapy against solid tumors .....	22
2.3.1 Immunosuppression in the tumor microenvironment .....	23
2.3.2 Limited tumor infiltration by chimeric antigen receptor modified T cells .....	25
2.3.3 Variability in antigen expression due to tumor heterogeneity.....	27
2.4 Research hypothesis and aims of the work.....	30
<b>3. Paper I .....</b>	<b>31</b>
<b>4. Paper II .....</b>	<b>45</b>
<b>References .....</b>	<b>57</b>
<b>Acknowledgements .....</b>	<b>67</b>

## List of abbreviations

Table 1: Abbreviations

ACT	Adoptive cell therapy
B7-H3	B7 homolog 3 protein
BiAb	Bispecific antibody
CAF	Cancer-associated fibroblast
CAR	Chimeric antigen receptor
CCL	Chemokine ligand
CCR	Chemokine receptor
CD	Cluster of differentiation
CRISPR	Clustered regularly interspaced short palindromic repeats
CTLA-4	Cytotoxic T-lymphocyte-associated protein 4
CXCL	C-X-C motif chemokine ligand
CXCR	C-X-C motif chemokine receptor
DNR	Dominant-negative receptor
EGFRvIII	Epidermal growth factor receptor variant 3
ELISA	Enzyme-linked immunosorbent assay
EpCAM	Epithelial cell adhesion molecule
Fc	Fragment crystallizable
GFP	Green-fluorescent protein
HER2	Human epidermal growth factor receptor 2
HP SCT	Hematopoietic stem cell transplant
i. p.	Intraperitoneally
i. v.	Intravenously
ICI	Immune checkpoint inhibitor
IFN(GR1)	Interferon (gamma receptor 1)
IHC	Immunohistochemistry
IL	Interleukin
LUC	Luciferase
(r)MCSP	(recombinant) Melanoma-associated chondroitin sulfate proteoglycan
MDSC	Myeloid-derived suppressor cell
MHC	Major histocompatibility complex

mRNA	Messenger ribonucleic acid
NK cell	Natural killer cell
NSG	NOD scid gamma
PD-1	Programmed cell death protein 1
qPCR	Quantitative polymerase chain rection
RAG2	Recombination activating gene 2
s. c.	Subcutaneously
SAR	Synthetic agonistic receptor
scFv	Single chain variable fragment
STAT1	Signal transducer and activator of transcription 1
TAA	Tumor-associated antigen
TAM	Tumor-associated macrophage
TCR	T cell receptor
TGF- $\beta$ (-R2)	Transforming growth factor $\beta$ (receptor 2)
TIL	Tumor-infiltrating lymphocyte
TME	Tumor microenvironment
TNF- $\alpha$	Tumor necrosis factor $\alpha$
Treg	Regulatory T cell
TYRP1	Tyrosinase-related protein 1
VEGF	Vascular endothelial growth factor

## List of publications summarized in this thesis

- I. **Märkl F**, Benmebarek MR, Keyl J, Cadilha BL, Geiger M, Karches C, Obeck H, Schwerdtfeger M, Michaelides S, Briukhovetska D, Stock S, Jobst J, Muller PJ, Majed L, Seifert M, Kluver AK, Lorenzini T, Grunmeier R, Thomas M, Gottschlich A, Klaus R, Marr C, von Bergwelt-Baildon M, Rothenfusser S, Levesque MP, Heppt MV, Endres S, Klein C, & Kobold S.  
Bispecific antibodies redirect synthetic agonistic receptor modified T cells against melanoma.  
*Journal for ImmunoTherapy of Cancer* 2023; 11(5).
  
- II. Cadilha BL, Benmebarek MR, Dorman K, Oner A, Lorenzini T, Obeck H, Vanttinen M, Di Pilato M, Pruessmann JN, Stoiber S, Huynh D, **Märkl F**, Seifert M, Manske K, Suarez-Gosalvez J, Zeng Y, Lesch S, Karches CH, Heise C, Gottschlich A, Thomas M, Marr C, Zhang J, Pandey D, Feuchtinger T, Subklewe M, Mempel TR, Endres S, & Kobold S.  
Combined tumor-directed recruitment and protection from immune suppression enable CAR T cell efficacy in solid tumors.  
*Science Advances* 2021; 7(24).



# 1. Contribution to the publications

## 1.1 Contribution to paper I: Bispecific antibodies redirect synthetic agonistic receptor modified T cells against melanoma

In the paper “Bispecific antibodies redirect synthetic agonistic receptor modified T cells against melanoma” we identified melanoma-associated chondroitin sulfate proteoglycan 4 (MCSP) and tyrosinase-related protein 1 (TYRP1) as suitable antigens for a targeted approach against melanoma. Furthermore, we applied the synthetic agonistic receptor (SAR) platform consisting of SAR T cells in combination with bispecific antibodies (BiAb) targeting these tumor-associated antigens (TAA). We could show conditional antigen-dependent SAR T cell activation, targeted melanoma cell lysis, potent anti-tumoral activity *in vitro* and *in vivo* and long-term survival of treated mice.

This paper was published with shared first authorship since the other first author and the author of this dissertation worked together on generating most of the data and writing the manuscript. The project was started in 2012, ten years before the publication of the paper and was since then elaborated with most of the data generated by the two first authors.

The author of this dissertation could show differential expression of TYRP1 and MCSP on messenger ribonucleic acid (mRNA) and protein level on melanoma cell lines A375 and MV3 and on tumor samples from patients with melanoma using quantitative polymerase chain reaction (qPCR)- and flow-cytometry-based readouts (Figure 1A and Supplementary Figure 1A). Additionally, the expression of TYRP1 on murine melanoma cell lines B16 and YUMM1.1, which were retrovirally transduced to express TYRP1, was demonstrated, whereas no expression

was detected on T cells nor on the antigen-negative control cell line Panc02-Ova (Supplementary Figure 1G and H).

In a next step, the author retrovirally transduced human and murine primary T cells with the E3 SAR or E3del construct which was confirmed by flow cytometric readouts (Figure 2A). The T cells featured a similar cluster of differentiation (CD) 4 to CD8 ratio and predominantly an effector-memory phenotype (negative for chemokine receptor 7 (CCR7) and positive for CD45RO) irrespective of the transduction with the E3 SAR or E3del construct (Figure 2B and C). In coculture experiments with the human melanoma cell line A375 the author could demonstrate specific activation of SAR T cells in conditions with the anti-TYRP1 x anti-epidermal growth factor receptor variant three (EGFRvIII) BiAb indicated by elevated levels of interferon (IFN)- $\gamma$ , interleukin 2 (IL-2), tumor necrose factor  $\alpha$  (TNF- $\alpha$ ), and granzyme B quantified in the supernatant with enzyme-linked immunosorbent assay (ELISA) (Figure 2D). Furthermore, the author demonstrated increased activation of the SAR T cells via CD69, 4-1BB and PD-1 expression, increased T cell counts and lysis of A375 and MV3 tumor cells following 48 hours of coculture only in conditions with MCSP- or TYRP1-targeting BiAb (Figure 2E – G). These results were obtained via a flow-cytometric readout. Three out of six assay repetitions were performed and measured by the author and the other three repetitions were performed under the supervision of the author. Similarly, the author measured increased concentrations of IFN- $\gamma$ , TNF- $\alpha$ , IL-2 and granzyme B in the supernatant of murine SAR T cells cocultured with antigen-positive B16 or YUMM1.1 TYRP1 melanoma cells in conditions with anti-TYRP1-targeting BiAb (Supplementary Figure 2A).

To probe the functionality of the platform with clinically more relevant cells, coculture experiments of human SAR T cells with primary melanoma samples with and without either one of the BiAb were conducted. The author could show specific activation of SAR T cells indicated by an increased expression of CD69, 4-1BB and PD-1, IFN- $\gamma$  secretion and CD3<sup>+</sup> T cell count (Figure 3A – C). Furthermore, the author demonstrated specific lysis of primary melanoma cells only in conditions with either the MCSP- or TYRP1-targeting BiAb via a flow cytometric readout (Figure 3D).

In a next step the influence of soluble forms of tumor antigen on the activation and killing capacity of the SAR-BiAb platform was analyzed. Therefore, wells were coated with increasing levels of recombinant MCSP (rMCSP) or rMCSP was directly pipetted in increasing concentrations to the medium. Then, human SAR T cells were added. The author demonstrated specific IFN- $\gamma$  release only with plate-bound antigen, whereas only low IFN- $\gamma$  concentrations were measured with soluble rMCSP via ELISA (Figure 4B). Similar results were obtained when the experiments were repeated with soluble recombinant TYRP1 and anti-TYRP1 x anti-EGFRvIII BiAb (Supplementary Figure 3B). Thus, these results suggest that the SAR-BiAb platform does not get activated by soluble antigen at the tested concentrations and that soluble antigen does not impact tumor cell lysis of the SAR-BiAb platform. In another coculture experiment with human SAR T cells, A375 melanoma cells and either one of the two BiAb molecules, the modularity, reversibility and controllability of the platform were tested. The author measured increased IFN- $\gamma$  concentrations in the supernatant after 24 hours in the conditions with either the MCSP- or TYRP1-targeting BiAb (Figure 4D). Then, the SAR T

cells were washed with PBS and pipetted to a new plate with tumor cells. Following transfer, the BiAb targeting the same antigen, the BiAb targeting the second antigen or vehicle solution was added to the medium. In the conditions with redosing of either the MCSP- or TYRP1-targeting BiAb, the IFN- $\gamma$  expression was maintained. However, in the condition where no BiAb was redosed the IFN- $\gamma$  concentration significantly dropped, indicating that the activation of SAR T cells can be reversed when no BiAb is added (Figure 4E). When redosing with anti-MCSP x anti-EGFRvIII BiAb (first dosing with anti-TYRP1 x anti-EGFRvIII), the SAR engineered T cells continued to secrete IFN- $\gamma$  indicating the lasting activation of the SAR T cells when redosing with either of the BiAb (Figure 4E). The author could demonstrate with this experiment that SAR modified T cells can sequentially target different antigens using BiAb with different antigen specificities indicating the modularity of the approach (Figure 4D and E).

Then several syngeneic and xenograft experiments were performed to analyze the functionality of the therapeutic platform *in vivo*. First, the author injected CD20-depleted C57/BL6 mice intravenously (i. v.) with murine YUMM1.1 TYRP1 cells expressing luciferase (LUC) and the green-fluorescent protein (GFP). After treating the mice with SAR T cells and TYRP1-targeting BiAb, SAR T cell persistence in the blood could be measured seven, 14 and 19 days after T cell transfer via flow cytometry by the author (Supplementary Figure 4A). The *in vivo* tumor growth was monitored by the author via bioluminescence readouts once per week. The mice treated with the SAR-BiAb combination had a reduced tumor growth compared to control mice and ultimately four out of ten mice cleared the tumor (Figure 5A and B, Supplementary Figure 4B). Along these lines, the author showed in a bioluminescence- and flow-cytometry-based readout that 80% of the

mice treated with SAR T cells and TYRP1-targeting BiAb featured no tumor cell signal in the lung (Figure 5C and Supplementary Figure 4C). The author was then able to show that treatment with a single dose of the TYRP1-targeting BiAb and SAR modified T cells led to an initial treatment effect but could not extend the survival compared to a control treatment (Supplementary Figure 4D and E). These results substantiate the *in vivo* reversibility and controllability of the therapeutic SAR-BiAb platform.

Additionally, the TYRP1-specificity was analyzed. The author injected C57/BL6 mice with TYRP1-negative YUMM1.1 LUC-GFP cells. Then, the author treated the mice four days later with SAR modified T cells and TYRP1-targeting BiAb or control treatment. The treatment did not alter antigen-negative tumor cell growth nor survival of treated mice (Supplementary Figure 4F and G), indicating the antigen specificity of the SAR-BiAb platform *in vivo*. In another experiment, the author injected mice *i. v.* with YUMM1.1 TYRP1-LUC-GFP tumor cells and 20 days later intraperitoneally (*i. p.*) with TYRP1- or Mesothelin-targeting control BiAb. Following incubation for 48 hours, tumor bearing lungs, the skin and heart, as those organs express TYRP1, were harvested and prepared for immunohistochemistry (IHC) by the author. In IHC-based stainings of the lung performed by co-authors it was shown that TYRP1 expressing GFP<sup>+</sup> tumor cells were specifically targeted by the anti-TYRP1 x anti-EGFRvIII BiAb (Figure 5D). Furthermore, no TYRP1 binding could be detected in the heart or skin (Supplementary Figure 4H).

In order to evaluate the treatment efficacy in human xenograft models NOD scid gamma (NSG) mice were subcutaneously (*s. c.*) injected with human MV3 melanoma cells and treated with SAR engineered T cells and MCSP-targeting BiAb

by one co-author. However, the generation and expansion of the SAR engineered T cells and the tumor growth measurements were done by the author. It was demonstrated that the treatment led to a decreased tumor growth and prolonged persistence of SAR modified T cells in the blood compared to control treatments (Figure 5E and F). In an endpoint experiment tumors were analyzed for SAR T cell infiltration via flow cytometry. Here, the generation and expansion of the SAR T cells and the tumor growth measurements were done by the author. The injections of the mice with tumor cells, T cells and BiAb were done by a co-author. More SAR T cells infiltrated into the tumor in mice injected with SAR T cells and MCSP-targeting BiAb compared to mice treated with SAR modified T cells alone (Figure 5G). Additionally, these SAR modified T cells featured a higher expression of programmed cell death protein 1 (PD-1) and had an effector memory phenotype, similar as before injection (Figure 5H and Supplementary Figure 4I). The preparation of single cell suspensions, staining with antibodies and flow-cytometric measurement were performed by the author and co-authors together. In another xenograft model with s. c. injected A375 human melanoma cells the authors could show a similar treatment efficacy and prolonged survival of the treated mice (Figure 5I and J). One experiment was conducted by one co-author and the repetition by the author. Furthermore, the author prepared primary patient samples and generated human SAR T cells for a patient-derived xenograft model. NSG mice were injected s. c. with these primary patient samples and then treated with the anti-TYRP1 x anti-EGFRvIII BiAb and SAR T cell combination by co-authors. The combination treatment resulted in decreased tumor growth compared to control treatments (Figure 5K).

## **1.2 Contribution to paper II: Combined tumor-directed recruitment and protection from immune suppression enable CAR T cell efficacy in solid tumors**

In the paper “Combined tumor-directed recruitment and protection from immune suppression enable CAR T cell efficacy in solid tumors” published in Science Advances [Cadilha *et al.*, 2021] we could show that equipping chimeric antigen receptor (CAR) T cells with the chemokine receptor 8 (CCR8) and the transforming growth factor beta (TGF- $\beta$ ) dominant negative receptor (DNR) induced increased migration to the tumor site and enhanced shielding from TGF- $\beta$  mediated immunosuppression. Furthermore, we identified chemokine ligand 1 (CCL1) secreted by activated T cells as a key player in a CCL1-CCR8 mediated positive feedback loop inducing improved infiltration and therapeutic efficacy in pancreatic cancer models.

The author contributed to this article by conducting several experiments investigating the migration pattern of CCR8 engineered T cells in a murine pancreatic cancer model. Panc02 tumor bearing mice were treated with a 1:1 ratio of CCR8-GFP and mCherry engineered murine T cells. In a flow cytometric readout 48 hours after adoptive cell transfer the amount of transduced T cells in blood, bone marrow, brain, intestine, kidney, liver, lymph nodes, lung, spleen, and subcutaneous tumor was analyzed. The highest numbers of T cells were found in the spleen, followed by liver, lymph nodes, lung, and tumor (Supplementary Figure S1B). CCR8-GFP transduced T cells were enriched compared to mCherry<sup>+</sup> T cells in the tumor, liver and lung likely driven by an increased CCL1 or CCL22 chemokine expression profile of these entities (Supplementary Figure S1C). Furthermore, the author could demonstrate in another experiment that four times more epithelial cell adhesion molecule (EpCAM)-specific CAR T cells additionally

---

equipped with CCR8 were found in Panc02-EpCAM subcutaneous tumors than CAR T cells without CCR8 underpinning the advantage of using CCR8 when targeting CCL1 expressing tumors (Supplementary Figure S1D).



## 2. Introductory summary

### 2.1 Tumor immunology

#### 2.1.1 History

Tumor immunology is defined as the field describing the complex interaction between the immune system with all its components and a neoplasm at various stages of development. The earliest hypothesis that the immune system is somehow linked to cancer development was put forward by Rudolf Virchow in 1863. He postulated that severe irritation in the tissues can lead to cancer development [Galon & Bruni, 2020]. The first case of cancer immunotherapy was conducted by William Bradley Coley who treated patients suffering from sarcomas with a mixture of live and inactivated *Streptococcus pyogenes* and *Serratia marcescens* causing tumor regression [Coley, 1893]. Two decades later Paul Ehrlich hypothesized that there was an intrinsic defense mechanism that inhibits tumor formation [Ehrlich, 1909]. In 1957 this initial thought of Paul Ehrlich was developed to the theory of cancer immunosurveillance by Frank MacFarlane Burnet [Burnet, 1957]. It was underpinned by the finding that the immune system can recognize newly arising tumor cells via the expression of tumor specific antigens and by the proof of the roles of IFN- $\gamma$  and granzyme B in the cancer immunosurveillance [Dighe *et al.*, 1994; van den Broek *et al.*, 1996]. Other than that oncology and immunology were mostly seen as separate disciplines and developed independently [Galon & Bruni, 2020]. In 2000, Hanahan and Weinberg [2000] postulated the hallmarks of cancer describing key characteristics for a cell to become cancerous completely leaving out the influence of the immune system. Tumor immunology had then a revival as a discipline about two decades ago. However, it can still be seen as an emerging field.

### 2.1.2 The immunoediting concept

The final experimental proof of the immunosurveillance hypothesis was performed with immunodeficient mice lacking a functional form of the recombination-activating gene 2 (RAG2) [Shankaran *et al.*, 2001]. It was shown that these mice developed tumors earlier and more often than wild-type mice after chemically induced tumor induction [Shankaran *et al.*, 2001]. Similar results were obtained with IFN- $\gamma$ -insensitive mice lacking either a functional IFN- $\gamma$  receptor 1 (IFNGR1) or signal transducer and activator of transcription 1 (STAT1) [Shankaran *et al.*, 2001], a transcription factor downstream of the IFNGR1 [Durbin *et al.*, 1996; Meraz *et al.*, 1996]. Furthermore, it was demonstrated that IFNGR1 x STAT1 double knockout mice also featured increased susceptibility to chemically induced tumors, but the incidences were not higher compared to mice with single knockouts [Shankaran *et al.*, 2001]. Thus, it was postulated that lymphocytes and IFN- $\gamma$  collaborate to prevent primary tumor formation and that the immune system acts as a potent tumor suppressor [Shankaran *et al.*, 2001]. Later, the immunosurveillance hypothesis was extended to the cancer immunoediting concept [Dunn *et al.*, 2004a; Schreiber *et al.*, 2011]. It describes a dynamic process on the interaction of tumor cells and the immune system (Figure 1).

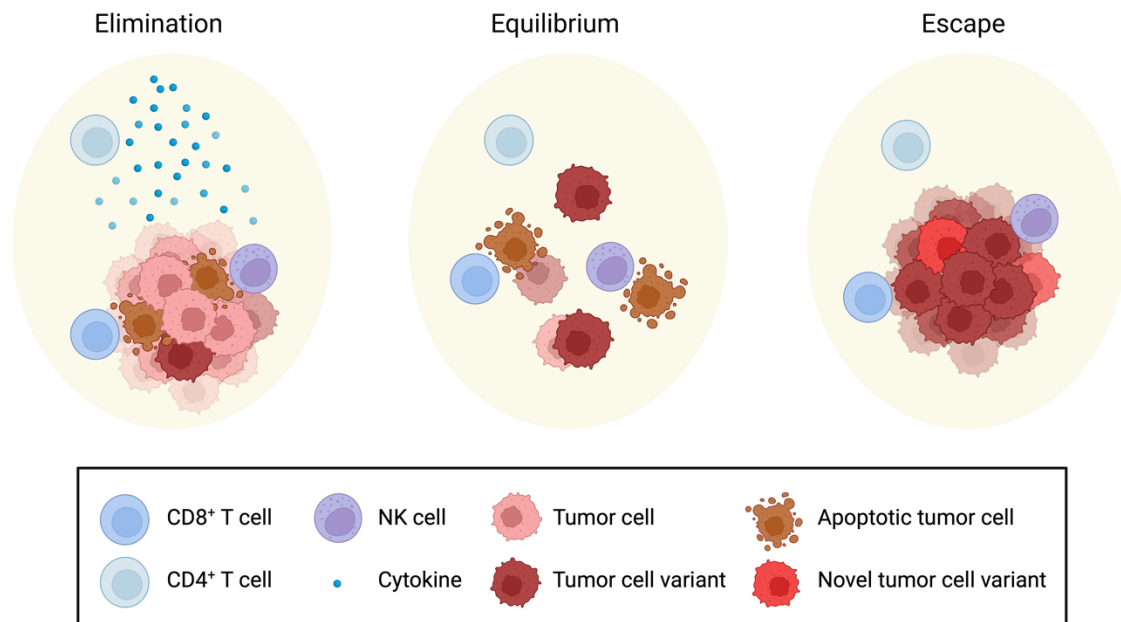


Figure 1: The three phases of immunoeediting: Elimination, equilibrium and escape. In the elimination phase tumor cells get recognized and lysed by effector immune cells, like CD8<sup>+</sup> T cells or natural killer (NK) cells. During the equilibrium phase, more resistant tumor cell variants evolve under the pressure of the immune system. Lastly, in the escape phase the tumor cell variants that are resistant to immune destruction grow out. Adapted from [Pradeu, 2020].

Three general phases can be described: elimination which is based on the classical immunosurveillance hypothesis, the equilibrium, and escape phase [Dunn *et al.*, 2004a]. During the equilibrium phase the immune system exerts selection pressure on the tumor cells that survived the elimination phase. Different mutations can occur during that time which provide increasing resistance to potent immune response [Dunn *et al.*, 2004a]. Thus, it is characterized by a continuous editing process which balances tumor cell destruction by the immune system and persistence of some resistant tumor cells [Dunn *et al.*, 2002]. This is the longest phase and can last over many years in humans [Dunn *et al.*, 2004b]. At some point the immune system fails to control tumor outgrowth leading to the immune escape phase. The escape process can be caused by changes directly at the tumor cell level which lead to the inability of the immune system to detect and

destruct the tumor or by tumor-derived factors or cells that suppress an effective immune response [Dunn *et al.*, 2004a].

### 2.1.3 Cancer immunotherapy

Along with an increased understanding of the impact of the immune system on cancer, more strategies to utilize the patient's own immune system to fight cancer were developed. First, systemic approaches, like the application of IFN- $\alpha$  in 1986 and IL-2 for renal cancer in 1992 were approved to boost the immune system in general and to enable an effective antitumoral immune response [Galon & Bruni, 2020]. Later, the first targeted therapy, the tyrosine kinase inhibitor Imatinib, was approved against chronic myeloid leukemia, the first cancer vaccine against prostate cancer in 2010 and the first immune checkpoint inhibitor (ICI), targeting cytotoxic T-lymphocyte-associated protein 4 (CTLA-4), for melanoma in 2011 [Cohen *et al.*, 2002].

In general, two different modes of cancer immunotherapy have been described: the stimulation of the patient's own antitumoral immune response and passive immunotherapy with immune cells and antibodies. Regarding the first strategy, patients can be vaccinated with tumor cells and tumor antigens or they can be treated with immunomodulators, like interleukins, interferons, chemokines, or immunomodulatory imide drugs, or with ICI [Naran *et al.*, 2018]. The second strategy relies on the administration of antibodies targeting tumor antigens or on the adoptive cell transfer [Naran *et al.*, 2018]. In 1957, the first patient suffering from leukemia was treated with bone marrow infusion from his genetically identical twin [Thomas *et al.*, 1957]. This was the first hematopoietic stem cell transplantation (HPSCT) and cellular therapy. For many decades HPSCT was the only clinically relevant cellular therapy. Recently, cellular therapies which utilize the

function of tumor-specific T cells have been developed and finally approved for treatment of hematological malignancies [Huang *et al.*, 2022].

## 2.2 Adoptive T cell therapy

Among the cellular therapies the adoptive T cell therapy (ACT) is so far the most successful one [Rohaan *et al.*, 2019]. There are three major applications to utilize T cells for therapy. Antigen specific T cells can be isolated from the tumor, expanded *ex vivo* and then reinfused into patients [Zhao *et al.*, 2022]. In 1988 the first patient was successfully treated with tumor-infiltrating lymphocytes (TIL) against melanoma [Rosenberg *et al.*, 1988]. However, this process also comes with several challenges. It requires accessible target lesions for TIL isolation and the product and response of the therapy can be heterogeneous partly due to the unknown specificity of the isolated and expanded T cells [Khong *et al.*, 2004; Zhao *et al.*, 2022].

Besides T cells with heterogeneous specificities against multiple tumor neoantigens, T cells can be genetically modified to become tumor-specific [Ellis *et al.*, 2021]. T cell receptors (TCRs) binding specific tumor antigens can be introduced into T cells *ex vivo*, generating a product known as TCR-engineered T cells [Shafer *et al.*, 2022]. The advantages of TCR-based approaches lie in the possibility of targeting any neoantigen via binding to major histocompatibility complex (MHC) and utilizing the endogenous TCR signaling moieties [Shafer *et al.*, 2022]. This contributes to a very sensitive recognition of suitable peptide-MHC complexes despite having binding affinities in the micromolar range [Hogquist & Jameson, 2014; Huang *et al.*, 2013; Sykulev *et al.*, 1996]. At the same time, MHC downregulation in tumor cells can cause treatment failure due to MHC-dependent activation of TCR engineered T cells [Taylor & Balko, 2022].

In contrast, synthetic receptors were developed to target surface antigens in an MHC-independent manner. These CAR molecules consist of a single chain variable fragment (scFv) for antigen specific binding, a transmembrane domain and at least one intracellular signaling domain [Guedan *et al.*, 2019]. For the first generation of CAR constructs only a CD3 $\zeta$  signaling domain was used [Subklewe *et al.*, 2019]. Later, by adding a costimulatory domain, either CD28 or 4-1BB, the efficacy of the approach improved drastically leading to the first approval of CD19 targeting CAR T cells in 2017 against relapsed and/or refractory B cell precursor acute lymphoblastic leukemia [Kershaw *et al.*, 2006; Maude *et al.*, 2018]. Direct comparison of CAR T cells with CD28 or 4-1BB-based costimulatory domains lead to similar response rates in clinical trials [Ying *et al.*, 2019].

Due to the mandatory genetic engineering step for the generation of CAR T cells, it is feasible to manipulate also other activating or inhibiting pathways simultaneously [Hong *et al.*, 2020].

### **2.3 Challenges of adoptive cell therapy against solid tumors**

So far, six different CAR T cell products have been approved for hematological malignancies [Asmamaw Dejenie *et al.*, 2022]. However, the response rate in patients with solid tumors remains limited due to the immunosuppressive tumor microenvironment (TME), poor migration to the tumor and tumor infiltration and lastly, due to antigen heterogeneity [Marofi *et al.*, 2021] (Figure 2).

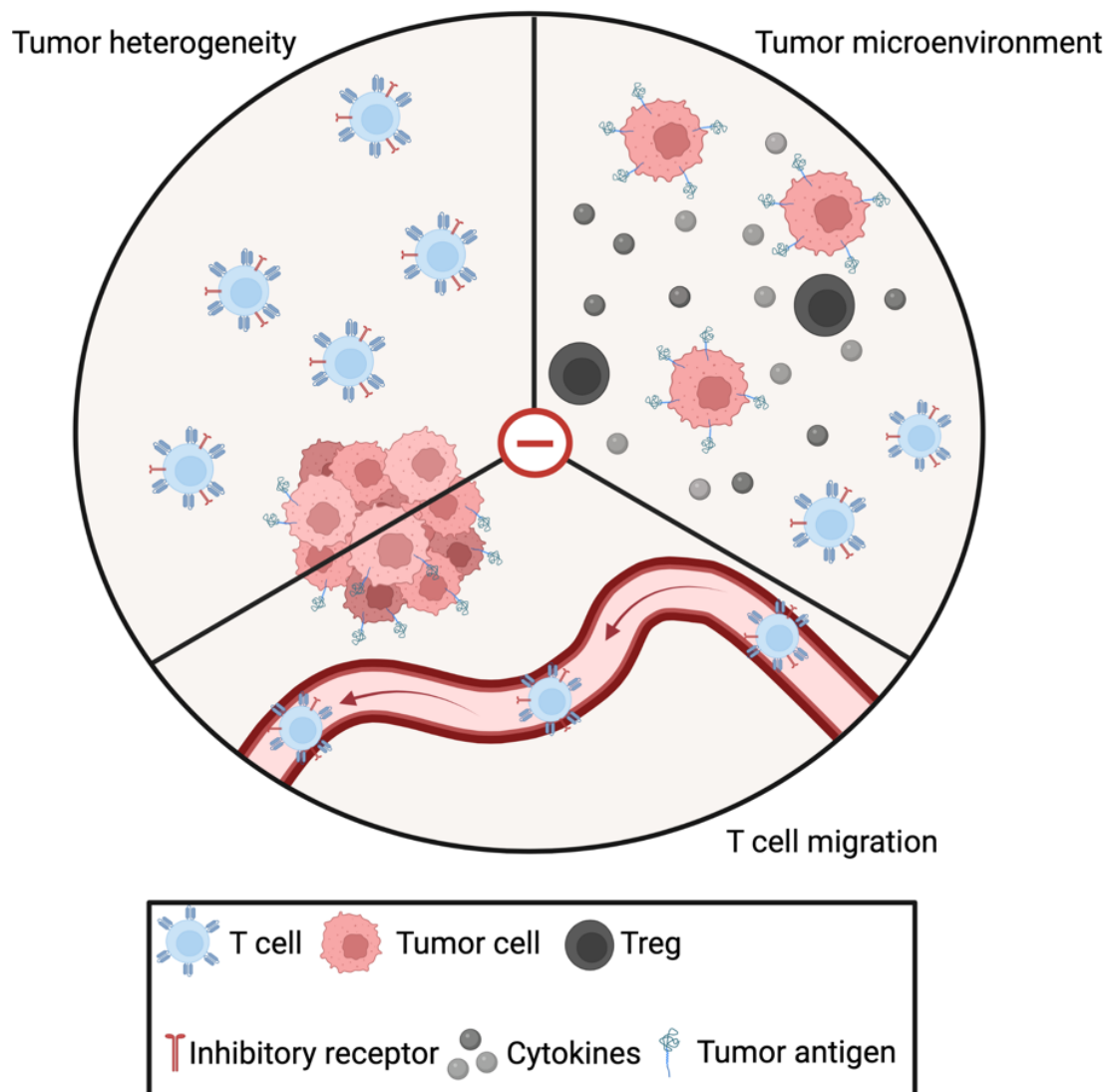


Figure 2: Challenges of CAR T cell therapy in solid tumors. Adapted from [Simon & Uslu, 2018].

### 2.3.1 Immunosuppression in the tumor microenvironment

Solid tumors can be highly infiltrated by immune and stromal cells that foster local immune suppression [Hanahan & Coussens, 2012]. Among these cells regulatory T cells (Treg), myeloid-derived suppressor cells (MDSC), cancer-associated fibroblasts (CAF) and tumor-associated macrophages (TAM) are the most prominent ones. The immunosuppression of T cells can be induced by cell-to-cell interactions with tumor cells directly or one of the afore mentioned cells in the TME. These immunosuppressive cell-to-cell interactions are often mediated via ICI molecules, like CTLA-4 or PD-1 on T cells [Nishimura *et al.*, 1999; Waterhouse

*et al.*, 1995]. One strategy to overcome ICI-mediated immunosuppression is to use antibodies blocking the interaction between the cells [Iwai *et al.*, 2002; Leach *et al.*, 1996]. Several ICI are now approved for mostly solid tumor entities [Johnson *et al.*, 2022]. This effect was also observed in a glioblastoma mouse model where PD-1-blockade enhanced EGFRvIII-CAR T cell efficiency and persistence [Song *et al.*, 2020]. Similarly, clustered regularly interspaced short palindromic repeats (CRISPR)-based knockout of PD-1 on EGFRvIII-CAR T cells had an *in vitro* growth inhibitory effect on EGFRvIII-expressing glioblastoma cells [Nakazawa *et al.*, 2020].

Another way of immunosuppression can be mediated via soluble factors derived from various cells in the TME. Cytokines, and chemokines that are locally secreted in solid tumors, including TGF- $\beta$ , vascular endothelial growth factor (VEGF), IL-4 and IL-10 facilitate tumor cell growth and proliferation [Marofi *et al.*, 2021]. TGF- $\beta$  generated by Treg directly impairs the functionality of cytotoxic CD8<sup>+</sup> T cells [Budhu *et al.*, 2017]. This effect correlated with a decrease in the abundance of the cytolytic effector molecule granzyme B and an increase of PD-1 on the T cells [Budhu *et al.*, 2017]. To overcome TGF- $\beta$ -mediated inhibition, T cells can be engineered to express a dominant negative version of the TGF- $\beta$  receptor 2 (TGF- $\beta$ -R2) which lacks a functional intracellular signaling domain [Bollard *et al.*, 2002; Wieser *et al.*, 1993] (Figure 3).



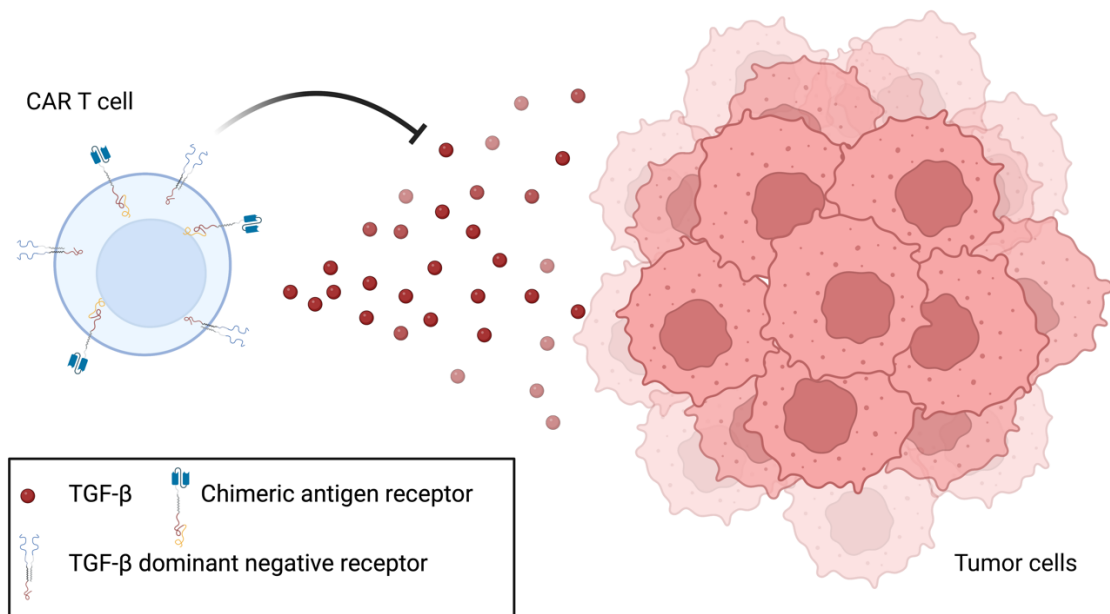


Figure 3: Schematic representation of DNR-mediated resistance to TGF- $\beta$ -induced immunosuppression.

Thus, TGF- $\beta$  is bound on the cell surface by the DNR leading to a scavenging effect but does not trigger intracellular signaling via SMAD2 [Bollard *et al.*, 2002]. In human prostate cancer mouse models, the expression of the TGF- $\beta$  DNR in CAR T cells enhanced proliferation, cytokine secretion and resistance to exhaustion of the T cells *in vivo* and lead to reduced tumor growth and prolonged survival [Kloss *et al.*, 2018].

### 2.3.2 Limited tumor infiltration by chimeric antigen receptor modified T cells

In many cancer types, among ovarian cancer, infiltration of cytotoxic CD8<sup>+</sup> T cells correlates with a prolonged survival of the patients [Barnes & Amir, 2018]. In contrast, the presence of immunosuppressive cells, like TAM or Treg, is often correlated with a worse prognosis [Qian *et al.*, 2011; Shou *et al.*, 2016]. Immune cells can be excluded from the tumor by an excessive extracellular matrix which is a protein network in the TME generated by cancer cells and CAF [Henze *et al.*,

2020]. The main driver of immune cell migration from the blood vessels to the tumor are chemokines. They are small, secreted proteins which induce chemotaxis towards increasing concentrations of the chemokine [Nagarsheth *et al.*, 2017]. In humans 50 chemokines and 19 chemokine receptors have been found indicating a high promiscuity in binding of chemokine ligand to chemokine receptor [Markl *et al.*, 2022]. Depending on the cell type and differentiation status different chemokine receptors are expressed. In cancer chemokines are expressed by tumor cells, immune cells and tumor-associated cells [Markl *et al.*, 2022]. In many cancer types chemokines are expressed that rather attract immunosuppressive cells than effector cells. In particular, CCL2 recruits CCR2<sup>+</sup> TAM to the tumor [Zhou *et al.*, 2020], while high levels of CCL2 correlate with reduced survival of patients suffering from breast cancer [Heiskala *et al.*, 2019]. Similarly, high levels of CCL1 were found in human breast cancers correlating with increased infiltration of CCR8<sup>+</sup> Treg and a worse prognosis [Kuehnemuth *et al.*, 2018; Shou *et al.*, 2016].

Activated T cells are mainly recruited to the tumor via C-X-C motif chemokine receptor (CXCR) 3 in melanoma, colorectal, and breast cancers [Harlin *et al.*, 2009; Mulligan *et al.*, 2013; Musha *et al.*, 2005]. The mismatch in chemokine ligand and secretion of cells in the TME and chemokine receptor expression on cytotoxic T cells can lead to a limited migration to the tumor and thus, treatment failure [Slaney *et al.*, 2014].

Several strategies have been applied to improve T cell trafficking and finally, treatment response. The expression profile of chemokine ligands in the TME can be altered towards a more pro-inflammatory and effector immune cell attracting

pattern [Moon *et al.*, 2018]. Another strategy harnesses the capability of genetically engineering CAR T cells to express chemokine receptors matching the chemokine ligand profile of the tumor (Figure 4).

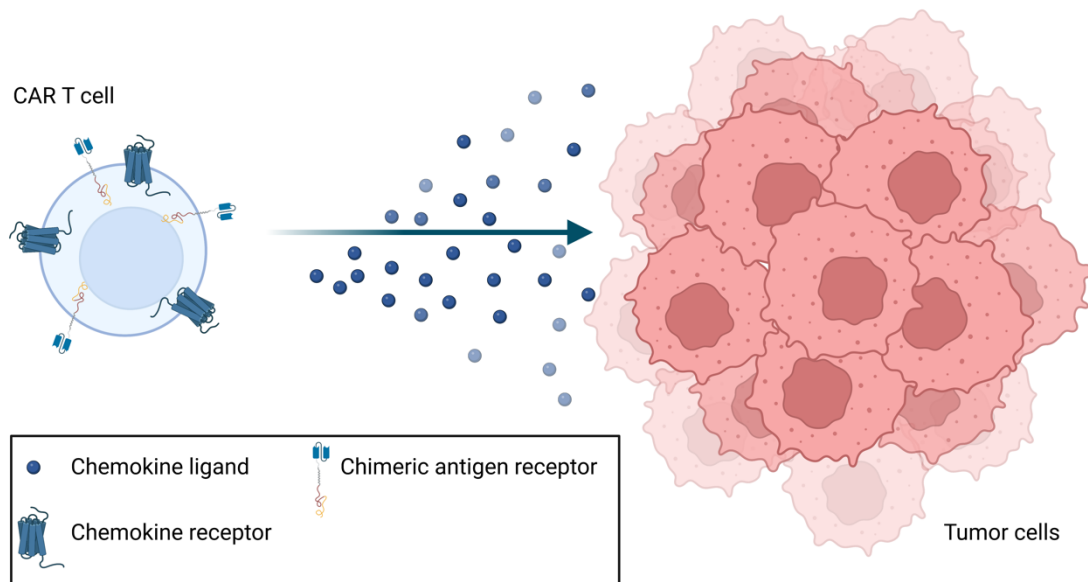


Figure 4: Chemotaxis of chemokine receptor transduced CAR T cells towards respective chemokine ligand secreting tumor cells.

CXCR6-modified mesothelin specific CAR T cells enhanced migration to pancreatic tumors expressing C-X-C motif chemokine ligand (CXCL) 16 in orthotopically transplanted tumor or patient-derived xenograft mouse models leading to a decrease in tumor growth and increased survival [Lesch *et al.*, 2021]. Thus, equipping CAR T cells with chemokine receptors has the potential to overcome one of the main challenges when targeting solid tumors with CAR T cell therapy.

### 2.3.3 Variability in antigen expression due to tumor heterogeneity

Apart from limited migration to the tumor and immunosuppression in the TME, antigen recognition is one of the main factors impeding the effectiveness of CAR T cell therapy [Guo & Cui, 2020]. Ideally, CAR T cells are targeting tumor-specific antigens that are exclusively expressed on all tumor cells. However, these are

rarely found in tumors. So far, TAA, like mesothelin, EpCAM or human epidermal growth factor receptor 2 (HER2) have been targeted with CAR T cells [Martinez & Moon, 2019]. The expression of TAA needs to be higher on tumor than on healthy cells to reduce the risk of on-target off-tumor toxicity. Unlike CD19 in B cell malignancies, lineage specific antigens that can be targeted without severe side effects have not been described for solid tumors yet [Guo & Cui, 2020]. In addition, heterogeneity in solid tumors is a challenge for targeted therapies. Especially, antigen expression differs in density and distribution between different subsets of malignant cells [Pak *et al.*, 2012]. Thus, targeting a single tumor antigen can lead to antigen escape by downregulation under therapeutic pressure [Anurathapan *et al.*, 2014]. This is considered one of the major causes of relapse when targeting CD19 in B cell malignancies [Gu *et al.*, 2022; Maude *et al.*, 2014].

Engineering T cells to target various antigens on tumor cells has the potential to overcome those challenges. Dual targeting CAR T cells contain two scFvs binding to different tumor antigens and can be activated by either one of the antigens. CAR T cells targeting simultaneously GD2 and B7 homolog 3 protein (B7-H3) were effective in solid tumor mouse models and prevented tumor escape due to low expression of tumor antigen [Hirabayashi *et al.*, 2021]. In addition, CAR T cells binding to tags on antibodies can provide a modular platform which is capable of switching the targeted tumor antigen by administration of a different antibody. This platform approach has been utilized by combining biotin-specific CAR T cells and biotinylated antibodies [Lohmueller *et al.*, 2017]. It was shown that the T cells can effectively lyse antigen positive tumor cells in presence of antibodies against CD19 or CD20 [Lohmueller *et al.*, 2017]. Similarly, CAR T cells recognizing the P329G-mutated fragment crystallizable (Fc) part of an antibody mediated modular targeting of HER2 and mesothelin in a human hepatocellular carcinoma

xenograft mouse model [Stock *et al.*, 2022]. Along these lines, BiAb can be utilized to render engineered T cells tumor specific. T cells that were modified to express a targetable SAR construct can be directed against a tumor antigen via a BiAb binding to the SAR and the target antigen (Figure 5) and thereby, mediate tumor cell killing in a reversible and modular fashion [Benmebarek *et al.*, 2021; Karches *et al.*, 2019]. The SAR construct contains the extracellular part of EGFRvIII, linked to a CD28 transmembrane domain and the signal transduction domains CD28 and CD3 $\zeta$  [Karches *et al.*, 2019]. EGFRvIII is known to be only expressed in glioblastoma but absent on healthy cells [Gupta *et al.*, 2010; Montano *et al.*, 2011].

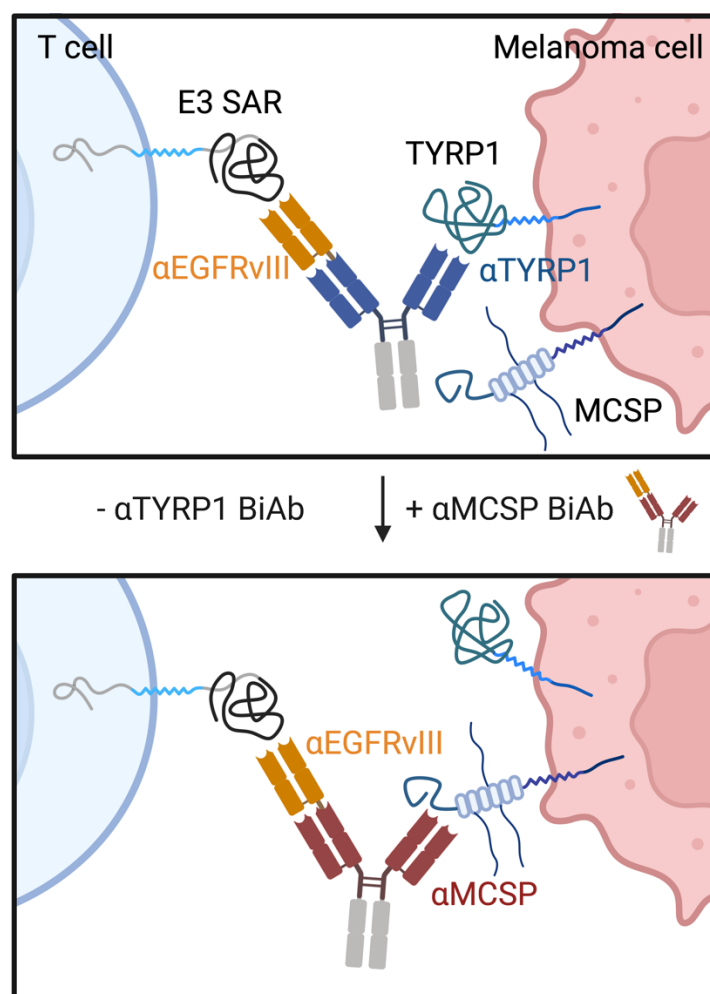


Figure 5: Modular therapeutic platform consisting of SAR engineered T cells in combination with BiAb targeting melanoma-associated antigens TYRP1 and MCSP utilized in this thesis. SAR T

cells are targeting TYRP1 via the anti-TYRP1 x anti-EGFRvIII BiAb ( $\alpha$ TYRP1 BiAb). Following removal of anti-TYRP1 x anti-EGFRvIII BiAb and addition of the anti-MCSP x anti-EGFRvIII BiAb ( $\alpha$ MCSP BiAb) SAR T cells are redirected against MCSP.

By administration of different BiAb molecules, SAR T cells can be redirected towards different melanoma antigens, like TYRP1 or MCSP (Figure 5).

## 2.4 Research hypothesis and aims of the work

Since its first approval in 2017, CAR T cell therapy had remarkable success in treating patients with hematological malignancies. However, clinical trials testing CAR T cells against solid tumor entities often had limited efficacy [Chen *et al.*, 2022]. This is mainly due to three challenges arising from intrinsic solid tumor characteristics: limited CAR T cell infiltration, immunosuppression of CAR T cells by the TME and tumor heterogeneity [Guo & Cui, 2020]. To overcome these challenges, T cell engineering needs to be optimized and possibly combined with other treatment approaches.

This present work focuses on (1) developing a modular platform consisting of engineered T cells in combination with BiAb to target multiple tumor antigens in melanoma and on (2) improving CAR T cell migration to the tumor and shielding from immunosuppression in pancreatic cancer by equipping CAR T cells with CCR8 and TGF- $\beta$  DNR.

### 3. Paper I


The original article “Bispecific antibodies redirect synthetic agonistic receptor modified T cells against melanoma” (doi: 10.1136/jitc-2022-006436) and the supplementary material can be found using the following link: <https://jitc.bmj.com/content/11/5/e006436>

Open access

Original research



## Bispecific antibodies redirect synthetic agonistic receptor modified T cells against melanoma

Florian Märkl <sup>1</sup>, Mohamed-Reda Benmebarek <sup>1</sup>, Julius Keyl,<sup>1</sup> Bruno L Cadilha,<sup>1</sup> Martina Geiger,<sup>2</sup> Clara Karches,<sup>1</sup> Hannah Obeck,<sup>1</sup> Melanie Schwerdtfeger,<sup>1</sup> Stefanos Michaelides,<sup>1</sup> Daria Briukhovetska,<sup>1</sup> Sophia Stock <sup>1,3,4</sup>, Jakob Jobst,<sup>1</sup> Philipp Jie Müller,<sup>1</sup> Lina Majed,<sup>1</sup> Matthias Seifert <sup>1</sup>, Anna-Kristina Klüver,<sup>1</sup> Theo Lorenzini <sup>1</sup>, Ruth Grünmejer <sup>1</sup>, Moritz Thomas <sup>5,6,7</sup>, Adrian Gottschlich,<sup>1</sup> Richard Klaus,<sup>8</sup> Carsten Marr,<sup>5,6</sup> Michael von Bergwelt-Baildon,<sup>3,4</sup> Simon Rothenfusser,<sup>1</sup> Mitchell P Levesque,<sup>9</sup> Markus Vincent Heppt,<sup>10,11</sup> Stefan Endres <sup>1,4,12</sup>, Christian Klein <sup>2</sup>, Sebastian Kobold <sup>1,4,12</sup>

**To cite:** Märkl F, Benmebarek M-R, Keyl J, et al. Bispecific antibodies redirect synthetic agonistic receptor modified T cells against melanoma. *Journal for ImmunoTherapy of Cancer* 2023;11:e006436. doi:10.1136/jitc-2022-006436

► Additional supplemental material is published online only. To view, please visit the journal online (<http://dx.doi.org/10.1136/jitc-2022-006436>).

FM and M-RB contributed equally.

Accepted 16 April 2023



© Author(s) (or their employer(s)) 2023. Re-use permitted under CC BY-NC. No commercial re-use. See rights and permissions. Published by BMJ.

For numbered affiliations see end of article.

#### Correspondence to

Professor Sebastian Kobold; [sebastian.kobold@med.uni-muenchen.de](mailto:sebastian.kobold@med.uni-muenchen.de)

#### ABSTRACT

**Background** Melanoma is an immune sensitive disease, as demonstrated by the activity of immune check point blockade (ICB), but many patients will either not respond or relapse. More recently, tumor infiltrating lymphocyte (TIL) therapy has shown promising efficacy in melanoma treatment after ICB failure, indicating the potential of cellular therapies. However, TIL treatment comes with manufacturing limitations, product heterogeneity, as well as toxicity problems, due to the transfer of a large number of phenotypically diverse T cells. To overcome said limitations, we propose a controlled adoptive cell therapy approach, where T cells are armed with synthetic agonistic receptors (SAR) that are selectively activated by bispecific antibodies (BiAb) targeting SAR and melanoma-associated antigens.

**Methods** Human as well as murine SAR constructs were generated and transduced into primary T cells. The approach was validated in murine, human and patient-derived cancer models expressing the melanoma-associated target antigens tyrosinase-related protein 1 (TYRP1) and melanoma-associated chondroitin sulfate proteoglycan (MCSP) (CSPG4). SAR T cells were functionally characterized by assessing their specific stimulation and proliferation, as well as their tumor-directed cytotoxicity, in vitro and in vivo.

**Results** MCSP and TYRP1 expression was conserved in samples of patients with treated as well as untreated melanoma, supporting their use as melanoma-target antigens. The presence of target cells and anti-TYRP1 × anti-SAR or anti-MCSP × anti-SAR BiAb induced conditional antigen-dependent activation, proliferation of SAR T cells and targeted tumor cell lysis in all tested models. In vivo, antitumoral activity and long-term survival was mediated by the co-administration of SAR T cells and BiAb in a syngeneic tumor model and was further validated in several xenograft models, including a patient-derived xenograft model.

**Conclusion** The SAR T cell-BiAb approach delivers specific and conditional T cell activation as well

#### WHAT IS ALREADY KNOWN ON THIS TOPIC

⇒ Melanoma has been shown to be sensitive to immunotherapy, though significant subsets of patients do not respond or relapse after initial response.

#### WHAT THIS STUDY ADDS

⇒ A modular and controllable adoptive T cell therapy approach to the treatment of melanoma.

#### HOW THIS STUDY MIGHT AFFECT RESEARCH, PRACTICE OR POLICY

⇒ This study puts forward the simultaneous and sequential targeting of melanoma-associated chondroitin sulfate proteoglycan and tyrosinase-related protein 1 as a strategy for the targeted therapy of melanoma.

as targeted tumor cell lysis in melanoma models. Modularity is a key feature for targeting melanoma and is fundamental towards personalized immunotherapies encompassing cancer heterogeneity. Because antigen expression may vary in primary melanoma tissues, we propose that a dual approach targeting two tumor-associated antigens, either simultaneously or sequentially, could avoid issues of antigen heterogeneity and deliver therapeutic benefit to patients.

#### BACKGROUND

Due to its high tumor mutational burden, likely driven by ultraviolet radiation, melanoma possesses a high number of neoantigens, making it one of the most immunogenic tumor types.<sup>1,2</sup> Melanoma treatment has been revolutionized by immune check-point blockade (ICB), reactivating T cells or preventing T cell dysfunction.<sup>3</sup> Despite these successes, many patients still either do not

## Open access



respond or relapse after an initial response.<sup>4</sup> For patients not carrying targetable mutations such as BRAFV600E or having already exhausted targeted treatments, limited options remain, resulting in an urgent need for innovative effective treatments.

While ICB-mediated prevention of T cell dysfunction has entered clinical practice in a wide array of indications beyond melanoma, the direct therapeutic use of T cells in non-hematological cancer entities has been largely ineffective.<sup>5</sup> Melanoma, however, has been an exception in this regard. Tumor infiltrating lymphocytes (TIL) are a prognostic factor in melanoma and correlate with response to ICB.<sup>6</sup> In fact, investigation using isolated, non-modified, and ex vivo expanded TIL as a treatment modality for patients with melanoma has already been explored in the pre-ICB era.<sup>7</sup> There, about 50% of treated patients were sensitive to TIL therapy, a fraction of which exhibiting complete and durable responses.<sup>8,9</sup> The success of ICB therapy then suspended further development of TIL-based therapies for some time. Recently, clinical studies have explored the potential of TIL therapy after ICB failure in patients with melanoma. Consistent with pre-ICB reports, TIL therapy yielded substantial response rates of up to 32%, indicating that even in such clinically challenging situations, TIL therapy might still be of benefit to patients (NCT00937625, NCT02379195 and NCT02354690).<sup>10</sup> Along these lines, ICB and TIL therapy impressively demonstrate the utility of T cells in melanoma treatment regardless of treatment line. TIL therapy, however, comes with significant challenges which limit its application: (1) requirement for accessible target lesions for resection and TIL selection and expansion, (2) failure to select and expand TIL, (3) heterogeneity of TIL products with often undefined specificities and consequently and (4) heterogeneous response patterns both in extent and in duration.<sup>11</sup>

T cells can be rendered tumor-specific through genetic engineering of a synthetic receptor, so called chimeric antigen receptor (CAR), that can recognize antigens on the cell surface independent of major histocompatibility complex molecules. Anti-CD19 CAR T cells have entered clinical routine after transformative results in the treatment of hematological malignancies.<sup>12,13</sup> CD19 as a target antigen allows for targeting of lymphoma and leukemic cells along with healthy B cells. The deleterious effects of depleting the entire B-cell compartment are clinically manageable.<sup>14</sup> In contrast to CD19<sup>+</sup> hematological malignancies, dispensable lineage-specific tumor-associated antigens are rarely found in solid cancer types.<sup>5</sup> Additionally, an immunosuppressive milieu and target antigen heterogeneity, among other factors, have resulted in melanoma CAR T cell therapy trials faring poorly thus far.<sup>15</sup> Detailed analysis of TIL therapy failure highlights that loss of dominant antigens under therapeutic pressure happens quite frequently, suggesting that a successful T cell product will need to target more than one antigen.<sup>16</sup> These results support the need for advances in melanoma cell therapy considering such a limitation.

As most of the targetable antigens are not entirely specific to melanoma but shared with other cells as well, we reasoned that any T cell therapeutic strategy would need to be controllable to allow application with a safety net. We have previously described a synthetic agonistic receptor (SAR) platform composed of the extracellular domain of epidermal growth factor receptor variant III (EGFRvIII), fused to intracellular T cell-activating domains (later referred to as E3 construct). The construct can be specifically activated by bispecific antibodies (BiAb) simultaneously targeting the SAR and the tumor antigen. The major advantages of modular adoptive cell therapy (ACT) platforms are the possibility to stop administration of the adaptor molecule in case of undesired therapy-associated toxicities and the ability to target multiple antigens by administering different T cell adaptor molecules.<sup>17,18</sup> In particular, we previously demonstrated that SAR-transduced T cell activity is conditional to the presence and binding of the BiAb, enabling a tunable activity that is advantageous in case of toxicities.<sup>19,20</sup> We hypothesized that this SAR platform could serve as a safe and effective way of targeting melanoma-associated antigens for melanoma treatment.<sup>20</sup>

For the present study, using the CrossMab technology,<sup>21,22</sup> we developed trivalent BiAb binding melanoma antigen and the E3 SAR. We demonstrate that SAR-transduced T cells were selectively and reversibly activated through the BiAb, solely in the presence of antigen-positive melanoma cells. We showcase substantial activity of the platform in primary melanoma cultures and in several xenograft and syngeneic mouse models, supporting further clinical development.

## MATERIAL AND METHODS

### Patient and healthy donor material

Frozen, primary and metastatic tumor samples from 13 patients with a histologically confirmed diagnosis of melanoma were used for this study. The samples were cultured in MCDB 153 medium (Merck) complemented with 20% Leibovitz's L-15 medium (Thermo Fisher), 2% fetal calf serum (Gibco), 10 µg/mL human insulin (Merck) and 2 M CaCl<sub>2</sub> solution and expanded until further use. Biological and clinical information were obtained from electronic medical records. Patient characteristics are summarized in online supplemental table 1. Human peripheral blood mononuclear cells (PBMCs) for the generation of human CAR and SAR T cells were isolated from healthy donors by Ficoll density gradient separation.

### Mice

Female C57BL/6N and NSG (NOD.Cg-Prkdcscid Il2rgtm1Wj/SzJ) mice were purchased from Charles River or Janvier Labs. Animals were housed in specific pathogen-free facilities in groups of 2–5 animals per cage. All experimental studies were approved and performed with mice aged 2–4 months and in accordance with guidelines and regulations implemented by the Regierung von





Oberbayern (ROB-55.2–2532.Vet\_02-20-208 and ROB-55.2–2532.Vet\_02-17-135). In accordance with the animal experiment application, tumor size, behavior, breathing, body weight and posture of mice were monitored three times per week. For survival analyses, the above-described criteria (in particular: curved back, apathy, weight loss >20%, piloerection, pronounced abdominal breathing and cyanosis, spasms, paralysis, tumor size >225 mm<sup>2</sup> or one of the two measure dimensions >15 mm or open wound in the tumor area) were taken as humane surrogates for survival and recorded in Kaplan-Meier plots.

#### Animal experiments

MV3, A375 and patient-derived (patient sample 2) xenograft models were established in NSG mice (in total n=96) following the subcutaneous (s.c.) injection of 0.2, 1 or 0.4×10<sup>6</sup> tumor cells, respectively, in 100 µL phosphate buffered saline (PBS) into the right flank of NSG mice. Syngeneic tumor model was established in C57BL/6 mice (in total n=84) by intravenous injection of YUMM1.1 overexpressing luciferase (and tyrosinase-related protein 1 (TYRP1) where mentioned) (2×10<sup>6</sup>) into the tail vein following a partial lymphodepletion of the B-cell compartment, using 250 µg murine IgG2a anti-CD20 monoclonal antibody (18B12, Roche). Animals were randomized into treatment groups according to tumor burden. Experiments were performed by a scientist blinded to treatment allocation and with adequate controls. No time points or mice were excluded from the experiments presented in the study. For s.c. models, tumor burden was measured three times per week and calculated as mm<sup>3</sup> given by volume=(length×width<sup>2</sup>)/2. Tumor burden of intravenous models were measured using a luciferase-based IVIS Lumina X5 imaging system. For ACT studies, 10<sup>7</sup>T cells with transduction efficiencies of 50–90% were injected intravenously in 100 µL PBS.

#### Cell line generation, culture and validation

A375, MV3, PANC-1 and B16 tumor cell lines were purchased from American Type Culture Collection. The ovalbumin overexpressing murine pancreatic cancer cell line Panc02-OVA has been previously described.<sup>20</sup> The murine YUMM1.1 cell line was kindly provided by Dr Bosenberg (Yale University, USA). YUMM1.1 tumor cells were stably transduced using retroviral pMP71 vector expressing TYRP1 protein (UNIPROT entry P17643) to generate YUMM1.1 TYRP1 tumor cells. Luciferase-eGFP (LUC-GFP) overexpressing cell line YUMM1.1 TYRP1-LUC-GFP and YUMM1.1 LUC-GFP were generated according to a previously described protocol.<sup>20</sup> All tumor lines were grown as previously described,<sup>20</sup> and used for experiments when in the exponential growth phase.

#### Virus production

293Vec-Galv, 293Vec-Eco and 293Vec-RD114 were a kind gift of Manuel Caruso, Québec, Canada, and have been previously described.<sup>23</sup> For virus production, retroviral pMP71 (kindly provided by C. Baum, Hannover) vectors

carrying the sequence of the relevant receptor were stably introduced in packaging cell lines. Single cell clones were generated and indirectly screened for virus production by determining transduction efficiency of primary T cells. This method was used to generate the producer cell lines 293Vec-RD114 for EGFRvIII-CD28-CD3ζ (E3), EGFRvIII with CD28 transmembrane domain lacking intracellular signaling domains (E3del) and anti-HER2-CD28-CD3ζ (HER2 CAR). 293Vec-Galv, 293Vec-Eco and 293Vec-RD114 were grown as previously described.<sup>24</sup> All cell lines used in experiments were regularly checked for mycoplasma species with the commercial testing kit MycoAlert (Lonza). Authentication of human cell lines by STR DNA profiling analysis was conducted in house.

#### T cell generation, retroviral transduction and culture

Human and murine SAR construct generation was previously described.<sup>20</sup> SAR-transduced T cells will be referred to as SAR T cells. The HER2 CAR was generated with a humanized single-chain variable fragment against HER2 (4D5).<sup>25</sup> Murine T cells were differentiated from splenocytes from donor mice. T cell isolation and transduction protocols have been previously described.<sup>26</sup> T cells were expanded or directly expanded with T cell medium supplemented with human interleukin (IL)-15 (PeproTech) every second day. Human T cells have been differentiated and transduced using previously described protocols<sup>27</sup> or directly taken into culture with human T cell medium in concentrations of 10<sup>6</sup>T cells per mL medium.

#### Cytotoxicity assays

For impedance-based real-time killing assays using a xCELLigence system (ACEA Bioscience), previously described,<sup>20</sup> 10<sup>4</sup> tumor cells were seeded per well in a 96-well plate. Cell number was monitored over the time frame of 10 hours for every 20 min. 10<sup>5</sup>T cells transduced with the indicated receptors were added to the tumor cells. For lactate dehydrogenase (LDH)-based killing assays, T cells were incubated with tumor cells and BiAb at indicated effector to target ratios and concentrations. Transduced T cells were added to the adherent tumor cells and co-cultured as indicated. LDH levels were measured according to the manufacturer's protocol (Promega). Additionally, the killing of melanoma patient samples was assessed using a flow cytometry-based readout after 48 hours of co-culture with human SAR T cells in the presence of either the anti-TYRP1/anti-EGFRvIII (αTYRP1/αE3) which is cross-reactive to human and murine TYRP1 or the anti-human melanoma-associated chondroitin sulfate proteoglycan (MCSP, also known as CSPG4)/anti-EGFRvIII BiAb (αMCSP/αE3). Tumor cells were stained with the cell proliferation dye eFluor 450 according to the manufacturer's protocol (eBioscience). Depending on the tumor cell size 2–4×10<sup>4</sup> cells per well were co-cultured with SAR T cells in an effector to target cell ratio of 2:1 in a 96-well plate. Tumor cells were detached using trypsin. Dead cells were stained using the violet fixable

## Open access



viability dye (BioLegend) for 15 min at room temperature. Following this, cell surface proteins were stained for 20 min at 4°C. For the characterization and quantification of the SAR T cells antibodies against CD3 (OKT3), CD4 (OKT4), CD8a (RPA-T8), PD-1 (EH12.2H7), 4-1BB (4B4-1), CD69 (FN50) and EGFR (A-13) (all from BioLegend) were used. Tumor and T cell counts were normalized to counting beads (Invitrogen).

#### Proliferation assays

SAR T cell proliferation was measured using a flow cytometry-based assay that compared fold proliferation of CD3<sup>+</sup> (17A2, BioLegend) T cells over a period of 48 hours normalized to the number of T cells per bead at indicated concentrations and effector to target ratio.

#### Biodistribution study

For the biodistribution study of the anti-TYRP1/anti-E3 BiAb ( $\alpha$ TYRP1/ $\alpha$ E3 BiAb),  $2 \times 10^6$  YUMM1.1 TYRP1-LUC-GFP tumor cells were intravenously injected into C57Bl/6 mice. IVIS imaging was used to verify tumor engraftment and distribution after 13 and 20 days.  $\alpha$ TYRP1/ $\alpha$ E3 or  $\alpha$ Mesothelin/ $\alpha$ E3 control BiAb (5  $\mu$ g/mouse or 10 mg/kg) were injected intraperitoneally (i.p.) into tumor-bearing (for each antibody n=3) and non-tumor-bearing mice (for each antibody n=2) on day 20. Experimental readout was taken 48 hours later. In addition to the metastasis in the lung, organs with the highest TYRP1 expression relative to baseline (skin and heart) were also harvested. Organ tissue was embedded and frozen in optimal cutting temperature compound before preparation for immunofluorescence staining and imaging.

#### Immunofluorescence

The 5  $\mu$ m tissue cryosections were stained on chip cytometry slides (Zellkraftwerk) with an antibody (polyclonal, AF555, Thermo Fisher Scientific) against the human IgG1-based  $\alpha$ TYRP1/ $\alpha$ E3 BiAb, a rabbit anti-GFP antibody (polyclonal, Novus Biologicals), a secondary antibody against rabbit IgG (polyclonal, PerCP, Jackson ImmunoResearch) and Hoechst 33342 (Thermo Fisher Scientific). The fluorescence was measured using the ZellScannerONE (Zellkraftwerk).

#### PCR and quantitative real-time PCR

All DNA constructs were generated by overlap extension PCR<sup>24</sup> and recombinant expression cloning into the retroviral pMP71 vector<sup>20</sup> using standard molecular cloning protocols.<sup>26</sup> RNA was extracted from cells using the InviTrap Spin Universal RNA extraction Kit (Strattec). Complementary DNA was synthesized using the SuperScript II kit (Life Technologies). Real-time PCR reactions were performed using SYBR Green PCR Master Mix (Applied Biosystems) and sequence specific primers for human MCSP, human and murine TYRP1.<sup>28–30</sup> The amplification was performed with CFX Connect Real-Time PCR Detection System (Bio-Rad Laboratories) running up to 50 cycles of 5 s at 95°C followed by 30 s at 60°C after

an initial step of 95°C for 2 min. Melting curves from 65°C to 95°C were performed to evaluate the specificity of the PCR. The messenger RNA (mRNA) expression levels of human TYRP1 and MCSP were normalized to the expression of phosphoglycerate kinase. The mRNA expression levels of murine TYRP1 were normalized to the expression of  $\beta$ -actin.

#### Cytokine release assays

Murine and human SAR T cell stimulation assays were set-up at indicated concentrations and effector to target ratios. Murine SAR T cells were co-cultured with B16, YUMM1.1 TYRP1 and Panc02-OVA cell lines. Human SAR T cells were co-cultured with MV3, A375 cell lines and human melanoma samples. Cytokine quantification was measured by ELISA for the following: interferon (IFN)- $\gamma$  (BD), IL-2 (BD), tumor necrosis factor (TNF)- $\alpha$  (R&D Systems) and granzyme B (R&D Systems).

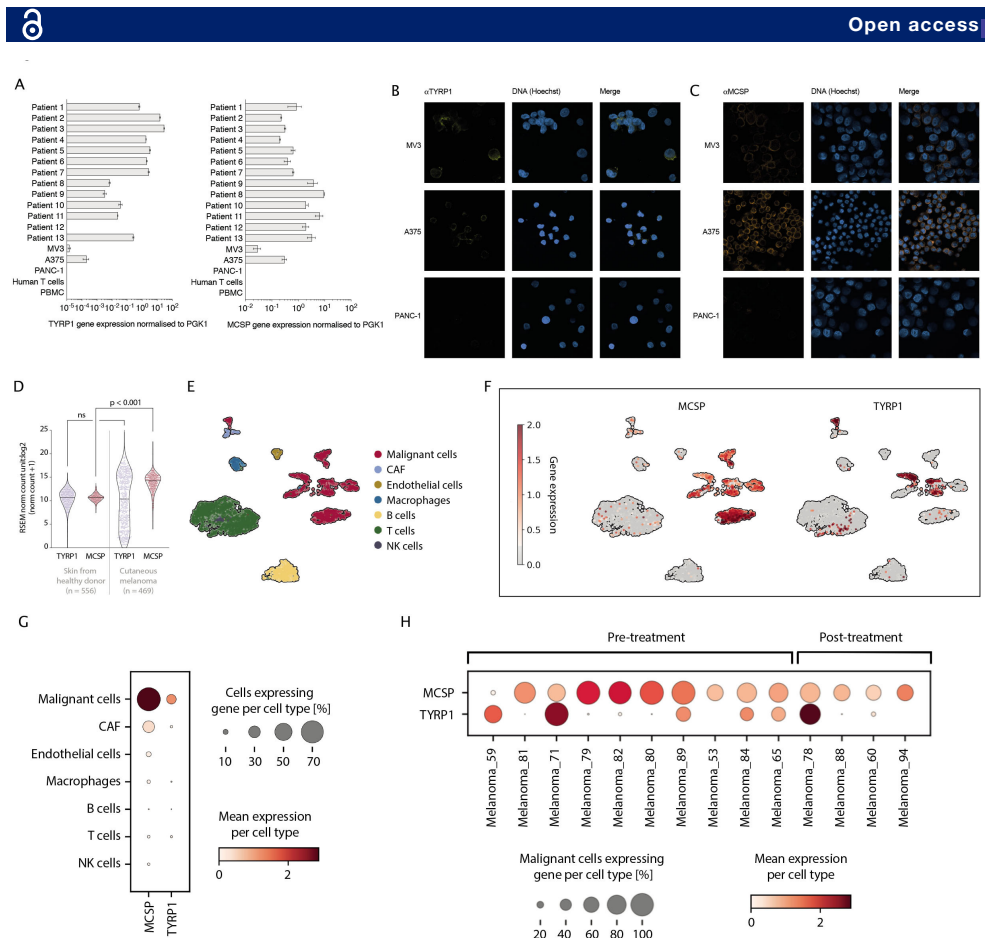
#### Statistical analysis

Two-tailed student's t-test was used for comparisons between two groups, while two-way analysis of variance with Bonferroni post-test (multiple time points) was used for comparisons across multiple groups. A log-rank (Mantel-Cox) test was used to compare survival curves. All statistical tests were performed with GraphPad Prism V.8 software, and  $p < 0.05$  was considered statistically significant and represented as \* $p < 0.05$ , \*\* $p < 0.01$  and \*\*\* $p < 0.001$ . No statistical methods were used to predetermine sample size. Investigators were blinded to treatment allocation during experiments and outcome assessment.

## RESULTS

### MCSP and TYRP1 are differentially expressed in melanoma

To identify suitable target structures, we assessed the expression of TYRP1 and MCSP in human melanoma cell lines as well as melanoma samples from treated and untreated patients. Both genes were shown to be highly expressed in melanoma relative to PBMC and human pancreatic cancer cell line PANC-1 control samples both at RNA and protein level (figure 1A–C, online supplemental figure 1A, online supplemental table 1). Analysis of The Cancer Genome Atlas RNA sequencing (RNA-seq) expression data also revealed MCSP to be differentially regulated in cutaneous melanoma tissue relative to skin tissue from healthy donors (figure 1D). Although the median expression of TYRP1 in cutaneous melanoma tissue was similar to the expression in skin from healthy donors, there was a far greater variability in its expression in patients with melanoma with a clear differential expression in a subset of patients (figure 1D). The expression of the targets was also analyzed across different cell types within the same patient (figure 1E), taking advantage of a single cell RNA-seq data set—GSE72056 of 3993 cells from 19 patients,<sup>31</sup> which revealed a distinct, only partially overlapping pattern of expression for each antigen in tumor tissue (figure 1F and G). Furthermore,



## Open access



MCSP expression on malignant cells was well-maintained in patients that received treatment (figure 1H). TYRP1 expression pattern was similar in pre-treatment and post-treatment samples but characterized by a high spread (figure 1H).

#### **$\alpha$ MCSP/ $\alpha$ E3 and $\alpha$ TYRP1/ $\alpha$ E3 BiAb bind MCSP<sup>+</sup> and TYRP<sup>+</sup> melanoma cells**

BiAb-mediated T cell activation is dependent on antibody aggregation on the target cell before their presentation to T cells in a polyvalent form. Our previous work on the SAR platform could show that BiAb must have a single specificity for E3 to ensure conditional SAR T cell activation in the presence of the target antigen.<sup>20</sup> This informed the BiAb design used in this study, with a trivalent and bispecific format with two specificities for the tumor antigen (TYRP1 or MCSP) and a single specificity for E3 (online supplemental figure 1B,C). The binding properties and apparent dissociation constant ( $K_D$ ) of BiAb (anti-MCSP/anti-E3 BiAb ( $\alpha$ MCSP/ $\alpha$ E3) and anti-TYRP1/anti-E3 BiAb ( $\alpha$ TYRP1/ $\alpha$ E3)) to both their targets (online supplemental figure 1D,E) and EGFRvIII (online supplemental figure 1F) were analyzed by flow cytometry. The previously characterized  $\alpha$ Mesothelin/ $\alpha$ E3 BiAb binding the SAR and mesothelin was used as a non-melanoma targeting control construct in subsequent experiments.<sup>20</sup>

#### **$\alpha$ MCSP/ $\alpha$ E3 and $\alpha$ TYRP1/ $\alpha$ E3 BiAb can mediate SAR T cell activation, proliferation and differentiation**

SAR constructs could be retrovirally transduced into primary murine and human T cells with high efficiencies (figure 2A). Following transduction and expansion protocols, CD4<sup>+</sup> and CD8<sup>+</sup> human SAR T cells were shown to be of similar frequencies and to predominantly have an effector memory phenotype (figure 2B,C). We assessed SAR T cell activation and cytokine release in both murine and human T cells. For murine T cells, we incubated SAR T cells with two TYRP1-expressing cell lines, B16 and YUMM1.1 TYRP1 and with the antigen-negative, pancreatic cancer cell line Panc02-OVA (online supplemental figure 1G-I) in the presence of  $\alpha$ TYRP1/ $\alpha$ E3 BiAb. Murine SAR T cells specifically released IFN- $\gamma$ , IL-2, TNF- $\alpha$  and granzyme B and expressed the activation markers programmed cell death protein 1 (PD-1) and CD69 on co-culture with TYRP1<sup>+</sup> melanoma cell lines, unlike in co-culture with antigen-negative Panc02-OVA tumor cells (online supplemental figure 2A,B). SAR T cells only proliferated in the presence of TYRP1-expressing tumor cells and BiAb (online supplemental figure 2C). Human SAR T cells were incubated with the MCSP<sup>+</sup> and TYRP1<sup>+</sup> cell lines, A375 and MV3, respectively. Only in the presence of the MCSP-targeting BiAb molecule and the target antigen, human SAR T cells released IFN- $\gamma$ , IL-2, TNF- $\alpha$  and granzyme B. In contrast, untransduced T cells (Unt) and control-E3del-transduced T cells remained inactive and did not produce cytokines or cytotoxic granules regardless of the presence of the BiAb and target

antigen (figure 2D). The frequency of CD69, PD-1 and 4-1BB-expressing SAR T cells was increased in the presence of either one of the two BiAb molecules and antigen-expressing target cells (figure 2E). CD4<sup>+</sup> and CD8<sup>+</sup> T cell proliferation was congruent with the activation observed, as stimulated SAR T cells proliferated more than control T cells or SAR T cells in the absence of BiAb (figure 2F).

#### **SAR T cells can target and lyse MCSP-expressing and TYRP1-expressing melanomas**

Using flow cytometry-based and impedance-based assays, we evaluated whether SAR T cells could selectively lyse MCSP-expressing and TYRP1-expressing melanoma cells in the presence of a bridging BiAb. Human SAR T cells specifically eliminated antigen-positive A375 and MV3 melanoma cells when co-cultured together with either an  $\alpha$ MCSP/ $\alpha$ E3 or  $\alpha$ TYRP1/ $\alpha$ E3 BiAb whereas no lysis was detected with the antigen-negative pancreatic cancer cell line PANC-1 (figure 2G). Similarly, murine SAR T cells only lysed TYRP1<sup>+</sup> B16 and YUMM1.1 TYRP1 melanoma cells in the presence of an  $\alpha$ TYRP1/ $\alpha$ E3 BiAb (online supplemental figure 2D,E). TYRP1-specific and MCSP-specific BiAb conditionally activated human SAR T cells in co-culture with patient-derived melanoma samples. SAR T cells showed increased expression of the activation markers CD69, PD-1 and 4-1BB, secretion of IFN- $\gamma$  and proliferation, relative to E3 only or Unt T cell in presence of either of the BiAb (figure 3A-C). Also, TYRP1-specific and MCSP-specific BiAb redirected SAR T cells to target and lyse all patient-derived melanoma samples tested, whereas Unt and BiAb controls had no effect on tumor cell lysis (figure 3D).

#### **Cleavable proteins do not impact SAR-BiAb platform efficacy and safety**

With elevated levels of MCSP having been reported in the sera of patients with melanoma,<sup>32</sup> we sought to better understand the potential impact of soluble MCSP or TYRP1 on the SAR T cell-BiAb approach. Therefore, soluble recombinant MCSP and TYRP1 proteins were used. Proteins were added in ascending concentrations to a T cell-tumor cell co-culture to study T cell killing efficiency and kinetics. Ascending concentrations of MCSP and TYRP1, including concentrations at a physiological level, did not impair SAR T cell killing (figure 4A and online supplemental figure 3A). We also sought to test whether free soluble protein targets would induce unwanted off-tumor SAR T cell activation. We found that soluble MCSP and TYRP1 did not induce SAR T cell activation in the presence of either relevant BiAb, both at physiological and supraphysiological concentrations that were tested. There, no significant changes in IFN- $\gamma$  levels were observed when comparing E3 and BiAb conditions to controls containing soluble recombinant MCSP or TYRP1 (figure 4B and online supplemental figure 3B). It should be noted that in this setting a higher basal SAR T cell activation was

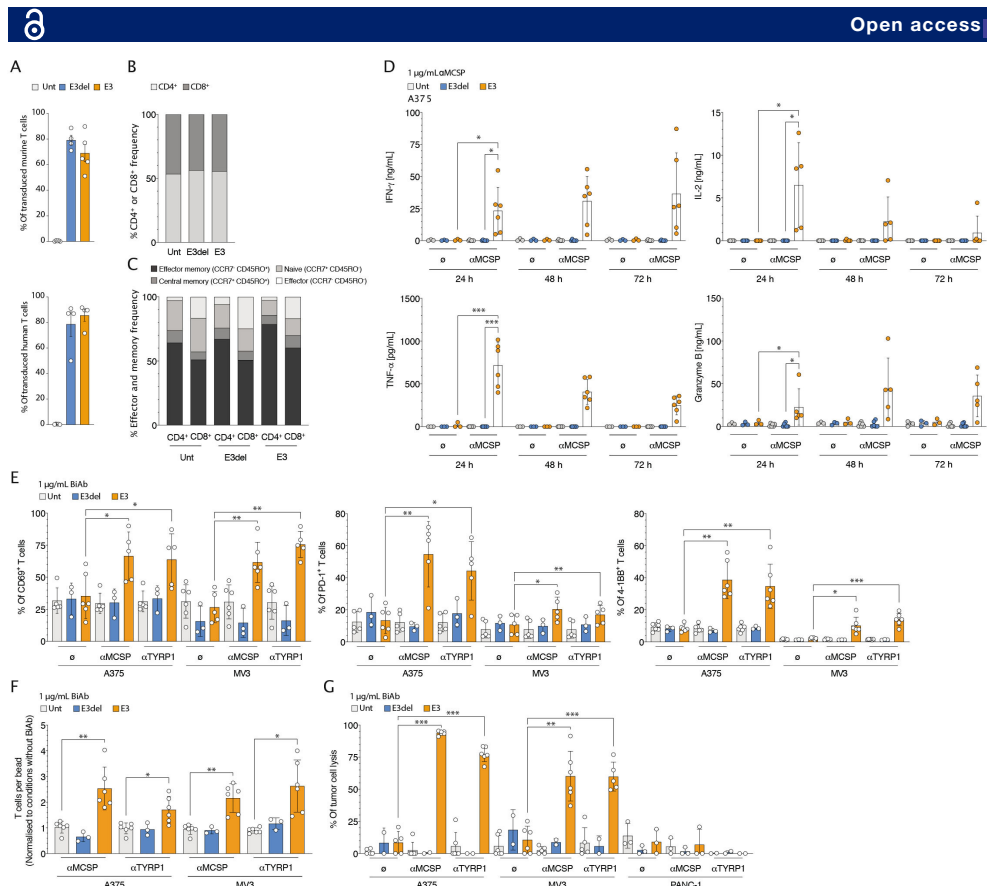


**Figure 2**  $\alpha$ MCSP/ $\alpha$ E3 and  $\alpha$ TYRP1/ $\alpha$ E3 BiAb activate SAR T cells to mediate specific cytotoxicity against human melanoma cell lines. (A) Expression of the constructs E3 and E3del on murine T cells and human T cells from healthy donors ( $n=4-5$ ). E3, E3 SAR-transduced T cells. E3del, T cells transduced with E3 SAR lacking intracellular signaling domains. (B) Frequency of CD4 and CD8 expression on human T cells. (C) Frequency of effector memory (CCR7<sup>-</sup> and CD45RO<sup>+</sup>), naive (CCR7<sup>+</sup> and CD45RO<sup>+</sup>), central memory (CCR7<sup>+</sup> and CD45RO<sup>-</sup>) and effector (CCR7<sup>-</sup> and CD45RO<sup>+</sup>) phenotype on human T cells. (D) ELISA for granzyme B, IFN- $\gamma$ , IL-2 and TNF- $\alpha$  in supernatant of human T cells in co-culture with human melanoma cell line A375 (E:T 2:1) and with or without  $\alpha$ MCSP/ $\alpha$ E3 BiAb ( $\alpha$ MCSP, 1  $\mu$ g/mL). Supernatant was taken after 24, 48 and 72 hours ( $n=3-6$ ). (E) Frequency of CD69, PD-1 and 4-1BB expression on T cells after 48 hours of co-culture with A375 or MV3 (E:T 2:1) and either with or without  $\alpha$ MCSP/ $\alpha$ E3 or  $\alpha$ TYRP1/ $\alpha$ E3 BiAb ( $\alpha$ MCSP or  $\alpha$ TYRP1, 1  $\mu$ g/mL) ( $n=3-6$ ). (F) Following 48 hours of co-culture, the CD3<sup>+</sup> T cell count per bead was assessed by flow cytometry. Counts were normalized to conditions without BiAb ( $n=3-6$ ). (G) The percentage lysis of melanoma cell lines A375, MV3, and antigen-negative, pancreatic cancer cell line PANC-1 by SAR T cells and either of the two BiAb was calculated using a flow cytometry-based readout after 48 hours of co-culture ( $n=3-6$ ). The values shown were normalized to the Unt T cells without BiAb control condition which was taken as 0% lysis. Statistical analysis was performed using the paired two-tailed Student's t-test. Statistics shown in (D) were calculated based on the 24-hour time points. Experiments show mean values  $\pm$  SD calculated from  $n$  independent biological replicates. BiAb, bispecific antibodies; E:T, effector to target ratio; IFN, interferon; IL, interleukin; MCSP, melanoma-associated chondroitin sulfate proteoglycan; PD-1, programmed cell death protein-1; SAR, synthetic agonistic receptor; TNF, tumor necrosis factor; TYRP1, tyrosinase-related protein 1; Unt, untransduced T cells.

observed with the  $\alpha$ TYRP1/ $\alpha$ E3 compared with the  $\alpha$ MCSP/ $\alpha$ E3 BiAb. It appears that the SAR T cell-BiAb platform is not easily impacted by alternative soluble sources of targeted proteins and requires

immobilization of these on the tumor cell surface, as previously described for other targets in one of our previous studies.<sup>20</sup> These findings align with the fact that the BiAb was designed only to bind a

## Open access

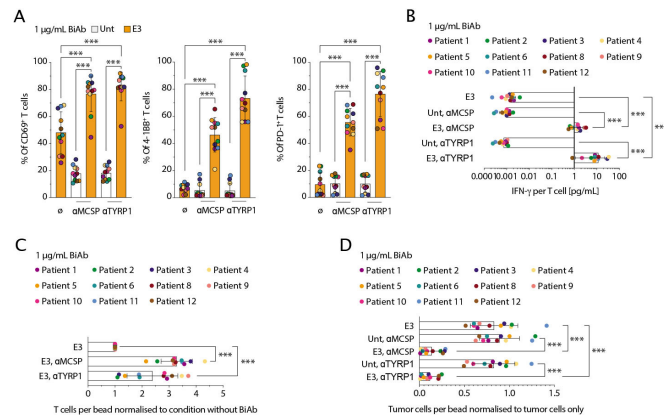


**Figure 3**  $\alpha$ MCSP/ $\alpha$ E3 and  $\alpha$ TYRP1/ $\alpha$ E3 BiAb activate SAR T cells to mediate specific cytotoxicity against patient-derived melanoma samples. (A) Human T cells were co-cultured with patient-derived melanoma samples (effector to target ratio 2:1) and either  $\alpha$ MCSP/ $\alpha$ E3 or  $\alpha$ TYRP1/ $\alpha$ E3 BiAb ( $\alpha$ MCSP or  $\alpha$ TYRP1, 1  $\mu$ g/mL) for 48 hours. The frequency of CD69, PD-1 and 4-1BB on T cells was assessed using flow cytometry. (B) Supernatant was taken and analyzed with ELISA for IFN- $\gamma$ . The values were normalized to the numbers of plated T cells. (C) The CD3<sup>+</sup> T cell count per bead was measured and normalized to conditions without BiAb. (D) The percentage lysis of the patient-derived melanoma samples by SAR T cells and either of the two BiAb was calculated based on flow cytometric readout after 48 hours of co-culture. The values shown were normalized to the tumor cells only control conditions. Statistical analysis was performed using the paired two-tailed Student's t-test. Experiments show mean values  $\pm$  SD. Each data point represents the mean of 2–3 biological replicates. BiAb, bispecific antibodies; IFN, interferon; MCSP, melanoma-associated chondroitin sulfate proteoglycan; PD-1, programmed cell death protein 1; SAR, synthetic agonistic receptor; TYRP1, tyrosinase-related protein 1; Unt, untransduced T cells.

membrane-proximal epitope that remains on the cell surface following cleavage.

#### Modular, selective and reversible activation of SAR T cells against melanoma

Melanomas are heterogeneous and stand to benefit from a modular and controllable therapeutic approach. Use of the melanoma differentiation antigens shared with other cells calls for control over these effects to antagonize potential unwanted excessive toxicities. While classic CAR T cell activity is maintained in the presence of a target antigen, SAR T cell activation is modular and controllable (figure 4C).<sup>19</sup> To demonstrate this in the melanoma setting, we used an in vitro stimulation assay to show how BiAb-dependent SAR activation enables greater control over T cell function (online supplemental figure 3C). As expected, following a 24-hour co-culture with MCSP<sup>+</sup> TYRP1<sup>+</sup> A375 tumor cells, SAR T cells could be activated in the presence of either of the two BiAb molecules (figure 4D). The same SAR T cells were then transferred to a new plate containing freshly plated A375 cells where they were co-cultured for a further 24 hours under different stimulation conditions. We found IFN- $\gamma$  expression was maintained when SAR T cells were redosed with either one of the two BiAb molecules (figure 4E). However, the concentration of IFN- $\gamma$  decreased in the absence of BiAb redosing, indicating the reversibility of SAR T cell activation. This was distinct from the lack of controllability seen with human anti-HER2 CAR T cells

when targeting HER2<sup>+</sup> A375 tumor cells, which continued to sense HER2<sup>+</sup> tumor cells<sup>33</sup> (figure 4E).

At the same time, sequential targeting of multiple antigen types would allow for more refined patient-specific tailoring of treatment and prevention of antigen-negative relapse. Through redosing with  $\alpha$ MCSP/ $\alpha$ E3 BiAb (first dosing with  $\alpha$ TYRP1/ $\alpha$ E3), the transferred SAR T cells remained activated, as shown by an elevated IFN- $\gamma$  concentration after 48 hours of co-culture (figure 4E).

By sequentially redirecting SAR T cells towards different melanoma targets with high efficiency, the modularity of the platform was demonstrated (figure 4D, E). Overall, this approach has the potential to target a variety of melanoma-associated antigens with a level of flexibility and controllability that is superior to that of CAR T cells.

#### SAR T cell-BiAb combination mediates effective tumor control in vivo

To probe the in vivo function of the SAR T cell-BiAb combination, we established and used both syngeneic and xenograft melanoma models. We engrafted the YUMM1.1 TYRP1-LUC-GFP murine melanoma cell line into C57BL/6 mice. The MV3 and A375 human melanoma cell lines and a sample from a patient with primary melanoma (sample 2) were implanted into NSG mice. In the syngeneic model, following adoptive transfer, SAR T cells were shown to persist well, where SAR<sup>+</sup> T cells could be tracked in the peripheral blood of mice at 7, 14 and 19 days post transfer (online supplemental figure 4A).

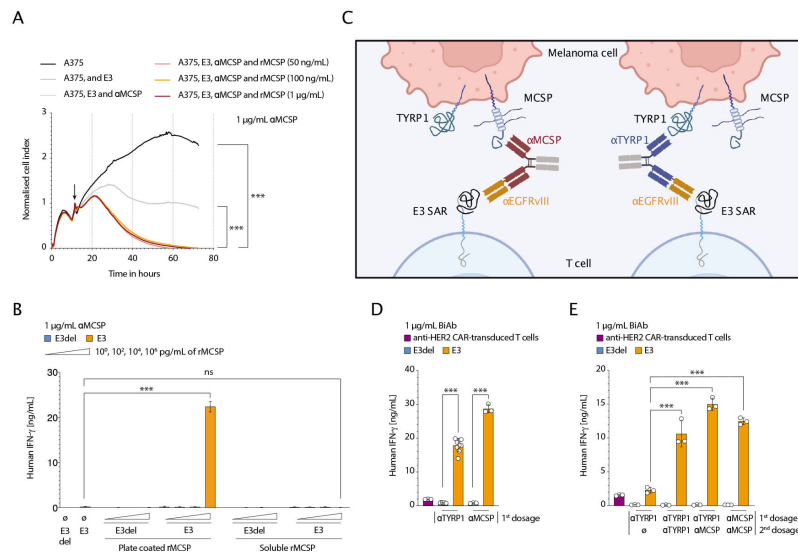


**Figure 4** Modular, selective and reversible activation of SAR T cells, irrespective of soluble forms of MCSP tumor antigen. (A) A375 melanoma cells were plated and co-cultured with human SAR T cells (E:T 2:1) and  $\alpha$ MCSP/ $\alpha$ E3 BiAb ( $\alpha$ MCSP, 1  $\mu$ g/mL). Different concentrations of soluble, recombinant MCSP (rMCSP) were added. The tumor cell lysis over time was assessed using xCELLigence (n=3). The cell index was normalized to the respective time point of T cell addition as indicated by an arrow. (B) Human SAR or E3del control T cells and  $\alpha$ MCSP/ $\alpha$ E3 BiAb (1  $\mu$ g/mL) were plated in wells either coated with different concentrations of rMCSP or where different concentrations of soluble rMCSP were added to the medium. After 48 hours the supernatant was taken and analyzed for IFN- $\gamma$  using ELISA (n=3). (C) Schematic overview of SAR-transduced T cells targeting TYRP1<sup>+</sup> MCSP<sup>+</sup> melanoma cells via an  $\alpha$ TYRP1/ $\alpha$ E3 or  $\alpha$ MCSP/ $\alpha$ E3 BiAb. (D and E) A modularity stress test was carried out using  $\alpha$ MCSP/ $\alpha$ E3 or  $\alpha$ TYRP1/ $\alpha$ E3 BiAb ( $\alpha$ MCSP or  $\alpha$ TYRP1, 1  $\mu$ g/mL). SAR or E3del control T cells were co-cultured with A375 tumor cells (E:T 2:1). HER2 CAR T cells were used as a control and co-cultured with HER2<sup>+</sup> A375 tumor cells (no BiAb was added). At assay start, co-cultures received either  $\alpha$ MCSP/ $\alpha$ E3 or  $\alpha$ TYRP1/ $\alpha$ E3 BiAb (first dosage). At 24 hours, the T cells were washed to remove residual BiAb and transferred to freshly plated A375 tumor cells. Co-cultures were then either redosed with the same BiAb, redosed with the BiAb against the other target, or not redosed after initial dosing (second dosage) and incubated for another 24 hours. At 24 (D) or 48 hours (E), supernatants were taken and ELISA for human IFN- $\gamma$  were performed (n=3). Analyses of differences between groups for (A) were performed using two-way analysis of variance with correction for multiple testing by the Bonferroni method. For statistical analysis of (B), (D) and (E), the unpaired two-tailed Student's t-test was used. Experiments show mean values  $\pm$  SD calculated from at least three biological replicates and are representative of three independent experiments. BiAb, bispecific antibodies; E:T, effector to target ratio; IFN, interferon; EGFRvIII, epidermal growth factor receptor variant III; MCSP, melanoma-associated chondroitin sulfate proteoglycan; SAR, synthetic agonistic receptor; TYRP1, tyrosinase-related protein 1; HER2, human epidermal growth factor receptor.

Mice that were treated with SAR T cells and repeated  $\alpha$ TYRP1/ $\alpha$ E3 BiAb dosing were able to clear the disease and achieved long-term survival (4 out of 10 mice with a complete response) (figure 5A,B, online supplemental figure 4B). In an endpoint experiment (19 days after T cell transfer) the lungs were harvested and analyzed using flow cytometry. SAR T cell and repeated  $\alpha$ TYRP1/ $\alpha$ E3 BiAb combination treatment led to a complete tumor clearance in four out of five mice based on a flow cytometry and IVIS readout (figure 5C and online supplemental figure 4C). In contrast, a single dose of the  $\alpha$ TYRP1/ $\alpha$ E3 BiAb in combination with SAR T cells only showed transient tumor control and did not lead to tumor clearance nor prolonged survival of the treated mice (online

supplemental figure 4D,E), indicating the necessity for redosing for maintained SAR activity in vivo. This necessity for redosing demonstrates a reversibility in SAR T cell activity on dosing cessation.

In order to analyze the antigen-specificity of the approach in vivo, mice bearing antigen-negative YUMM1.1 LUC-GFP tumors were treated with SAR T cell-BiAb combination. Treatment of antigen-negative tumors did not impact tumor growth and survival compared with control mice treated with SAR T cells or the vehicle solution (online supplemental figure 4F,G) underpinning the necessity of target antigen expression for the functionality of the approach. To further analyze the specificity of the  $\alpha$ TYRP1/ $\alpha$ E3 BiAb, TYRP1-expressing organs

## Open access

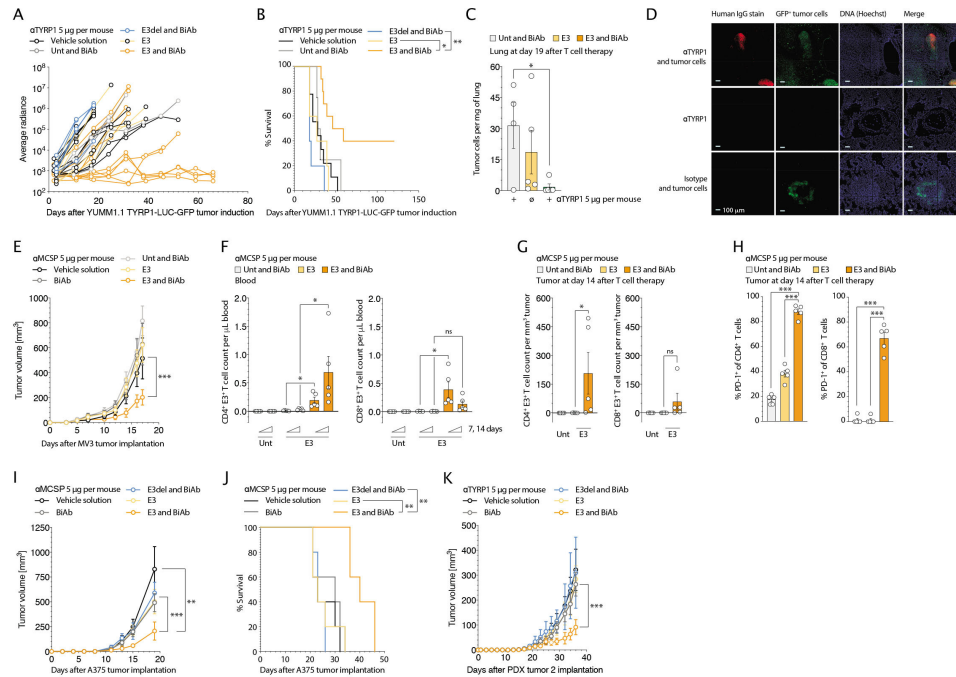


**Figure 5** Treatment with the SAR T cell-BiAb combination is effective in syngeneic and xenograft melanoma models and enhances survival in vivo. (A) C57BL/6 mice were injected i.p. weekly with an anti-CD20 depleting antibody (250  $\mu\text{g}/\text{injection}$ ) starting 7 days before tumor cell injection. Mice were inoculated intravenously with  $2 \times 10^6$  YUMM1.1 TYRP1-LUC-GFP tumor cells. Mice were treated with a single intravenous injection of T cells 4 days after tumor cell injection. Simultaneously, antibody treatment was given by i.p. injections of the  $\alpha\text{TYRP1}/\alpha\text{E3}$  BiAb ( $\alpha\text{TYRP1}$ , 5  $\mu\text{g}/\text{injection}$ ) which was redosed two times per week. In vivo luminescent signal imaging was performed one time per week using IVIS. Treatment groups were as follows: SAR T cells and  $\alpha\text{TYRP1}/\alpha\text{E3}$  BiAb ( $n=10$ ), E3del T cells and  $\alpha\text{TYRP1}/\alpha\text{E3}$  BiAb ( $n=5$ ), SAR T cells and  $\alpha\text{TYRP1}/\alpha\text{E3}$  BiAb ( $n=4$ ), and the vehicle solution ( $n=9$ ). (B) Percentage survival readout. (C) Tumor burden per mg of lung tissue 19 days after T cell therapy using a flow cytometry-based readout. Mice were treated with either SAR T cells and  $\alpha\text{TYRP1}/\alpha\text{E3}$  BiAb ( $n=5$ ), Unt T cells and  $\alpha\text{TYRP1}/\alpha\text{E3}$  BiAb ( $n=4$ ), SAR T cells only ( $n=5$ ), SAR T cells and  $\alpha\text{TYRP1}/\alpha\text{E3}$  BiAb ( $n=5$ ), Unt T cells and  $\alpha\text{TYRP1}/\alpha\text{E3}$  BiAb ( $n=4$ ), SAR T cells only ( $n=5$ ), BiAb only ( $n=5$ ), and the vehicle solution ( $n=5$ ). (D) Immunofluorescence imaging of the  $\alpha\text{TYRP1}/\alpha\text{E3}$  BiAb and tumor cell-derived GFP in lung tissue was carried out with anti-human IgG and anti-GFP stainings. Mice were injected intravenous either with  $2 \times 10^6$  YUMM1.1 TYRP1-LUC-GFP cells or with vehicle solution. After 20 days the mice were injected either with 5  $\mu\text{g}$   $\alpha\text{TYRP1}/\alpha\text{E3}$  BiAb, an isotype BiAb or with the vehicle solution. Following 48 hours of incubation, the lung, heart and skin were harvested, stained and imaged using ZellScannerONE. The groups were as follows: Tumor and  $\alpha\text{TYRP1}/\alpha\text{E3}$  BiAb ( $n=3$ ),  $\alpha\text{TYRP1}/\alpha\text{E3}$  BiAb only ( $n=2$ ), tumor and isotype BiAb ( $n=3$ ). (E) NSG mice were inoculated s.c. with  $1 \times 10^6$  MV3 tumor cells. Mice were treated with a single intravenous injection of T cells 5 days after tumor cell injection. Simultaneously, antibody treatment was given by i.p. injections of the  $\alpha\text{MCSP}/\alpha\text{E3}$  BiAb ( $\alpha\text{MCSP}$ , 5  $\mu\text{g}/\text{injection}$ ) which was redosed two times per week. Treatment groups were as follows: SAR T cells and the  $\alpha\text{MCSP}/\alpha\text{E3}$  BiAb ( $n=5$ ), Unt T cells and  $\alpha\text{MCSP}/\alpha\text{E3}$  BiAb ( $n=4$ ), SAR T cells only ( $n=5$ ), BiAb only ( $n=5$ ), and the vehicle solution ( $n=5$ ). (F) In an endpoint experiment, SAR T cell persistence in the blood and in the tumor was analyzed using a flow cytometry-based readout 14 days after T cell transfer. The mice were treated with either SAR T cells and  $\alpha\text{MCSP}/\alpha\text{E3}$  BiAb, Unt T cells and  $\alpha\text{MCSP}/\alpha\text{E3}$  BiAb or SAR T cells only (for each group  $n=5$ ). (G) SAR T cell infiltration per  $\text{mm}^3$  tumor. (H) Frequency of PD-1 expression on human  $\text{CD4}^+$  and  $\text{CD8}^+$  T cells in the tumor. (I) NSG mice were injected s.c. with  $0.2 \times 10^6$  A375 tumor cells. The mice were treated according to the experiment in (E) 11 days after tumor induction (for E3del and  $\alpha\text{MCSP}/\alpha\text{E3}$  BiAb:  $n=4$ , for other groups:  $n=5$ ). (J) Percentage survival readout. (K) NSG mice were injected s.c. with  $0.4 \times 10^6$  patient-derived melanoma cells (patient sample 2). The mice were treated according to the experiment in (E) 12 days after tumor induction with  $\alpha\text{TYRP1}/\alpha\text{E3}$  BiAb (for E3del and  $\alpha\text{TYRP1}/\alpha\text{E3}$  BiAb, and vehicle solution:  $n=4$ , for other groups:  $n=5$ ). For statistical analysis of survival data, the log-rank test was applied. Analyses of differences between groups for (E), (I) and (K) were performed using two-way analysis of variance with correction for multiple testing by the Bonferroni method. For statistical analysis of (C), (F), (G) and (H) the unpaired two-tailed Student's t-test was used. Experiments show mean values  $\pm$  SEM calculated from  $n$  biological replicates, one experiment for (B), (C), (F), (G), (H) and (K), and one representative of two independent experiments in (A), (E), (I) and (J). BiAb, bispecific antibodies; i.p., intraperitoneally; MCSP, melanoma-associated chondroitin sulfate proteoglycan; PD-1, programmed cell death protein 1; PDX, patient-derived xenograft; SAR, synthetic agonistic receptor; s.c., subcutaneously; TYRP1, tyrosinase-related protein 1; Unt, untransduced T cells.





(heart and skin) and tumor-bearing lungs were harvested 48 hours after BiAb injection and the BiAb was stained using immunofluorescence.  $\alpha$ TYRP1/ $\alpha$ E3 BiAb specifically bound to YUMM1.1 TYRP1-LUC-GFP tumor cells in the lung, while no comparable binding of the BiAb could be detected in other TYRP1-expressing tissues, indicative of its selectivity for melanoma cells (figure 5D and online supplemental figure 4H).

In the human MV3 xenograft model, a strong antitumoral response was again observed in the group treated with SAR T cells and  $\alpha$ MCSP/ $\alpha$ E3 BiAb compared with all controls (figure 5E). In this group, durable persistence of SAR-transduced T cells was seen by flow cytometry at 7 and 14 days post transfer (figure 5F). At the experimental endpoint, tumors were harvested and analyzed by flow cytometry. Higher numbers of tumor infiltrating SAR T cells were found in mice that received the SAR T cell-BiAb treatment combination (figure 5G), with CD4<sup>+</sup> T cells persisting better than CD8<sup>+</sup> T cells in contrast to any of the controls. Phenotyping of transferred T cells at the experimental endpoint revealed maintenance of the effector memory phenotype they had prior to adoptive transfer (as determined by CD45RO and CCR7 expression) (online supplemental figure 4I). Furthermore, PD-1 expression was increased in SAR T cell-BiAb treated mice compared with SAR T cell only or Unt T cells and BiAb control conditions (figure 5H). Similar to the MV3 model, the A375 xenograft model, demonstrated comparable sensitivity to SAR T cells and BiAb resulting in improved tumor control and prolonged survival (figure 5I and J). Additionally, in a patient-derived xenograft model, treatment with the  $\alpha$ TYRP1/ $\alpha$ E3 BiAb and SAR T cells resulted in reduced tumor growth in mice receiving SAR T cell and BiAb combination (figure 5K).

## DISCUSSION

We could demonstrate that MCSP and TYRP1 expression remains differentially expressed on primary melanoma samples of patients pre-treatment or post-treatment. We reasoned that their targeting using a modular and controllable T cell therapy platform, in the form of the SAR T cell-BiAb approach, could be an effective strategy and probed this hypothesis in vitro and in vivo. In order to demonstrate the translational relevance of the approach, we selected a series of relevant in vitro and in vivo models. We used immunocompetent syngeneic mouse models to better control for the immune system's impact on the treatment approach and primary human melanoma models and cell lines to test the efficacy of the approach in treated as well as untreated melanoma models.

Our results demonstrate the efficacy of the approach in several in vitro and in vivo models. SAR-engineered T cells could be redirected towards MCSP-expressing and TYRP1-expressing melanoma cells in the presence of the  $\alpha$ MCSP/ $\alpha$ E3 or  $\alpha$ TYRP1/ $\alpha$ E3 BiAb. SAR T cells efficiently targeted and lysed MCSP-expressing and TYRP1-expressing melanoma cell lines. Targeted specificity and

killing capacity were retained when targeting patient-derived melanomas, using in vitro co-cultures, as well as several syngeneic and xenograft in vivo mouse models.

The potent cytolytic effects of the platform in the syngeneic model resulted in 4 out of 10 mice completely curing the tumor in the observed period. We also observed strong treatment effects in xenograft models which are comparable to results shown in preclinical approaches using melanoma-specific CAR T cells.<sup>33–36</sup> In these studies, HER2 and GD2 were the targeted antigens. HER2 CAR T cells have been shown to pose a risk of lethal toxicity, with cytokine release syndrome from on-target off-tumor recognition of HER2.<sup>37</sup> While efforts are being made to create safer HER2-targeting CAR T cells,<sup>38</sup> we demonstrate herein that the SAR T cell-BiAb approach, with its controllable and reversible facets, can be a ready-made solution for lowering and controlling toxicity.<sup>39</sup>

MCSP is differentially expressed on the surface of over 85% of melanomas.<sup>40</sup> It provides tumorigenic signals to melanoma cells that stimulate growth, motility, and tissue invasion.<sup>41–44</sup> It was therefore unsurprising to discover its expression was retained on patient with primary melanoma samples irrespective of the treatment history. Furthermore, we could show expression on human melanoma cell lines on transcript and protein level which was in line with the functional readouts. MCSP has been described as potential target for CAR T cell therapy in melanoma and glioblastoma.<sup>39, 45</sup> TYRP1, a transmembrane glycoprotein naturally involved in melanin production,<sup>46</sup> has been identified as an antigen highly expressed in melanoma and stably expressed during disease progression.<sup>47</sup> TYRP1 expression could also be observed on primary patient samples and human melanoma cell lines. Discrepancies between transcript and protein expression could be partly caused by internalization of TYRP1.<sup>48, 49</sup> The influence of target antigen internalization on treatment outcome must be investigated in further studies. Nonetheless, potent treatment effects were shown when targeting TYRP1<sup>+</sup> cells with the SAR-BiAb approach in syngeneic and human xenograft models. In a phase I study an anti-TYRP1 monoclonal antibody was administered in patients with relapsed or refractory melanoma, where no serious adverse events were observed, indicating the potential safety of targeting.<sup>50</sup>

With low off-tumor expression detected in some healthy tissues for both targets, it was necessary to design antibodies that would bind MCSP and TYRP1 with sufficient avidity, while minimizing the potential for off-tumor toxicity. Melanoma-specific BiAb were designed with two binding arms for the tumor target. This increased the binding avidity of the BiAb to melanoma cells showing higher target expression compared with healthy cells. Thus, the binding strength could be increased while minimizing the risk of on-target off-tumor toxicity that is often associated with increased binding affinities. Similarly, the risk of targeting endogenous T cells is limited since no expression of the target antigens was observed on human T cells. The modular facets of the SAR platform were

## Open access



previously demonstrated in an acute myeloid leukemia xenograft model,<sup>19</sup> and again substantiated herein. The simultaneous, or in the event of antigen loss, sequential targeting of multiple tumor antigens has proven to be an effective approach in the treatment of B-cell malignancies,<sup>51</sup> and is further evidenced by several approaches attempting to render CAR T cells more adaptable.<sup>52</sup> We thereby reason, that a platform allowing change or simultaneous targeting of multiple antigens, with one cellular construct comes with clear advantages of feasibility and flexibility.

MCSP levels have been shown to be elevated in the sera of patients with advanced melanoma.<sup>32</sup> We experimentally tested the potential impact of soluble MCSP on the conditional specificity of the SAR T cell-BiAb approach. At physiological levels, free-MCSP did not activate SAR T cells in the presence of BiAb. Free targeted protein in the tumor microenvironment must be considered as a potential hindrance to the efficacy of the SAR T cell-BiAb combination, as well as other adoptive T cell therapies. This could become especially problematic in targeting cleavable proteins, such as MCSP, and the targeting of membrane-associated forms of proteins could maximize efficiency in this regard.<sup>32</sup> In fact, shed glypican-3 was shown to induce a blocking effect on CAR T cells targeting glypican-3-expressing hepatocellular carcinoma.<sup>53</sup> Probably because of the peculiarities of the SAR T cell-BiAb platform, we have not found such mechanism to impact efficacy or activity.

Anti-melanoma CAR T cell therapy has shown limited efficacy in the clinic thus far.<sup>54</sup> Results from the CARPETS phase I trial (NCT02107963) showed limited persistence of GD2 CAR T cells in patients with metastatic melanoma, with CAR transgenes only detected at low levels in patient peripheral blood after 4 months. T cell exhaustion and activation induced cell death have been shown to hinder the persistence and function of adoptively transferred T cells.<sup>55,56</sup> Recent work from Weber and colleagues showed that transient rest, using enforced CAR molecule downregulation via a drug-regulatable system, could restore CAR T cell functionality.<sup>57</sup> An advantage of the SAR T cell-BiAb system is that it is an adaptor platform inherently regulatable, via its BiAb facet. The reversibility of SAR T cell activation was demonstrated with the cessation of BiAb dosing in vitro and in vivo. This makes it very straightforward to incorporate a transient rest period simply by modifying the dosing schedule of the BiAb, thus recapitulating the previously mentioned regulatable system. Recent work by Philipp and colleagues also showed that transient BiAb dosing reduced T cell exhaustion and improved CD3<sup>+</sup> T cell engager efficacy.<sup>58</sup> The BiAb molecules we used have an IgG format, which extends their half-life in comparison to Fc-deficient BiAb.<sup>59</sup> Engineering the half-life of BiAb to offer greater flexibility towards patient needs would be a straightforward approach, that could also be beneficial. Importantly, we could previously demonstrate the use of different antibody formats and half-lives to activate and redirect SAR T cells,<sup>19,20</sup> opening the door to

such optimizations. Inadequate T cell infiltration into the tumor and a suppressive milieu therein are the subject of ongoing investigation that could broadly improve the therapeutic success of adoptive T cell therapies in solid tumors,<sup>5</sup> including melanoma. Equipping SAR T cells with relevant chemokine receptors while shielding them from local immune suppression could further improve treatment efficacy and warrant further investigation.<sup>24,26</sup>

Harnessing the apparent advantages of the SAR T cell-BiAb platform for melanoma therapy has yielded very promising results in our preclinical models. With evident potential for improved clinical benefit, we believe these findings warrant further characterization in more advanced preclinical models and ultimately clinical studies.

## Author affiliations

- <sup>1</sup>Department of Medicine IV, Division of Clinical Pharmacology, Klinikum der Universität München, Munich, Germany  
<sup>2</sup>Roche Innovation Center Zurich, Roche Pharma Research & Early Development, Schlieren, Switzerland  
<sup>3</sup>Department of Medicine III, Klinikum der Universität München, Munich, Germany  
<sup>4</sup>German Cancer Consortium (DKTK), Partner Site Munich, Munich, Germany  
<sup>5</sup>Institute of AI for Health, Helmholtz Center Munich, German Research Center for Environmental Health, Neuherberg, Germany  
<sup>6</sup>Institute of Computational Biology, Helmholtz Center Munich, German Research Center for Environmental Health, Neuherberg, Germany  
<sup>7</sup>School of Life Sciences Weihenstephan, Technical University of Munich, Munich, Freising, Germany  
<sup>8</sup>Division of Pediatric Nephrology, Department of Pediatrics, Dr. v. Hauner'sches Kinderspital, Klinikum der Universität München, Munich, Germany  
<sup>9</sup>Department of Dermatology, University Hospital Zurich, Schlieren, Switzerland  
<sup>10</sup>Department of Dermatology, Universitätsklinikum Erlangen, Friedrich-Alexander-Universität Erlangen-Nürnberg (FAU), Erlangen, Germany  
<sup>11</sup>Deutsches Zentrum Immuntherapie (DZI), Friedrich-Alexander-Universität Erlangen-Nürnberg, Erlangen, Germany  
<sup>12</sup>Einheit für Klinische Pharmakologie (EKLiP), Helmholtz Center Munich, German Research Center for Environmental Health, Neuherberg, Germany

**Twitter** Mohamed-Reda Benmebarek @MRbenmebarek, Julius Keyl @JuliusKeyl, Bruno L. Cadihla @bcadihla and Sophia Stock @SophiaStock\_

**Acknowledgements** The authors acknowledge the Core Facility Flow Cytometry of the University Hospital, LMU Munich, for assistance with the generation of flow cytometry data. Figure 4C was created with BioRender.com. SS was supported by the Else Kröner-Fresenius Clinician Scientist Program Cancer Immunotherapy, the Munich Clinician Scientist Program (MCSP) and the DKTK School of Oncology. SM, JJ, MS, A-KK, TL and RK were supported by a grant from the Förderprogramm für Forschung und Lehre (FöFoLe) of the Ludwig Maximilian University (LMU) of Munich.

**Contributors** Conceptualization: M-RB, FM, CK and SK. Methodology: FM, M-RB, DB, PJM, JJ, MT, JK, LM, CK and MS. Investigation: M-RB, FM, HO and MT. Validation: HO, MS, A-KK, TL, SS, SM and RG. Writing—original draft: M-RB and FM. Writing—review and editing: M-RB, FM, BLC, JK, MG, MS, MT, MVH, SE, CK and SK. Funding acquisition: SE and SK. Resources: DB, AG, CM, SR, MPL, MVH, SE, CK and SK. Supervision: RK, CM and SK. Guarantor: M-RB and FM.

**Funding** The in vivo imaging device was funded by the Deutsche Forschungsgemeinschaft (DFG, German Research Foundation) – INST 409/231-1. MT is funded by the Volkswagen Foundation (project OntoTime). CM has received funding from the European Research Council (ERC) under the European Union's Horizon 2020 research and innovation programme (grant agreement number 866411). This study was supported by the Marie-Sklodowska-Curie Program Training Network for Optimizing Adoptive T Cell Therapy of Cancer funded by the H2020 Program of the European Union (Grant 955575, to SK); by the Hector Foundation (to SK); by the International Doctoral Program i-Target: Immunotargeting of Cancer funded by the Elite Network of Bavaria (to SK and SE); by Melanoma Research Alliance Grants 409510 (to SK); by the Else Kröner-Fresenius-Stiftung (to SK and RK); by the German Cancer Aid (to SK); by the Ernst-Jung-Stiftung (to



SK); by the LMU Munich's Institutional Strategy LMUexcellent within the framework of the German Excellence Initiative (to SE and SK); by the Go-Bio initiative (to SK); by the m4 Award of the Bavarian Ministry of Economical Affairs, by the Bundesministerium für Bildung und Forschung (SK); by the European Research Council Grant 756017, ARMOR-T (to SK) and the ERC proof-of-concept Grant 101100460 (to SK); by the Deutsche Forschungsgemeinschaft (DFG, German Research Foundation) (KO5055-2-1 and 510821390 to SK); by the SFB-TRR 338/1 2021-452881907 (to SK); by the Wilhelm-Sander-Stiftung, by the Fritz-Bender Foundation (to SK) and by the Deutsche José-Carreras Leukämie Stiftung (to SK).

**Competing interests** Parts of this work were performed in partial fulfillment of the requirements of the Munich Medical Research School for doctoral graduation of FM. SK has received honoraria from TCR2 Miltenyi Biotec, Novartis, BMS and GSK. SK and SE are inventors of several patents in the field of immuno-oncology. SK and SE received license fees from TCR2 and Carina Biotech. SK and SE received research support from TCR2, Arcus Bioscience, Plectonic GmbH and Tabby Therapeutics for work unrelated to the manuscript. MG and CK declare employment, patents and stock ownership with Roche.

**Patient consent for publication** Not applicable.

**Ethics approval** Written informed consent was obtained from all patients after approval by the local committees of the Klinikum der Universität München and the Cantonal Ethics Committee of Zürich.

**Provenance and peer review** Not commissioned; externally peer reviewed.

**Data availability statement** Data are available upon reasonable request. Data supporting this manuscript is attached. Raw data and reagents will be made available upon reasonable request to the authors.

**Supplemental material** This content has been supplied by the author(s). It has not been vetted by BMJ Publishing Group Limited (BMJ) and may not have been peer-reviewed. Any opinions or recommendations discussed are solely those of the author(s) and are not endorsed by BMJ. BMJ disclaims all liability and responsibility arising from any reliance placed on the content. Where the content includes any translated material, BMJ does not warrant the accuracy and reliability of the translations (including but not limited to local regulations, clinical guidelines, terminology, drug names and drug dosages), and is not responsible for any error and/or omissions arising from translation and adaptation or otherwise.

**Open access** This is an open access article distributed in accordance with the Creative Commons Attribution Non Commercial (CC BY-NC 4.0) license, which permits others to distribute, remix, adapt, build upon this work non-commercially, and license their derivative works on different terms, provided the original work is properly cited, appropriate credit is given, any changes made indicated, and the use is non-commercial. See <http://creativecommons.org/licenses/by-nc/4.0/>.

#### ORCID iDs

Florian Märkl <http://orcid.org/0000-0003-4285-0380>  
 Mohamed-Reda Benmebarek <http://orcid.org/0000-0002-1201-7067>  
 Sophia Stock <http://orcid.org/0000-0002-5072-5013>  
 Matthias Seifert <http://orcid.org/0000-0002-6581-6196>  
 Theo Lorenzini <http://orcid.org/0000-0003-3377-032X>  
 Ruth Grünmeier <http://orcid.org/0000-0002-9044-3600>  
 Moritz Thomas <http://orcid.org/0000-0002-8422-2414>  
 Stefan Endres <http://orcid.org/0000-0002-4703-537X>  
 Christian Klein <http://orcid.org/0000-0001-7594-7280>  
 Sebastian Kobold <http://orcid.org/0000-0002-5612-4673>

#### REFERENCES

- Hodis E, Watson IR, Kryukov GV, et al. A landscape of driver mutations in melanoma. *Cell* 2012;150:251-63.
- Cohen CJ, Gartner JJ, Horovitz-Fried M, et al. Isolation of neoantigen-specific T cells from tumor and peripheral lymphocytes. *J Clin Invest* 2015;125:3981-91.
- Blank CU, Rozeman EA, Fanchi LF, et al. Neoadjuvant versus adjuvant ipilimumab plus nivolumab in macroscopic stage III melanoma. *Nat Med* 2018;24:1655-61. 10.1038/s41591-018-0198-0
- Larkin J, Chiarion-Sileni V, Gonzalez R, et al. Five-Year survival with combined nivolumab and ipilimumab in advanced melanoma. *N Engl J Med* 2019;381:1535-46.
- Lesch S, Benmebarek M-R, Cadilha BL, et al. Determinants of response and resistance to CAR T cell therapy. *Semin Cancer Biol* 2020;65:80-90.
- Maibach F, Sadozai H, Seyed Jafari SM, et al. Tumor-Infiltrating lymphocytes and their prognostic value in cutaneous melanoma. *Front Immunol* 2020;11:2105.
- Rosenberg SA, Packard BS, Aebbersold PM, et al. Use of tumor-infiltrating lymphocytes and interleukin-2 in the immunotherapy of patients with metastatic melanoma. *N Engl J Med* 1988;319:1676-80.
- Hont AB, Cruz GR, Ulrey R, et al. Immunotherapy of relapsed and refractory solid tumors with ex vivo expanded multi-tumor associated antigen specific cytotoxic T lymphocytes: a phase I study. *J Clin Oncol* 2019;37:2349-59.
- Chandran SS, Klebanoff CA. T cell receptor-based cancer immunotherapy: emerging efficacy and pathways of resistance. *Immunity* 2019;290:127-47.
- Borch TH, Andersen R, Ellebaek E, et al. Future role for adoptive T-cell therapy in checkpoint inhibitor-resistant metastatic melanoma. *J Immunother Cancer* 2020;8:e000668.
- Sim GC, Chacon J, Haymaker C, et al. Tumor-infiltrating lymphocyte therapy for melanoma: rationale and issues for further clinical development. *BioDrugs* 2014;28:421-37.
- June CH, O'Connor RS, Kawalekar OU, et al. Car T cell immunotherapy for human cancer. *Science* 2018;359:1361-5.
- Neelapu SS, Locke FL, Bartlett NL, et al. Axicabtagene ciloleucel CAR T-cell therapy in refractory large B-cell lymphoma. *N Engl J Med* 2017;377:2531-44.
- Hill JA, Giralt S, Torgerson TR, et al. CAR-T and a side order of IgG, to go? -immunoglobulin replacement in patients receiving CAR-T cell therapy. *Blood Rev* 2019;38:S0268-960X(19)30067-0.
- Beatty GL, O'Hara MH, Lacey SF, et al. Activity of mesothelin-specific chimeric antigen receptor T cells against pancreatic carcinoma metastases in a phase 1 trial. *Gastroenterology* 2018;155:29-32.
- Khong HT, Wang QJ, Rosenberg SA. Identification of multiple antigens recognized by tumor-infiltrating lymphocytes from a single patient: tumor escape by antigen loss and loss of MHC expression. *J Immunother* 2004;27:184-90.
- Rataj F, Jacobi SJ, Stoiber S, et al. High-Affinity CD16-polymorphism and fc-engineered antibodies enable activity of CD16-chimeric antigen receptor-modified T cells for cancer therapy. *Br J Cancer* 2019;120:79-87.
- Stock S, Benmebarek M-R, Kluever A-K, et al. Chimeric antigen receptor T cells engineered to recognize the P329G-mutated Fc part of effector-silenced tumor antigen-targeting human IgG1 antibodies enable modular targeting of solid tumors. *J Immunother Cancer* 2022;10:e005054.
- Benmebarek M-R, Cadilha BL, Herrmann M, et al. A modular and controllable T cell therapy platform for acute myeloid leukemia. *Leukemia* 2021;35:2243-57.
- Karches CH, Benmebarek M-R, Schmidbauer ML, et al. Bispecific antibodies enable synthetic agonistic receptor-transduced T cells for tumor immunotherapy. *Clin Cancer Res* 2019;25:5890-900.
- Schaefer W, Regula JT, Böhner M, et al. Immunoglobulin domain crossover as a generic approach for the production of bispecific IgG antibodies. *Proc Natl Acad Sci U S A* 2011;108:11187-92.
- Surovka M, Schaefer W, Klein C. Ten years in the making: application of crossmab technology for the development of therapeutic bispecific antibodies and antibody fusion proteins. *MAbs* 2021;13:1967714.
- Ghani K, Wang X, de Campos-Lima PO, et al. Efficient human hematopoietic cell transduction using RD114- and GALV-pseudotyped retroviral vectors produced in suspension and serum-free media. *Hum Gene Ther* 2009;20:966-74.
- Lesch S, Blumenberg V, Stoiber S, et al. T cells armed with C-X-C chemokine receptor type 6 enhance adoptive cell therapy for pancreatic tumours. *Nat Biomed Eng* 2021;5:1246-60.
- Carter P, Presta L, Gorman CM, et al. Humanization of an anti-p185HER2 antibody for human cancer therapy. *Proc Natl Acad Sci U S A* 1992;89:4285-9.
- Cadilha BL, Benmebarek M-R, Dorman K, et al. Combined tumor-directed recruitment and protection from immune suppression enable CAR T cell efficacy in solid tumors. *Sci Adv* 2021;7:eabi5781.
- Kobold S, Grassmann S, Chaloupka M, et al. Impact of a new fusion receptor on PD-1-mediated immunosuppression in adoptive T cell therapy. *J Natl Cancer Inst* 2015;107:djv146.
- Journe F, Id Boufker H, Van Kempen L, et al. Tyrp1 mRNA expression in melanoma metastases correlates with clinical outcome. *Br J Cancer* 2011;105:1726-32.
- Erfurt C, Sun Z, Haendle I, et al. Tumor-reactive CD4+ T cell responses to the melanoma-associated chondroitin sulphate proteoglycan in melanoma patients and healthy individuals in the absence of autoimmunity. *J Immunol* 2007;178:7703-9.

## Open access



- 30 Pérez-Lorenzo R, Erjavec SO, Christiano AM, et al. Improved therapeutic efficacy of unmodified anti-tumor antibodies by immune checkpoint blockade and kinase targeted therapy in mouse models of melanoma. *Oncotarget* 2021;12:66–80.
- 31 Tirosh I, Izar B, Prakadan SM, et al. Dissecting the multicellular ecosystem of metastatic melanoma by single-cell RNA-seq. *Science* 2016;352:189–96.
- 32 Vergilis IJ, Szarek M, Ferrone S, et al. Presence and prognostic significance of melanoma-associated antigens CYT-MAA and HMW-MAA in serum of patients with melanoma. *J Invest Dermatol* 2005;125:526–31.
- 33 Forsberg EMV, Lindberg MF, Jespersen H, et al. Her2 CAR-T cells eradicate uveal melanoma and T-cell therapy-resistant human melanoma in IL2 transgenic NOD/SCID IL2 receptor knockout mice. *Cancer Res* 2019;79:899–904.
- 34 Yu J, Wu X, Yan J, et al. Anti-GD2/4-1BB chimeric antigen receptor T cell therapy for the treatment of Chinese melanoma patients. *J Hematol Oncol* 2018;11:1.
- 35 Beard RE, Zheng Z, Lagisetty KH, et al. Multiple chimeric antigen receptors successfully target chondroitin sulfate proteoglycan 4 in several different cancer histologies and cancer stem cells. *J Immunother Cancer* 2014;2:25.
- 36 Geldres C, Savoldo B, Hoyos V, et al. T lymphocytes redirected against the chondroitin sulfate proteoglycan-4 control the growth of multiple solid tumors both in vitro and in vivo. *Clin Cancer Res* 2014;20:962–71.
- 37 Morgan RA, Yang JC, Kitano M, et al. Case report of a serious adverse event following the administration of T cells transduced with a chimeric antigen receptor recognizing ErbB2. *Molecular Therapy* 2010;18:843–51.
- 38 Liu X, Zhang N, Shi H. Driving better and safer HER2-specific cars for cancer therapy. *Oncotarget* 2017;8:62730–41.
- 39 Wang Y, Geldres C, Ferrone S, et al. Chondroitin sulfate proteoglycan 4 as a target for chimeric antigen receptor-based T-cell immunotherapy of solid tumors. *Expert Opin Ther Targets* 2015;19:1339–50.
- 40 Campoli MR, Chang C-C, Kageshita T, et al. Human high molecular weight-melanoma-associated antigen (HMW-MAA): a melanoma cell surface chondroitin sulfate proteoglycan (MSCP) with biological and clinical significance. *Crit Rev Immunol* 2004;24:267–96.
- 41 Eisenmann KM, McCarthy JB, Simpson MA, et al. Melanoma chondroitin sulphate proteoglycan regulates cell spreading through Cdc42, Ack-1 and p130Cas. *Nat Cell Biol* 1999;1:507–13.
- 42 Yang X, Kovalenko OV, Tang W, et al. Palmitoylation supports assembly and function of integrin-tetraspanin complexes. *J Cell Biol* 2004;167:1231–40.
- 43 Yang J, Price MA, Li GY, et al. Melanoma proteoglycan modifies gene expression to stimulate tumor cell motility, growth, and epithelial-to-mesenchymal transition. *Cancer Res* 2009;69:7538–47.
- 44 Iida J, Wilhelmson KL, Ng J, et al. Cell surface chondroitin sulfate glycosaminoglycan in melanoma: role in the activation of pro-MMP-2 (pro-gelatinase A). *Biochem J* 2007;403:553–63.
- 45 Pellegatta S, Savoldo B, Di Ianni N, et al. Constitutive and TNF $\alpha$ -inducible expression of chondroitin sulfate proteoglycan 4 in glioblastoma and neurospheres: implications for CAR-T cell therapy. *Sci Transl Med* 2018;10:430.
- 46 Ghanem G, Fabrice J. Tyrosinase related protein 1 (TYRP1/gp75) in human cutaneous melanoma. *Mol Oncol* 2011;5:150–5.
- 47 Asgarov K, Bailand J, Tirele C, et al. A new anti-mesothelin antibody targets selectively the membrane-associated form. *MAbs* 2017;9:567–77.
- 48 Bulterma JJ, Boyle JA, Malenke PB, et al. Myosin Vc interacts with Rab32 and Rab38 proteins and works in the biogenesis and secretion of melanosomes. *J Biol Chem* 2014;289:33513–28.
- 49 Truschel ST, Simoes S, Setty SRG, et al. Escrt-1 function is required for TYRP1 transport from early endosomes to the melanosome limiting membrane. *Traffic* 2009;10:1318–36.
- 50 Khamil DN, Postow MA, Ibrahim N, et al. An open-label, dose-escalation phase I study of Anti-TYRP1 monoclonal antibody IMC-20D7S for patients with relapsed or refractory melanoma. *Clin Cancer Res* 2016;22:5204–10.
- 51 Spiegel JY, Patel S, Muffly L, et al. CAR T cells with dual targeting of CD19 and CD22 in adult patients with recurrent or refractory B cell malignancies: a phase 1 trial. *Nat Med* 2021;27:1419–31.
- 52 Darowski D, Kobold S, Jost C, et al. Combining the best of two worlds: highly flexible chimeric antigen receptor adaptor molecules (CAR-adaptors) for the recruitment of chimeric antigen receptor T cells. *MAbs* 2019;11:621–31.
- 53 Sun L, Gao F, Gao Z, et al. Shed antigen-induced blocking effect on CAR-T cells targeting glypican-3 in hepatocellular carcinoma. *J Immunother Cancer* 2021;9:e001875.
- 54 Gargett T, Yu W, Dotti G, et al. GD2-specific CAR T cells undergo potent activation and deletion following antigen encounter but can be protected from activation-induced cell death by PD-1 blockade. *Mol Ther* 2016;24:1135–49.
- 55 Long AH, Haso WM, Shern JF, et al. 4-1Bb costimulation ameliorates T cell exhaustion induced by tonic signaling of chimeric antigen receptors. *Nat Med* 2015;21:581–90.
- 56 Stoiber S, Cadilha BL, Benmebarek M-R, et al. Limitations in the design of chimeric antigen receptors for cancer therapy. *Cells* 2019;8:472.
- 57 Weber EW, Parker KR, Sotillo E, et al. Transient rest restores functionality in exhausted CAR-T cells through epigenetic remodeling. *Science* 2021;372:6537.
- 58 Philipp N, Kazerani M, Nicholls A, et al. T-cell exhaustion induced by continuous bispecific molecule exposure is ameliorated by treatment-free intervals. *Blood* 2022;140:1104–18.
- 59 Labrijn AF, Janmaat ML, Reichert JM, et al. Bispecific antibodies: a mechanistic review of the pipeline. *Nat Rev Drug Discov* 2019;18:585–608.

## 4. Paper II

The original article “Combined tumor-directed recruitment and protection from immune suppression enable CAR T cell efficacy in solid tumors” (doi: 10.1126/sciadv.abi5781) and the supplementary material can be found using the following link: <http://advances.sciencemag.org/cgi/content/full/7/24/eabi5781/DC1>

SCIENCE ADVANCES | RESEARCH ARTICLE

CANCER

### Combined tumor-directed recruitment and protection from immune suppression enable CAR T cell efficacy in solid tumors

Bruno L. Cadiilha<sup>1,\*†</sup>, Mohamed-Reda Benmebarek<sup>1†</sup>, Klara Dorman<sup>1,2</sup>, Arman Oner<sup>1</sup>, Theo Lorenzini<sup>1</sup>, Hannah Obeck<sup>1</sup>, Mira Vänttinen<sup>1</sup>, Mauro Di Pilato<sup>3,4</sup>, Jasper N. Pruessmann<sup>3,5</sup>, Stefan Stoiber<sup>1</sup>, Duc Huynh<sup>1</sup>, Florian Märkl<sup>1</sup>, Matthias Seifert<sup>1</sup>, Katrin Manske<sup>1</sup>, Javier Suarez-Gosalvez<sup>1</sup>, Yi Zeng<sup>1</sup>, Stefanie Lesch<sup>1</sup>, Clara H. Karches<sup>1</sup>, Constanze Heise<sup>1</sup>, Adrian Gottschlich<sup>1</sup>, Moritz Thomas<sup>6,7</sup>, Carsten Marr<sup>6</sup>, Jin Zhang<sup>1</sup>, Dharmendra Pandey<sup>1</sup>, Tobias Feuchtinger<sup>8,9</sup>, Marion Subklewe<sup>2</sup>, Thorsten R. Mempel<sup>3</sup>, Stefan Endres<sup>1</sup>, Sebastian Kobold<sup>1,10,11\*</sup>

CAR T cell therapy remains ineffective in solid tumors, due largely to poor infiltration and T cell suppression at the tumor site. T regulatory (T<sub>reg</sub>) cells suppress the immune response via inhibitory factors such as transforming growth factor-β (TGF-β). T<sub>reg</sub> cells expressing the C-C chemokine receptor 8 (CCR8) have been associated with poor prognosis in solid tumors. We postulated that CCR8 could be exploited to redirect effector T cells to the tumor site while a dominant-negative TGF-β receptor 2 (DNR) can simultaneously shield them from TGF-β. We identified that CCL1 from activated T cells potentiates a feedback loop for CCR8<sup>+</sup> T cell recruitment to the tumor site. This sustained and improved infiltration of engineered T cells synergized with TGF-β shielding for improved therapeutic efficacy. Our results demonstrate that addition of CCR8 and DNR into CAR T cells can render them effective in solid tumors.

#### INTRODUCTION

The implementation of immune-checkpoint blockade into the standard of care for a growing number of malignant diseases has established the role of T cells in therapeutically inducible antitumor immunity (1, 2). Likewise, the therapeutic use of T cells, also termed adoptive T cell therapy (ACT), has been developed. This includes the ex vivo expansion and reinfusion of tumor-infiltrating lymphocytes or engineering patient T cells to express a cancer antigen-specific T cell receptor (TCR) bearing improved tumor-targeting capacities (3). Alternatively, patient T cells can be engineered to express a chimeric antigen receptor (CAR), which combines the specificity of an antibody with T cell-activating and costimulatory domains that acts as a fully synthetic receptor triggering a full-blown T cell response (4). CAR T cells have shown unparalleled efficacy in refractory patients with hematological malignancies such as acute lymphatic leukemia or diffuse large B cell lymphoma (5, 6). Nevertheless, a large proportion of patients acquire resistance during the course of their therapy due to target loss or mutation (7). In the more frequent solid cancer

indications, efficacy of CAR T cells remains to be demonstrated, despite the strong proof-of-concept studies in xenograft models (8). These immunocompromised models should be complemented with immune-competent syngeneic models that can demonstrate the immune system's impact on CAR T cells (9, 10). However, we and others have repeatedly observed that tumor control by TCR-specific T cells and also CAR T cells, despite appropriate target selection, is limited or absent in syngeneic models (11–13). This reflects the growing body of clinical observations with CAR T cells (7) and demonstrates the need for alternative methods to improve the activity of CAR T cells against solid tumors.

Major unaddressed obstacles to CAR T cell efficacy in solid tumors are poor infiltration at the tumor site and T cell suppression (14). Clinically relevant CAR T cell efficacy is unlikely to occur unless both aspects are tackled simultaneously. T regulatory (T<sub>reg</sub>) cells are key drivers of immunosuppression in solid tumors (15) largely via release of transforming growth factor-β (TGF-β) (16). More recently, another mechanism of immunosuppression by T<sub>reg</sub> cells has been identified and involves the ligand CCL1 binding to its receptor C-C chemokine receptor 8 (CCR8) (16). Accumulation of these CCR8<sup>+</sup> T<sub>reg</sub> cells is associated with poor prognosis in breast cancer (15, 16). So far, this chemokine axis has not been exploited therapeutically. Since tumors of different origins actively recruit T<sub>reg</sub> cells through the CCL1-CCR8 axis, we reasoned that this axis could be therapeutically exploited by arming effector T (T<sub>eff</sub>) cells with CCR8 to improve recruitment to tumor sites. However, recruitment of CCR8-engineered T cells to the same sites as T<sub>reg</sub> cells will directly expose them to T<sub>reg</sub> cell-mediated suppression. To overcome this immunosuppression, we sought to use the well-characterized truncated variant of the TGF-β receptor 2 (17, 18). Combining a previously unused tumor recruitment mechanism with a well-established mechanism of immunosuppression prevention would generate the first T cell product that can address the two major limitations of ACT in solid tumors. We probed this hypothesis in murine and human models

Copyright © 2021  
The Authors, some  
rights reserved;  
exclusive licensee  
American Association  
for the Advancement  
of Science. No claim to  
original U.S. Government  
Works. Distributed  
under a Creative  
Commons Attribution  
NonCommercial  
License 4.0 (CC BY-NC).

<sup>1</sup>Center of Integrated Protein Science Munich and Division of Clinical Pharmacology, Department of Medicine IV, Klinikum der Universität München, Munich, Germany. <sup>2</sup>Department of Internal Medicine III, University of Munich, Munich, Germany. <sup>3</sup>Center for Immunology and Inflammatory Diseases, Massachusetts General Hospital and Harvard Medical School, Boston, MA, USA. <sup>4</sup>Department of Immunology, The University of Texas, MD Anderson Cancer Center, Houston, TX, USA. <sup>5</sup>Department of Dermatology, Allergology, and Venerology, University of Lübeck, Lübeck, Germany. <sup>6</sup>Institute of Computational Biology, Helmholtz Zentrum München-German Research Center for Environmental Health, Neuherberg, Germany. <sup>7</sup>Technical University of Munich, School of Life Sciences Weihenstephan, Freising, Germany. <sup>8</sup>Department of Pediatric Hematology, Oncology, Hemostaseology and Stem Cell Transplantation, Dr. von Hauner University Children's Hospital, Ludwig Maximilian University Munich. <sup>9</sup>German Center for Infection Research (DZIF), Munich, Germany. <sup>10</sup>German Center for Translational Cancer Research (DKTK), Partner Site Munich, Germany. <sup>11</sup>Einheit für Klinische Pharmakologie (EKLP), Helmholtz Zentrum München, German Research Center for Environmental Health (HMGU), Neuherberg, Germany. \*Corresponding author. Email: bcadiilha@gmail.com (B.L.C.); sebastian.kobold@med.uni-muenchen.de (S.K.)

†These authors contributed equally to this work.

## SCIENCE ADVANCES | RESEARCH ARTICLE

in vitro and in vivo and show that CAR T cell therapy can be rendered effective in various tumor models with this novel combinatorial approach.

## RESULTS

**CCL1 recruits CCR8<sup>+</sup> T cells to tumors in a murine pancreatic cancer model**

To further understand the determinants of successful infiltration of adoptively transferred antigen-specific T cells, we transferred ovalbumin (OVA)-specific, in vitro expanded T cells (OT-1 T cells) transduced with green fluorescent protein (GFP) to mice bearing Panc02-OVA tumors (Fig. 1A). A week after transfer, we isolated the transferred T cells from spleen and tumor and performed reverse transcription polymerase chain reaction (RT-PCR)-based microarray analysis on predefined genes associated with T cell exhaustion and homing. As expected, markers of activation and exhaustion such as PD-1 (Programmed cell death protein 1) were up-regulated in tumor-infiltrating T cells (Fig. 1B). Of all the chemokine receptors, the only target that was significantly up-regulated was CCR8 (Fig. 1B), implying its role in facilitating T cell accumulation at the tumor site. Homing of CCR8<sup>+</sup> cells is mainly driven by CCL1 (16, 19), which could be detected in ex vivo Panc02 tumors at both the RNA (Fig. 1C) and protein level (Fig. 1, D and E), and was detected in the tumor microenvironment at considerably higher levels than other organs (Fig. 1D). Activated T cells have previously been reported to produce CCL1 (20). Consistent with this, we found that tumor-

infiltrating T cells produced high amounts of CCL1 upon stimulation (Fig. 1F). Upon antigen recognition, T cells produced more CCL1 with increasing effector-to-target ratios (Fig. 1G), highlighting a positive feedback loop, whereby local activation of T cells in the tumor induces their expression of CCL1, which, in turn, will further amplify the recruitment of CCR8-expressing immune cells. In contrast, the Panc02 tumor cells themselves did not release CCL1 (Fig. 1G).

**CCR8-transduced T cells improve ACT efficacy through CCL1-dependent tumor trafficking**

The presence of CCR8 on tumor-infiltrating T cells implies that the CCL1-CCR8 axis recruits T cells to the tumor site. CCR8 is a chemokine receptor predominantly present on effector T<sub>reg</sub> cells. There, its expression is substantially higher compared to central T<sub>reg</sub> or conventional T<sub>eff</sub> cells (Fig. 2A) and may contribute to their infiltration into CCL1-expressing tumors. Thus, by ectopically introducing CCR8 into tumor-specific T<sub>eff</sub> cells, these cells may be able to mirror T<sub>reg</sub> cell migration patterns. However, CCR8 is not the only chemokine receptor found in T<sub>reg</sub> cells. CCL22 is the ligand of CCR4, which, similar to CCR8, is expressed on T<sub>reg</sub> cells, fostering an immunosuppressive environment in ovarian carcinoma and predicting poor survival (21). We therefore compared the relative expression of these two axes across several human tissues. We found substantial expression of CCL22 in numerous healthy tissues including the central nervous system, gastrointestinal tract, lung, and skin. In contrast, CCL1 was expressed at lower levels and restricted to the spleen, lung, testes, and brain (fig. S1A). These data suggest a favorable specificity

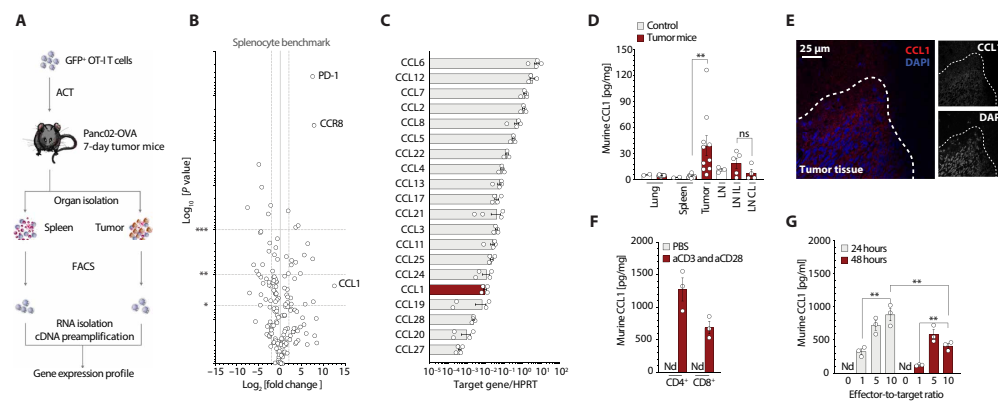


**Fig. 1. CCR8 is used by a subset of transferred antigen-specific T cells to traffic to a murine pancreatic cancer in a CCL1-dependent manner.** (A) Schematic experimental layout to determine the gene expression profile of OT-1 T cells after adoptive transfer. (B) Volcano plot for gene expression profile of tumor-infiltrating OT-1 T cell compared to a splenocyte benchmark. Gene expression is depicted on the x axis versus the P value depicted on the y axis. ( $n = 3$  mice). (C) RT-PCR gene analysis of explanted Panc02-OVA tumors ( $n = 4$ ). HPRT, hypoxanthine-guanine phosphoribosyltransferase. (D) Enzyme-linked immunosorbent assay (ELISA) for murine CCL1 on organ lysates of control animals ( $n = 3$ ) or Panc02-OVA tumor-bearing animals ( $n = 10$ ). LN.I, lymph node ipsilateral to the tumor; LN.C, lymph node contralateral to the tumor. (E) Fourteen-day Panc02-OVA tumor explants, embedded in OCT medium and frozen for cryosectioning and stained with CCL1 and 4',6-diamidino-2-phenylindole (DAPI) (representative of  $n = 3$  mice). (F) ELISA for murine CCL1 on CD4<sup>+</sup> or CD8<sup>+</sup> magnetic-activated cell-sorted T cells after 24-hour stimulation with anti-CD3 and anti-CD28 antibodies or vehicle solutions only (representative of  $n = 3$  independent experiments). (G) ELISA for murine CCL1 of supernatants generated upon 24- or 48-hour culture of different effector to target ratios, namely, 0, 1, 5, or 10 OT-1 T cells to 1 tumor target cell (a constant number of 20,000 Panc02-OVA tumor cells was used) (representative of  $n = 3$  independent experiments). nd stands for nondetectable. ns stands for nonsignificant  $P > 0.05$ . Experiments show mean values  $\pm$  SEM of at least three triplicates and are representative of at least three independent experiments. P values are based on two-sided unpaired t test. Data shown in (D) are pooled from three independent experiments.

## SCIENCE ADVANCES | RESEARCH ARTICLE

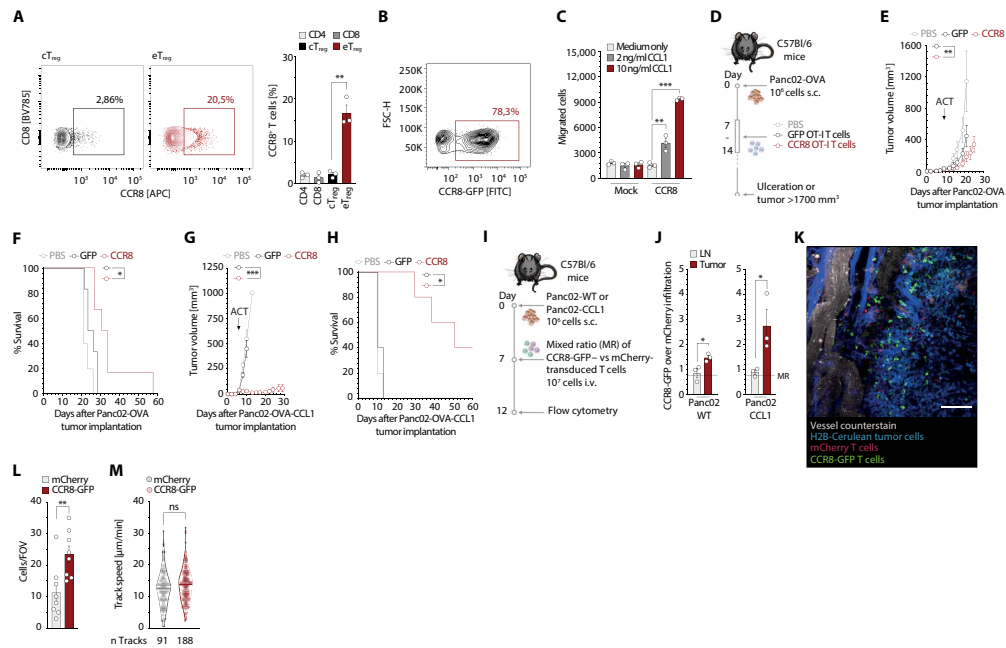


**Fig. 2. CCR8 transduction in OT-I T cells improves ACT efficacy through CCL1-dependent tumor trafficking.** (A) CCR8 staining of live, CD4<sup>+</sup>CD3<sup>+</sup>CD4<sup>+</sup>FoxP3<sup>+</sup>CD44<sup>high</sup>CD62L<sup>+</sup>eTreg and CD44<sup>low</sup>CD62L<sup>+</sup>cTreg Panc02-OVA-infiltrating cells. CCR8 expression on CD4<sup>+</sup>CD8<sup>+</sup>eTreg and cTreg T cells. (*n* = 3 mice). APC, Allophycocyanin. (B) CCR8-GFP transduction efficiency of murine T cells. FITC, fluorescein isothiocyanate. (C) In vitro migration of murine T cells to CCL1. (D) Experimental layout for (E) to (H). (E) Tumor growth curves of mice treated with a single intravenous (i.v.) injection of phosphate-buffered saline (PBS) or 10<sup>7</sup> GFP-transduced or CCR8-transduced OT-I T cells (*n* = 5 mice per group). (F) Tumor survival curves of (E). (G) Panc02-OVA-CCL1 tumor growth curves of mice treated with a single intravenous injection of PBS or 10<sup>7</sup> GFP-transduced or CCR8-transduced OT-I T cells (*n* = 5 mice per group). (H) Tumor survival curves of (G). (I) ACT tracking experiments in Panc02 or Panc02-CCL1 tumors by flow cytometry. s.c., subcutaneous. (J) Live, CD45.1<sup>+</sup> tumor-infiltrating T cells (*n* = 3 mice). (K and L) ACT tracking in mice with tumors in a dorsal skinfold chamber to enable multiphoton intravital imaging (L) and speed quantification of tumor-infiltrating T cells (M) (*n* = 8 mice). FOV, field of view. Experiments show mean values ± SEM and are representative of three independent experiments, except (G) and (H) that are representative of two independent experiments. *P* values for (C), (J), (L), and (M) are based on a two-sided unpaired *t* test. Analyses of differences between groups for (E) and (G) were performed using two-way analysis of variance (ANOVA) with correction for multiple testing by the Bonferroni method. Comparison of survival rates for (F) and (H) was performed with the log-rank (Mantel-Cox) test.

profile with less off-target accumulation of CCR8-CAR T cells and increased specificity of the CCL1-CCR8 axis to tumors.

We next probed the hypothesis that forced expression of CCR8 in T cells would enable their migration toward CCL1, thereby enhancing tumor access. We first inserted this gene in a retroviral vector followed by a 2a-linker peptide fused to GFP and assessed that CCR8 was expressed efficiently upon retroviral transduction into primary T cells (Fig. 2B). There, CCR8 proved functional upon ligand binding, facilitating dose-dependent migration toward recombinant CCL1 (Fig. 2C). We then set up an in vivo experiment, on the Panc02-OVA model used previously, to assess the therapeutic efficacy of CCR8-transduced T<sub>eff</sub> cells (Fig. 2D). A single transfer of CCR8-transduced OT-I T cells resulted in significantly improved tumor growth control and prolonged survival of tumor-bearing mice compared to GFP-transduced OT-I T cells (Fig. 2, E and F).

To test the impact of CCR8-expressing T<sub>eff</sub> cells on tumors that produce CCL1 themselves, we generated a Panc02-OVA variant overexpressing CCL1. Using the same treatment protocol as before, treatment of tumor-bearing mice with CCR8-transduced OT-I T cells almost completely abolished tumor growth and more markedly prolonged survival compared to control OT-I T cells (Fig. 2, G and H). To evaluate whether the observed phenotype did indeed rely on enhanced recruitment of T cells to the tumor site, we analyzed immune cell infiltrates by flow cytometry. Analysis of the tumor environment after transfer of an equal mix of CCR8-GFP- and mCherry-transduced T cells (Fig. 2I) revealed increased infiltration of CCR8 OT-I T cells compared to OT-I T cells in tumor tissues, which was further enhanced in tumors overexpressing CCL1 (Fig. 2J). Using the same experimental setup, we looked at the antigen-nonspecific infiltration of the ACT in multiple organs. We found CCR8-GFP T cells

## SCIENCE ADVANCES | RESEARCH ARTICLE

to preferentially infiltrate the liver, lung, and tumor relative to the spleen (fig. S1, B and C). We then wondered whether, in addition to amplifying the infiltration of tumors, CCR8 expression enhanced their intratumoral motility, which may promote tumor invasion and further increase their antitumor activity. For this purpose, we performed intravital microscopy that recapitulated the enhanced infiltrative capacity of CCR8-transduced T cells (Fig. 2, K and L). However, no significant changes in the motility of CCR8-transduced T cells compared to mCherry-transduced T cells were observed (Fig. 2M). Together, these data point toward enhanced tumor-directed migration, which is further enhanced by continued CCL1 production in the presence of a tumor target, as the mode of action of CCR8 in ACT.

### Dominant-negative receptor-transduced T cells retain proliferative capacity despite TGF- $\beta$

As CCR8 is typically used by T<sub>reg</sub> cells for directed migration toward tumor tissues, effector cells recruited to the same site would be at increased risk of T<sub>reg</sub> suppression. We first quantified T<sub>reg</sub> cell infiltrates in Panc02 tumors (Fig. 3, A and B). The fraction of T<sub>reg</sub> cells in the immune cell infiltrate in this tumor model was higher than in lymphoid organs (Fig. 3B) and was essentially entirely composed of CD44<sup>hi</sup> effector T<sub>reg</sub> cells (Fig. 3C). Given that TGF- $\beta$  is one of the main suppressive mechanisms used by T<sub>reg</sub> cells, and that tumor-infiltrating T<sub>reg</sub> cells produce this cytokine in the Panc02-OVA tumor model (Fig. 3D), we considered that shielding the transferred T cells from this suppressive cytokine would improve their tumor-ablating function. We also found large amounts of TGF- $\beta$  in supernatants derived from *in vitro* cultures of Panc02 cells, further corroborating

the immunosuppressive role of this cytokine in this model (Fig. 3E). To counteract the deleterious effects of this cytokine on gene-engineered cells, we used the well-described truncated version of the TGF- $\beta$  receptor 2 [dominant-negative receptor (DNR); Fig. 3F]. This receptor lacks the intracellular signaling motifs required for TGF- $\beta$  signal transduction and directly competes with wild-type TGF- $\beta$  receptor 2 for binding to TGF- $\beta$ . Binding of TGF- $\beta$  to DNR-transduced T cells will scavenge TGF- $\beta$ , preventing its activity on untransduced T cells (22, 23). Upon retroviral transduction, DNR was readily expressed in primary murine T cells (Fig. 3G). DNR efficiently shielded transduced T cells from TGF- $\beta$ , as TGF- $\beta$  did not negatively affect the proliferation of transduced T cells in contrast to control T cells (Fig. 3H). We next used DNR-transduced OT-I T cells to treat mice bearing Panc02-OVA tumors with the same treatment schedule as outlined previously (Fig. 3I). DNR-transduced OT-I T cells showed enhanced tumor control and prolonged survival of mice compared to GFP-transduced OT-I T cells (Fig. 3, J and K). In contrast to the chemokine receptor-engineered T cells, as expected, DNR-transduced cells did not show a preferential accumulation at the tumor tissue compared to control OT-I T cells (Fig. 3L). Together, these results indicate that DNR could be a suitable combination partner for CCR8 overexpression in antigen-specific T cells by shielding these cells from immune suppression.

### CCR8-DNR-transduced CAR T cells show *in vivo* efficacy in murine pancreatic solid tumors

Considering the enhanced tumor control we observed by generating conventional T<sub>eff</sub> cells expressing either ectopic CCR8 or DNR,

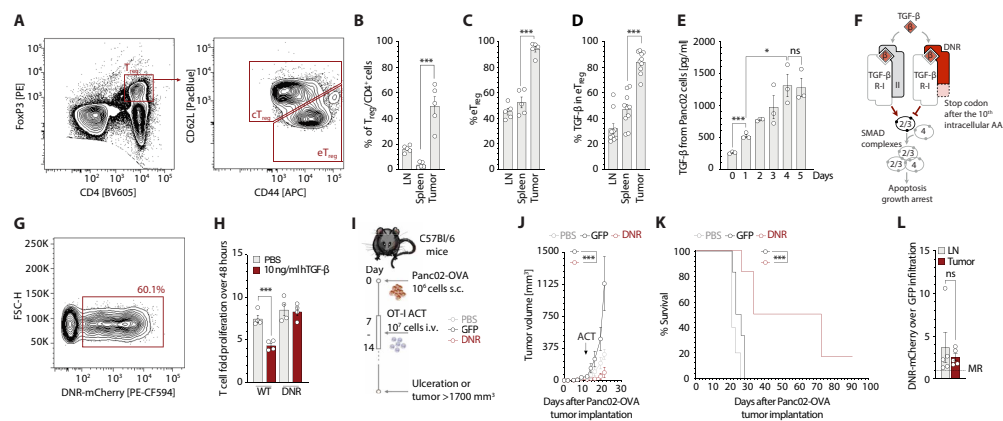


**Fig. 3. DNR-transduced T cells retain proliferative capacity despite TGF- $\beta$ .** (A) CD45<sup>+</sup>CD3<sup>+</sup>CD4<sup>+</sup>FoxP3<sup>+</sup>CD44<sup>high</sup>CD62L<sup>+</sup>eT<sub>reg</sub> and CD44<sup>low</sup>CD62L<sup>+</sup>cT<sub>reg</sub> Panc02-OVA infiltrating cells ( $n = 5$  mice). PE, Phycoerythrin. (B) Percentage of T<sub>reg</sub>/CD4<sup>+</sup> in (A) ( $n = 5$  mice). T<sub>reg</sub> cells: lymph nodes 15406  $\pm$  5351, spleen 6992  $\pm$  9702, and tumor 893  $\pm$  244 (mean absolute cells  $\pm$  SD). (C) Percentage eT<sub>reg</sub> cells in T<sub>reg</sub> cells. (D) Percentage TGF- $\beta$ <sup>+</sup> cells in eT<sub>reg</sub> ( $n = 10$ ). (E) Murine TGF- $\beta$  ELISA on 20,000 tumor cells supernatant ( $n = 3$ ). (F) DNR downstream signaling. AA, amino acid. (G) Transduction efficiency of murine T cells with DNR. (H) T cell proliferation measured through flow cytometry ( $n = 3$ ). (I) Experimental layout for tumor challenge with Panc02-OVA. (J) Tumor growth curve in mice treated with a single intravenous injection of PBS or 10<sup>7</sup> GFP-transduced or DNR-transduced OT-I T cells ( $n = 5$ ). (K) Tumor survival curves of (J). (L) Flow cytometry ACT tracking in Panc02 tumor-bearing mice treated with an equal mix of DNR-mCherry T cells and GFP T cells ( $n = 3$ ). Experiments show mean values  $\pm$  SEM and are representative of three independent experiments, except (A) to (C), which was performed for a total of 5 mice, and (D) a total of 10 mice. *P* values for (B), (C), (D), (E), and (L) are based on two-sided unpaired *t* test. Analyses of differences between groups for (J) were performed using two-way ANOVA with correction for multiple testing by the Bonferroni method. Comparison of survival rates for (K) was performed with the log-rank (Mantel-Cox) test.



## SCIENCE ADVANCES | RESEARCH ARTICLE

we wanted to test whether this approach could also be used to improve the function of CAR T cells, and whether their combined expression produced synergistic effects. To this end, we developed polycistronic constructs allowing for coexpression of a CAR targeting the murine epithelial cell adhesion molecule (EpCAM), along with CCR8, DNR, or both in a single plasmid (Fig. 4A). We were able to efficiently introduce these receptor combinations into primary murine T cells (Fig. 4B). CCR8-equipped T cells migrated toward CCL1 gradients in vitro (Fig. 4C). T cells transduced with the DNR were shielded from TGF- $\beta$ , allowing for TGF- $\beta$ -unhindered proliferation (Fig. 4D). Last, the CAR conferred EpCAM antigen specificity as shown by interferon- $\gamma$  (IFN- $\gamma$ ) release (Fig. 4E) and impedance-based killing assays (Fig. 4F) in coculture experiments. In vivo, tracking the infiltration of ACT in an antigen-specific setting revealed that CCR8-CAR T cells were enriched only in the tumor and not in any other of the organs analyzed when compared to CAR T cells (fig. S1D). Next, mice bearing Panc02-EpCAM tumors were treated with CAR, CCR8-CAR, DNR-CAR, or CCR8-DNR-CAR T cells (Fig. 4G). CAR and DNR-CAR T cells only modestly prolonged survival, and CCR8-CAR T cells led to one tumor rejection (10% of mice). CCR8-DNR-CAR T cells outperformed all other groups both in terms of antitumoral activity (with three of seven mice clearing the tumor) and prolongation of survival (Fig. 4, H and I). Together,

these results indicate a synergy between CCR8 and DNR in the CAR setting, which warranted testing the applicability of this strategy to enable ACT in human solid tumor models.

### CCR8-DNR-CAR T cells are functional in human xenograft tumor models

To provide further rationale for the translational potential of our findings from murine models, we next probed our underlying hypothesis in publicly available databases: If CCR8 is a relevant chemokine receptor for the access of immunosuppressive cells ( $T_{reg}$  cells) to different cancer tissues, then this should be reflected within these samples. Mining The Cancer Genome Atlas (TCGA) database, we indeed found high expression of the genes CCR8, FOXP3 (expressed in  $T_{reg}$  cells), and TGF $\beta$ 1 in pancreatic ductal adenocarcinoma (PDAC) (fig. S2A). Similar associations were found across the diverse disease entities studied such as breast invasive carcinoma, stomach adenocarcinoma, colon adenocarcinoma, rectum adenocarcinoma, skin cutaneous melanoma, lung adenocarcinoma, lung squamous cell carcinoma, and mesothelioma (fig. S2A). Along these lines, CCL1, the main ligand of CCR8, and also the other minor ligands (CCL4, CCL17, and CCL18) were found to be up-regulated in pancreatic cancer compared to healthy tissue (fig. S2B). CCR8 and TGF $\beta$ 1 expression were strongly associated

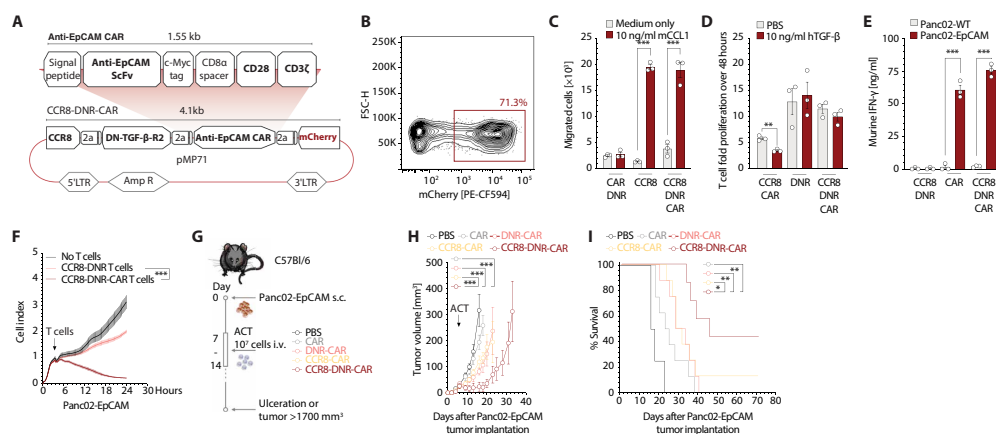


**Fig. 4. CCR8-DNR-transduced CAR T cells mediate superior in vivo efficacy in pancreatic solid tumors.** (A) Schematic representation of murine retroviral construct for T cell engineering. 5' LTR, long terminal repeat; Amp R, Ampicillin resistance. (B) Transduction efficiency of primary murine T cells with CCR8-DNR-CAR. (C) Boyden chamber assay to assess in vitro migration of primary murine T cells to recombinant murine CCL1 measured by flow cytometry. Migrated cells were normalized for CCR8 expression.  $n = 3$ . (D) T cell fold expansion over 48 hours with or without TGF- $\beta$  on the culture media, measured through flow cytometry (representative of  $n = 3$  independent experiments). (E) ELISA for murine IFN- $\gamma$  was performed on supernatants generated after 24-hour culture of T cells with Panc02-EpCAM tumor cells, in a ratio of 10 effector cells to 1 target cell (representative of  $n = 3$  independent experiments). (F) Panc02-EpCAM tumor cell killing by different T cell conditions, in a 10-fold concentration, measured over time through xCELLigence. Representative of  $n = 3$  independent experiments. (G) Experimental layout for the ACT experiments depicted in (H) and (I). (H) Growth curves of Panc02-OVA-EpCAM tumors in C57Bl/6 mice that were treated with a single intravenous injection of PBS ( $n = 5$  mice) or  $10^7$  CAR-transduced, DNR-CAR-transduced, CCR8-CAR-transduced ( $n = 8$  mice) or CCR8-DNR-CAR-transduced T cells ( $n = 7$  mice). (I) Tumor survival curves of a tumor challenge experiment with Panc02-OVA-EpCAM tumors. Mice were treated with a single intravenous injection of PBS ( $n = 5$  mice) or  $10^7$  CAR-transduced, DNR-CAR-transduced, CCR8-CAR-transduced ( $n = 7$  mice), or CCR8-DNR-CAR-transduced T cells ( $n = 8$  mice). Experiments show mean values  $\pm$  SEM and are representative of three independent experiments.  $P$  values for (C) to (E) are based on two-sided unpaired  $t$  test. Analyses of differences between groups for (F) and (H) were performed using two-way ANOVA with correction for multiple testing by the Bonferroni method. Comparison of survival rates for (I) was performed with the log-rank (Mantel-Cox) test.

## SCIENCE ADVANCES | RESEARCH ARTICLE

with the  $T_{reg}$  cell up-regulated marker, FOXP3, indicating that  $T_{reg}$  cells indeed express CCR8 and TGFB1 across these studied tumor entities (fig. S2C).

We scrutinized PDAC patient data and found that high CCR8 expression correlated with more advanced tumor staging and thus a more rapid disease progression (fig. S3A). High CCR8 expression also correlated with a lower TIDE (Tumor immune dysfunction and exclusion) exclusion score and trended with a higher dysfunction score, which corroborates a previous analysis that CCR8 can induce recruitment of immune cells to the tumor microenvironment and is associated with lower effector functions on-site (fig. S3B) (15). This was accompanied by higher lymphocyte infiltration,  $T_{reg}$  and TGFB1 scores, and a significantly lower proliferation score (fig. S3C). Together, these data strengthen the rationale that CCR8 is an attractive

target molecule for immune cell recruitment to human cancer tissue and that  $T_{reg}$  cells are an important source of TGF- $\beta$  at the tumor site correlating with T cell proliferation arrest.

To translate these findings into a therapeutic application, we engineered primary human T cells with an anti-mesothelin (MSLN) CAR, previously described (24), together with human CCR8, DNR, or both (Fig. 5A). The constructs were successfully transduced into primary human T cells (Fig. 5B), where we observed comparable CAR transduction efficiency and surface expression independent of construct design (fig. S4A). The anti-MSLN CAR allowed effective recognition and elimination of MSLN antigen-positive cells, as assessed by impedance measurements of cell killing and by IFN- $\gamma$  release (Fig. 5, C and D). As seen in the murine cells, activated human T cells produced CCL1 upon coculture with tumor cells, the amount

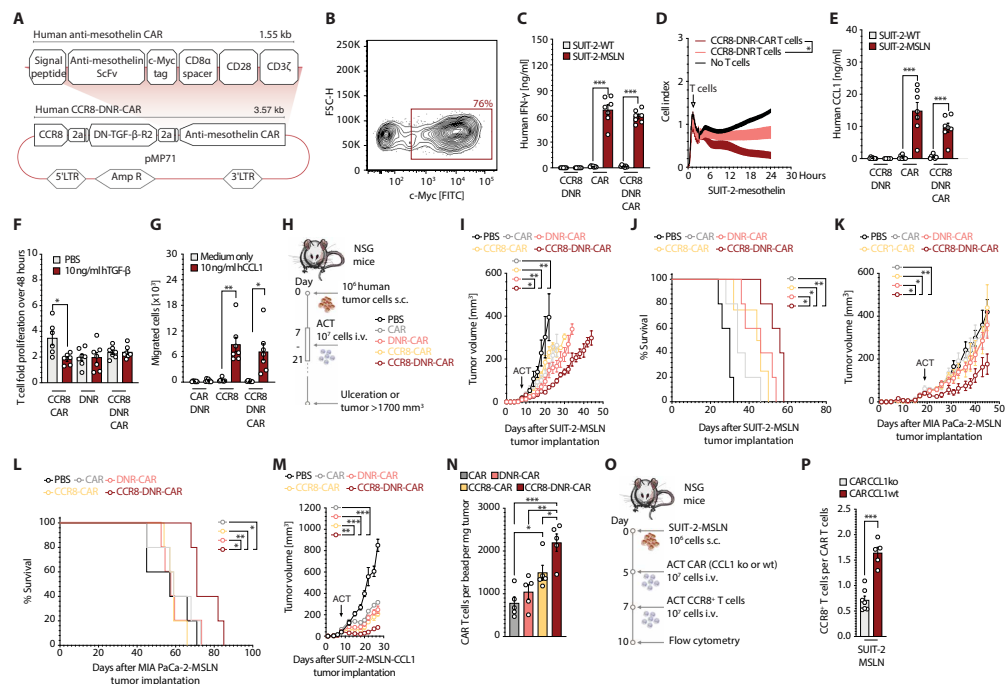


**Fig. 5. CCR8-DNR-CAR T cells are effective in human tumor models.** (A) Schematic representation of construct. (B) Transduction efficiency of human T cells with CCR8-DNR-CAR. (C) Human IFN- $\gamma$  ELISA on 24-hour coculture supernatants. (D) SUIT-2-MSLN killing measured by xCELLigence. (E) Human CCL1 ELISA on 24-hour coculture supernatants. (C to E) 10:1 effector to target cells. (F) Forty-eight-hour T cell expansion, flow cytometry. (G) In vitro migration of T cells to CCL1, flow cytometry. (H) Experimental layout for (I) to (M). Tumor growth and survival curves of SUIT-2-MSLN (I and J), MIA PaCa-2-MSLN (K and L), and SUIT-2-MSLN-CCL1 (M) treated with a single intravenous injection of PBS or  $10^7$  CAR-, DNR-CAR-, CCR8-CAR-, or CCR8-DNR-CAR-transduced T cells ( $n = 5$  mice per group). (N) Flow cytometry quantification of CAR T cells per bead per milligram on day 27 after tumor implantation ( $n = 5$  mice). (O) Experimental layout for (P). (P) SUIT-2-MSLN tumor-bearing mice were administered with  $10^7$  CAR T cells that were either wild-type (wt) or CCL1 knockout (ko). This was followed by a treatment with  $10^7$  CCR8-transduced T cells ( $n = 7$  mice). Experiments show mean values  $\pm$  SEM of  $n = 7$  healthy donors for (B) to (G), one experiment for (I) to (L) and (P), and two independent experiments for (M) and (N).  $P$  values for (C), (E), (F), (G), (N), and (P) are based on a two-sided unpaired  $t$  test. (D), (I), (K), and (M) were assessed through two-way ANOVA with correction for multiple testing by the Bonferroni method. (J and L) Survival rate comparison through the log-rank (Mantel-Cox) test.

## SCIENCE ADVANCES | RESEARCH ARTICLE

of which correlated with the amount of IFN- $\gamma$  released (Fig. 5E). DNR, in turn, improved proliferation of transduced T cells in the presence of TGF- $\beta$  compared to control-transduced T cells (Fig. 5F). DNR functionality was further validated via phosphoflow, revealing no phosphorylation of SMAD2/3 downstream of TGF- $\beta$  when DNR was expressed by T cells (fig. S4B). CCR8 enabled migration toward human CCL1 gradients compared to control-transduced T cells (Fig. 5G).

We next sought to provide a more in-depth characterization of the phenotype and function of CCR8-DNR-CAR-modified T cells over the single- or double-modified T cells. We could observe that in vitro over a prolonged period with repeat antigen exposures, DNR-CAR and CCR8-DNR-CAR T cell conditions (for short, DNR conditions) had an increased and more durable proliferative capacity (fig. S4C). DNR conditions did not alter CD4 and CD8 ratios (fig. S4D) nor significantly change the effector or memory phenotype compared to CCR8-CAR or CAR conditions (fig. S4E). DNR conditions did not alter PD-1, TIM-3 (T-cell immunoglobulin and mucin-domain containing-3), or LAG-3 (Lymphocyte-activation gene 3) levels (fig. S4F). The impact of CCR8 and DNR expression on the secretion profile of these CAR T cells revealed that the DNR conditions show a modest increase in T helper 2 (T<sub>H</sub>2) cytokines [such as interleukin-4 (IL-4) and IL-10] and T<sub>H</sub>1 cytokines (such as IL-2 and granzyme B) (fig. S4G). DNR conditions also showed a more robust secretion of the chemokines probed (including CCL1, CCL3, and CCL4) (fig. S4G). As expected, TGF- $\beta$  levels measured within this coculture gradually rose as T cells decreased in their proliferative capacity (fig. S4G).

To investigate whether T cell-derived CCL1 would indeed be necessary and sufficient to recruit CCR8<sup>+</sup> T cells and mediate therapeutic benefits, we went on to assess the impact in CCL1-negative tumor cell models. We tested CCR8-DNR-CAR T cells in human pancreatic xenograft tumor models where SUIT-2-MSLN and MIA PaCa-2-MSLN tumors were implanted in nonobese diabetic (NOD)-scid (Severe Combined Immunodeficiency)-IL2 $\gamma$  null (NSG) mice (Fig. 5H). CCR8-DNR-CAR T cells controlled tumor growth and prolonged survival in both human pancreatic tumor models, demonstrating the necessity of both CCR8 and DNR transduction into the CAR T cells for effective tumor control in solid tumors (Fig. 5, I to L). Together, these data indicate that T cell-derived CCL1 is sufficient to mediate CCR8-associated therapeutic benefit.

Given that CCL1 expression is elevated in patient cohorts of specific disease subtypes, including pancreatic cancer, we further engineered the abovementioned SUIT-2-MSLN pancreatic cancer xenograft model to overexpress CCL1. SUIT-2-MSLN-CCL1 tumors were implanted in NSG mice. We tested CCR8-DNR-CAR T cells in this model, where they outperformed single- or double-transduced T cells in controlling tumor growth (Fig. 5M).

Next, to test whether therapeutic advantage was indeed paralleled by increased T cell access to the tumor site, we analyzed infiltration into the implanted tumors following T cell transfer. At the probed time point, there was an enhanced accumulation of transferred T cells in the tumor, showing increased CCR8-DNR-CAR T cell numbers compared to all other groups (Fig. 5N). At the tumor site, we found a preferential accumulation of CD8<sup>+</sup> T cells compared to the spleen where most of the cells were CD4<sup>+</sup> T cells with a skew toward a central memory phenotype (fig. S4, H and I).

Last, to test whether increased T cell access was indeed due to CCL1 production from the transferred T cells, we used the SUIT-2-MSLN tumor model and a two-step ACT starting with CAR T cells

(wild-type or CCL1 knockout) followed by CCR8-transduced T cells (Fig. 5O). CCL1 knockout using CRISPR-Cas9 editing on primary T cells was technically validated by measuring CCL1 levels 24 hours after T cell stimulation (fig. S4J). We show that tumor infiltration of CCR8-transduced T cells was mostly abolished when CAR T cells had lost the ability to produce CCL1 (Fig. 5P), highlighting that CCL1 produced by activated T cells is necessary to generate a robust positive feedback loop recruitment of CCR8<sup>+</sup> T cells.

## DISCUSSION

T cell therapies have shown remarkable results in hematological cancer (25), but this success has yet to be successfully translated to solid malignancies. Appropriate trafficking to the tumor site and resistance to the tumor microenvironment-induced suppression are major hurdles to the employment of T cell therapies in solid tumors (14). Improved trafficking of T cells through chemokine receptors has been shown to be a reliable approach in tumor models (26). At the same time, CAR T cell therapy has entered the clinical realm for selected hematological malignancies, with newer generations of CAR T cells in clinical trials. Nevertheless, only two clinical trials are using chemokine receptors, CXCR2 (NCT01740557) and CCR4 (NCT03602157), to improve trafficking of T cells to the tumor site, with results pending.

The plethora of chemokine receptors and their respective ligands, as well as their promiscuity, means that sophisticated screening of targets and careful patient selection are required. Chemokines expressed in tumor cells and in tumor stroma cells can be subject to posttranslational changes that modify their function (27). In addition, atypical chemokine receptors can scavenge secreted ligands rendering them unavailable to trigger migration of T<sub>eff</sub> cells (28). Furthermore, the chemokine receptor-ligand choice for engineering CAR T cells should not only aim at improving migration into the given tumor but also target critical axes for the tumor's immune evasion. Here, we reason that the CCR8-CCL1 axis fulfills these criteria, as it has been demonstrated to be a pivotal receptor-ligand pair for recruiting T<sub>reg</sub> cells to the tumor and for potentiating their immunosuppressive capacity across different cancer entities, as well as being associated with poor disease prognosis (15, 16). Down-regulation or loss of an immunosuppression-enabling axis appears highly unlikely to occur in the tumor environment.

Our TCGA analysis confirms both the correlation of CCR8 and FOXP3 and the correlation of T<sub>reg</sub> cells with poor prognosis and further expands it to several solid tumors so far impervious to CAR T cell therapy. CCR8<sup>+</sup> T<sub>reg</sub> cells have been proposed to be master drivers of immune regulation as specific binding of CCL1 to CCR8 increases the suppressive capacity of T<sub>reg</sub> cells. The CCL1-CCR8 axis is, however, incapable of inducing a switch from FOXP3<sup>-</sup> to FOXP3<sup>+</sup> (16). Furthermore, the low endogenous CCR8 expression in T<sub>eff</sub> cells increases the likelihood of an improved migration upon overexpression.

Transduction of different chemokine receptors—namely, CXCR2 (29), CCR4 (26), CCR2 (30), and CX3CR1 (31)—has been used in the past to improve ACTs for solid tumor entities (26, 29). Out of these, CCR4 is the only other chemokine receptor expressed in T<sub>reg</sub> cells, thus making it an approach that is directly comparable to the strategy in the present study. CCR4 transduction improved CAR T cell efficacy in a model of Hodgkin lymphoma, which was dependent on the availability of CCL22 (26). CCR4 and CCR8 ACT highjack

two distinct axes—CCL22 and CCL1, respectively—that can enable  $T_{reg}$  cell trafficking to solid tumors. The CCL1-CCR8 therapeutic axis is more specific to tumors and can directly counterbalance  $T_{reg}$  cell infiltration in solid tumors, making it a superior choice for chemokine receptor enhanced ACT in solid tumors when compared to the CCL22-CCR4 axis. Considering the tumor specificity and potential safety, our TCGA analysis on expression levels of CCL1 and CCL22 reveals that CCL22 is broadly expressed in different healthy tissues. This may lead to redirection of  $CCR4^+$  CAR T cells into off-target CCL22<sup>+</sup> tissue, on the one hand diminishing the antitumor effect and on the other increasing the risk for off-tumor toxicity. On the contrary, CCL1 expression is lower and more restricted in healthy tissue, which can enable a more specific homing of CCR8-transduced CAR T cells to the tumor site.

Besides the need for improved tumor infiltration, there is also a fundamental need for CAR T cell activity and proliferation at the tumor site. TGF- $\beta$  is a hallmark of the immunosuppressive tumor milieu in pancreatic and other solid tumors (32). It can control T cell homeostasis by inhibiting both T cell proliferation and activation (33). In addition, it can inhibit  $T_{eff}$  cell activity through an anticytotoxic program of transcriptional repression, down-regulating the expression of perforin, granzyme A, granzyme B, Fas ligand, and IFN- $\gamma$  (34). The DNR is a well-characterized receptor in which binding by TGF- $\beta$  will not trigger downstream signaling in the cell. Moreover, TGF- $\beta$  scavenging will prevent its detrimental effects on other  $T_{eff}$  cells. Such a receptor harbors multiple advantages when compared to anti-TGF- $\beta$  antibody therapy as the effect with DNR is limited to the proximity of the DNR-expressing cell. It will also be specific for the tumor tissue expressing the CAR-targeted antigen. Thus, endogenous T cells with different TCR specificities will remain unaffected, reducing the risk of self-reactivity (23). In addition to TGF- $\beta$ , other  $T_{reg}$  cell-derived cytokines such as IL-10 can be found in abundance in the tumor microenvironment. IL-10 has been described to impair dendritic cell functionality and hamper  $T_{eff}$  cell cytotoxicity. This cytokine may also play a role in promoting tumor rejection instead of inducing immunosuppression (35). Genome editing technologies such as CRISPR-Cas9 are an equally valid alternative approach for relieving T cell immunosuppression. However, the knowledge on safety and efficacy of these approaches is still limited, and more evidence will be needed for a comprehensive assessment. The advanced stage of testing, including use in clinical trials, as well as knowledge of the safety profile of current DNR-based therapies, makes it an attractive tool for the relief of T cell immunosuppression (23).

Similar to human breast tumors (15), we were able to show that FOXP3, CCR8 (as well as its ligands), and the TGF $\beta$ 1 genes are up-regulated in human pancreatic adenocarcinoma compared to healthy pancreatic tissue and to verify that there are strong correlations between the expression of these genes. This highlights the potential relevance of the CCL1-CCR8 axis and of TGF- $\beta$  expression in this disease and provides the rationale for targeting them in pancreatic cancer and in other tumor entities with comparable expression profiles.

Despite the improvement that targeting this axis had on the efficacy of CAR T cell therapy, some limitations must be considered. Beyond improving migration to the tumor site and relieving immunosuppression on T cells, CAR T cell therapy still stands to benefit from continued improvement in the design (8), precise integration (36), and regulation of the CAR construct itself (37), as outlined by

the recent studies. Furthermore, antigen-specificity is still a major hurdle and a pivotal requirement to ensure the feasibility of any tumor-targeted T cell therapy (38). Similar studies using the same murine Panc02 tumor cell line were able to show T cell memory formation (39); nonetheless, this analysis was not performed in the present study. Targeting the model antigen EpCAM in the murine tumor models of the present study did not reveal any signs of toxicity. However, C57Bl/6 mice are typically highly resistant to immune-mediated side effects, which may only occur with added modifications to the treatment schedule (40). Thus, toxicity associated with CCR8- and DNR-transduced CAR T cells could not be comprehensively assessed in this model. Furthermore, the herein presented human CCL1 tissue expression data, while suggestive of a safer T cell infiltration profile, cannot fully rule out potential side effects when treating patients. Nonetheless, the addition of chemokine receptors or DNR to T cells has not been associated with acute toxicity events, such as cytokine release syndrome and tumor lysis syndromes, which have been observed for CAR T cell therapy (41). Autoimmunity has been described as a long-term deleterious effect of T cell TGF- $\beta$  deprivation for DNR-based T cell therapy (42), and transgenic mice expressing DNR have been reported to develop lymphoproliferative disorder (43). Currently, a clinical trial is assessing the safety and efficacy of DNR transduction in Epstein-Barr virus-specific T cells for lymphoma (NCT00368082) (23). A recent preclinical study investigating the potential of expressing DNR in CAR T cells similarly showed superior proliferation and antitumoral function in prostate cancer (18), with a clinical trial assessing its safety and feasibility currently underway (NCT03089203).

From the long-term in vitro coculture assays, we could better understand the effect the DNR has on the cytokine profile of T cells. We saw increased levels in a variety of cytokines associated with both the innate and adaptive immune response when the DNR was expressed.  $T_H1$ - and  $T_H2$ -associated cytokine levels were both elevated and more balanced, while chemokine levels were also increased. Overall, the expression of the DNR appears to confer  $T_{eff}$  cells with greater functionality, and the expression of CCR8 does not seem to affect the phenotype of  $T_{eff}$  cells.

The treatment experiments in human xenograft tumor models revealed that only in the presence of DNR could CCR8-CAR T cells mediate significant tumor control. This supports the notion that a feedback loop mechanism sustained by CCL1 from activated T cells stands to benefit from immunosuppression shielding. Beyond TGF- $\beta$ , we postulate that relieving other immunosuppressive axes can further sustain this CCL1 feedback loop mechanism, thereby improving the antitumoral function of  $CCR8^+$  ACT. In the model using CCL1 overexpression, the treatment effect was more pronounced as continued recruitment of CCR8-DNR-CAR T cells no longer solely relied on T cell-derived CCL1 to effectively migrate into the tumor, given the tumor itself was overexpressing the chemokine ligand. A better understanding of other suppressive axes that could be additionally targeted could potentiate the effectiveness of this approach. Furthermore, anti-PD-1 checkpoint blockade therapy was recently shown to improve the proliferation and suppressive capacity of  $PD-1^+$   $T_{reg}$  cells (44). Added to the fact that CCL1 levels will rise in the tumor after checkpoint blockade therapy-induced T cell activation, it is reasonable to postulate that simultaneously targeting the CCR8-CCL1 axis might also prove beneficial.

Hence, given appropriate antigen targeting, we propose that CCR8- and DNR-transduced CAR T cells can exploit two critical biological

## SCIENCE ADVANCES | RESEARCH ARTICLE

axes to render CAR T cell therapy effective in solid tumors such as pancreatic cancer. The therapeutic potential of this approach could extend to other T<sub>reg</sub>-rich solid tumor entities where limited infiltration into the tumor and intratumoral T cell proliferation prevent therapeutic success. The novel combination described in the present study may harness the power of CAR T cell therapy for solid tumors with as dismal a prognosis as pancreatic cancer.

**MATERIALS AND METHODS****Study design**

This study was designed to evaluate the benefit of the addition of CCR8 and DNR to CAR T cell therapy in solid tumors using controlled laboratory experiments. We used 6- to 10-week-old female mice from OT-1, C57Bl/6, or NSG strains as donors or recipients of matching appropriate tumor cell lines as described for each experiment. Mice have been implanted with 10<sup>6</sup> tumor cells. Mice were randomized and the investigator was blinded when tumors reached a volume of at least 50 mm<sup>3</sup>. No time points or mice were excluded from the experiments presented in the study. For ethical reasons, endpoints of survival studies were defined as tumor ulceration, tumor sizes exceeding 15 mm in any dimension, weight loss above 20%, or clinical signs of distress. These endpoints were used as surrogate endpoints for survival and are used as such throughout the study. Peripheral blood mononuclear cells were collected from healthy individuals. The murine tumor cell lines used for this study were Panc02, Panc02-OVA, Panc02-OVA-EpCAM, Panc02-H2B-Cerulean, or Panc02-OVA-CCL1 as described in the respective figures. The human cell lines used for this study were SUIT-2-WT, SUIT-2-MSLN, SUIT-2-MSLN-CCL1, or MIA PaCa-2-MSLN as described. Effects have been assessed through quantitative PCR, enzyme-linked immunosorbent assay (ELISA), tumor measurement, flow cytometry, or multiphoton intravital microscopy as described. No outliers have been excluded from any of the experiments. At least three biological replicates were performed for each experiment and  $n > 5$  for each group unless otherwise indicated in the figure legends. One-way analysis of variance (ANOVA) with Tukey's posttest, two-way ANOVA with Bonferroni posttest, or unpaired Student's *t* tests were performed with an  $\alpha$  value of <0.05 to detect differences between group means.

**Mice**

C57BL/6Rj and NSG (NOD.Cg-Prkdc<sup>scid</sup> Il2rg<sup>tm1Wjl</sup>/SzJ) mice were purchased from Charles River Laboratories. OT-1 mice were bred at the animal facilities at the Klinikum der Universität München or Massachusetts General Hospital (MGH). Animals were housed in specific pathogen-free facilities. All experimental studies were approved and performed in accordance with guidelines and regulations implemented by the Regierung von Oberbayern and the MGH Institutional Animal Care and Use Committee. All experiments were carried out randomized and performed blinded and with adequate controls. In accordance with the animal experiment application, tumor growth and health status of mice were checked every other day. For survival analyses, the above-defined criteria were taken as surrogates for survival and recorded in Kaplan-Meier plots.

**Tumor growth studies and treatments**

All tumor cell lines were subcutaneously injected in 100  $\mu$ l of phosphate-buffered saline (PBS) into the flanks of mice. Animals were randomized into treatment groups according to tumor volumes. Tumor

volumes were measured before and every other day after treatment was started and calculated as  $V = (\text{length} \times \text{width}^2)/2$ . For ACT studies, 10<sup>7</sup> T cells were injected intravenously in 100  $\mu$ l of PBS once average group tumor volumes had reached at least 50 mm<sup>3</sup>.

**Cell line generation, culture, and validation**

Murine Panc02, Panc02-OVA, and Panc02-EpCAM (11) have been previously described. The human SUIT-2, SUIT-2-MSLN, and MIA PaCa-2-MSLN tumor cell lines have been previously described (11). The Panc02-OVA cell line has been modified with retroviruses to express the murine CCL1 chemokine (UniProt entry P10146) (Panc02-CCL1) or a blue fluorescent protein tagged to a Histone protein (Panc02-H2B-Cerulean). The SUIT-2-MSLN tumor cell line has been modified with retroviruses to express the human CCL1 chemokine (UniProt entry P22362) (SUIT-2-MSLN-CCL1). All tumor lines were grown as previously described (11) and used for experiments when in exponential growth phase. 293Vec-Galv, 293Vec-Eco, and 293Vec-RD114 were a gift of M. Caruso, Québec, Canada and have been previously described (45). For virus production, retroviral pMP71 (provided by C. Baum, Hannover) vectors carrying the sequence of the relevant receptor were stably introduced in packaging cell lines. Single-cell clones were generated and indirectly screened for the highest level of virus production by determining transduction efficiency of primary T cells. This method was used to generate the producer cell lines 293Vec-RD114 for GFP, mCherry, CCR8, -DNR, CAR-MSLN, CCR8-CAR-MSLN, DNR-CAR-MSLN, and CCR8-DNR-CAR-MSLN or 293Vec-Eco for GFP, mCherry, H2B-Cerulean, CCR8, DNR, CCR8-DNR, CAR-EpCAM, CCR8-CAR-EpCAM, DNR-CAR-EpCAM, CCR8-DNR-CAR-EpCAM. 293Vec-Galv, 293Vec-Eco, and 293Vec-RD114 were grown as previously described (45). Primary murine and human T cells were cultured according to previously described protocols (46). All cell lines used in experiments were regularly checked for mycoplasma species with the commercial testing kit MycoAlert (Lonza). Authentication of human cell lines by STR DNA profiling analysis was conducted in-house.

**T cell generation, retroviral transduction, CRISPR, and culture**

Murine T cells have been differentiated from splenocytes from donor mice. T cell isolation and transduction have been previously described (47) and then expanded or directly expanded with T cell medium supplemented with human IL-15 (PeproTech) every second day. Human T cells have been differentiated and transduced using previously described protocols (39) or directly taken into culture with human T cell medium in concentrations of 10<sup>6</sup> T cells per milliliter medium. CCL1 knockout human T cells were generated using a two-component guide RNA (gRNA) CRISPR method as previously described (48) after magnetic removal of DynaBeads, using the EH-115 pulse code on a 4D-Nucleofector (Lonza). gRNAs [crRNA (Transactivating CRISPR RNA) CCL1 AA: TGTAACACAGGATTGCCCTCAGG; and crRNA CCL1 AF: CGGAGCAAGAGATCCCCTGAGG] were selected from CHOPCHOPv3 (49), synthesized by IDT (Integrated DNA technologies), and used simultaneously for human CCL1 knockout. T cells were used in experiments 5 days after genetic modifications.

**Migration assays**

Cell migration was evaluated using Transwell plates (Corning) as previously described (39). A total of  $5 \times 10^5$  T cells were placed on a 3- $\mu$ m pore membrane in the upper chamber of a Transwell plate

## SCIENCE ADVANCES | RESEARCH ARTICLE

with the lower chamber containing different concentrations of recombinant murine or human CCL1 (BioLegend). After 3 hours of incubation at 37°C, the migrated cells in the lower chamber were analyzed by flow cytometry.

#### Cytotoxicity assays

For impedance-based real-time killing assays using an xCELLigence system (ACEA Biosciences, USA), previously described (11),  $10^4$  tumor cells were seeded per well in a 96-well plate. The cell number was monitored over the time frame of 10 hours for every 20 min. A total of  $10^5$  T cells transduced with the indicated receptors were added to the tumor cells.

#### Cytokine protein level quantification

Murine and human IFN- $\gamma$  were quantified using ELISA sets from BD Biosciences (555138 and 555142, respectively). Murine and human CCL1 were quantified using DuoSet ELISA from R&D Systems (DY845 and DY272, respectively). Murine TGF- $\beta$  was quantified using a DuoSet ELISA from R&D Systems (DY1679). Other cytokine quantifications are further described in Supplementary Methods.

#### Proliferation assays

Proliferation was measured using a flow cytometry–based assay that compared fold proliferation of T cells over a period of 48 hours normalized to the number of T cell per condition upon assay start. Recombinant human TGF- $\beta$  (Cell Signaling Technology) or vehicle solution was added to concentrations of 20 ng/ml to test for proliferation arrest of T cells cultured with murine T cell medium supplemented with IL-15.

#### Preparation of single-cell suspensions, antibody staining, and flow cytometry

LNs (lymph nodes) and spleens were passed through 30- $\mu$ m cell strainers, followed by erythrocyte lysis in the spleens. Tumors were digested with collagenase IV (1.5 mg/ml) and deoxyribonuclease I (50 U/ml) for 30 min at 37°C under agitation. Dead cells were stained using the fixable viability violet dye Zombie Red or Violet (BioLegend) for 15 min at room temperature, followed by blocking of Fc receptors with TruStain FcX (BioLegend) for 20 min at 4°C. Following this, cell surface proteins were stained for 20 min at 4°C with anti-CCR8 (SA214G2), anti-CD4 (GK1.5), anti-CD45.1 (A20), anti-CD45.2 (104), anti-CD8 $\alpha$  (53-6.7), anti-CD90.1 (OX-7), anti-CD90.2 (30-H12), CD62L (MEL-14), and CD44 (IM7) (all from BioLegend) or anti-c-myc (SH1-26E7.1.6, Miltenyi Biotec) for detection of CAR constructs. Nuclear proteins were stained for 60 min at room temperature after permeabilization and fixation (Mouse Regulatory T cell Staining Kit, eBioscience) using Foxp3 (MF-14, BioLegend) and TGF- $\beta$  (TW7-16B4, BioLegend). Antibodies used for flow cytometry of human samples are further detailed in Supplementary Methods. Cells were analyzed on a Canto or LSRFortessa flow cytometer (BD Biosciences), and data were analyzed with FlowJo software version 9.9.5 or version 10.3.

#### PCR and quantitative RT-PCR

All DNA constructs were generated by overlap extension PCR (50) and recombinant expression cloning into the retroviral pMP71 vector (51) using standard molecular cloning protocols (50). RNA was extracted from cells using the InviTrap Spin Universal RNA

Extraction Kit (Stratagene). cDNA was synthesized using the Superscript II kit (Life Technologies). PCR primers for real-time PCR were designed automatically from the National Center for Biotechnology Information GenBank sequences in the assay design center from the Roche Universal ProbeLibrary and have been previously published (39). Real-time PCR was performed using a Kapa Probe Universal MasterMix (VWR) in a LightCycler 480 instrument (Roche Diagnostics).

#### Immunofluorescence

Tissue samples obtained from tumors were embedded and frozen in OCT (Optimal cutting temperature compound). Sections of 5  $\mu$ m were stained with a primary antibody for goat anti-CCL1 (R&D Systems) and an Alexa Fluor 488 (Life Technologies) secondary antibody and DAPI (4',6-diamidino-2-phenylindole) (VECTASHIELD) according to previously described standard procedures (52).

#### Multiphoton intravital microscopy

A total of  $5 \times 10^6$  CCR8-GFP–transduced T cells were coinjected with  $5 \times 10^6$  mCherry-transduced T cells. Tumor cells that expressed the H2B-Cerulean fluorescent protein were implanted in the back of mice after removal of hair. Five days later, a dorsal skinfold chamber was implanted around engrafted tumors through an aseptic surgical procedure under general isoflurane inhalation anesthesia and buprenorphine analgesia, as previously described (53). Mice were monitored daily for tumor growth as well as for pain and local or systemic inflammatory signs. Imaging took place every other day under isoflurane anesthesia, and Qtracker 655 nontargeted quantum dots (Invitrogen) were injected intravenously to visualize blood vessels. Multiphoton excitation was achieved with a MaiTai Ti:sapphire laser (Spectra-Physics) tuned to 950 nm to excite all fluorescent probes used. Stacks of 18 to 24 square optical sections with 500- $\mu$ m width and 4- to 5- $\mu$ m z spacing were acquired on an Ultima In Vivo multiphoton microscope (Bruker) every 60 s. Emitted fluorescence was detected through 460/50, 525/50, 595/50, and 660/40 band-pass filters and nondescanned detectors to generate four-color images. Image processing and quantification of cell motility were performed with Imaris software (Bitplane).

#### Statistical analysis

Two-tailed Student's *t* test was used for comparisons between two groups, while two-way ANOVA with Bonferroni posttest (multiple time points) or one-way ANOVA with Tukey's posttest (single time points) was used for comparisons across multiple groups. A log-rank (Mantel-Cox) test was used to compare survival curves. All statistical tests were performed with GraphPad Prism 8 software, and  $P < 0.05$  was considered statistically significant and represented as \* $P < 0.05$ , \*\* $P < 0.01$ , and \*\*\* $P < 0.001$ . No statistical methods were used to predetermine sample size. Investigators were blinded to allocation during experiments and outcome assessment.

#### SUPPLEMENTARY MATERIALS

Supplementary material for this article is available at <http://advances.sciencemag.org/cgi/content/full/7/24/eabi5781/DC1>

#### REFERENCES AND NOTES

1. M. Kalos, B. L. Levine, D. L. Porter, S. Katz, S. A. Grupp, A. Bagg, C. H. June, T cells with chimeric antigen receptors have potent antitumor effects and can establish memory in patients with advanced leukemia. *Sci. Transl. Med.* **3**, 95ra73 (2011).

## SCIENCE ADVANCES | RESEARCH ARTICLE

2. S. L. Topalian, F. S. Hodi, J. R. Brahmer, S. N. Gettinger, D. C. Smith, D. F. McDermott, J. D. Powderly, R. D. Carvajal, J. A. Sosman, M. B. Atkins, P. D. Leming, D. R. Spigel, S. J. Antonia, L. Horn, C. G. Drake, D. M. Pardoll, L. Chen, W. H. Sharfman, R. A. Anders, J. M. Taube, T. L. McMiller, H. Xu, A. J. Korman, M. Jure-Kunkel, S. Agrawal, D. McDonald, G. D. Kollia, A. Gupta, J. M. Wigginton, M. Szoln, Safety, activity, and immune correlates of anti-PD-1 antibody in cancer. *N. Engl. J. Med.* **366**, 2443–2454 (2012).
3. S. A. Roseberg, N. P. Restifo, Adoptive cell transfer as personalized immunotherapy for human cancer. *Science* **348**, 62–68 (2015).
4. M.-R. Bennebarek, H. C. Karches, L. B. Cadiha, S. Lesch, S. Endres, S. Kobold, Killing mechanisms of chimeric antigen receptor (CAR) T cells. *Int. J. Mol. Sci.* **20**, 1283 (2019).
5. J. H. Park, I. Rivière, M. Gonen, X. Wang, B. Sénéchal, K. J. Curran, C. Sauter, Y. Wang, B. Santomaso, E. Mead, M. Roshal, P. Maslak, M. Davila, R. J. Brentjens, M. Sadelain, Long-term follow-up of CD19 CAR therapy in acute lymphoblastic leukemia. *N. Engl. J. Med.* **378**, 449–459 (2018).
6. S. S. Neelapu, F. L. Locke, N. L. Bartlett, L. J. Lekakis, D. B. Miklos, C. A. Jacobson, I. Braunschweig, O. O. Oluwole, T. Siddiqui, Y. Lin, J. M. Timmerman, P. J. Stiff, J. W. Friedberg, L. W. Flinn, A. Goy, B. T. Hill, M. R. Smith, A. Deol, U. Farooq, P. McSweeney, J. Munoz, I. Avivi, J. E. Castro, J. R. Westin, J. C. Chavez, A. Ghobadi, K. V. Komanduri, R. Levy, E. D. Jacobsen, T. E. Witzig, P. Reagan, A. Bot, J. Rossi, L. Navale, Y. Jiang, J. Aycock, M. Elias, D. Chang, J. Wieszorek, W. Y. Go, Axicabtagene ciloleucel CAR T-cell therapy in refractory large B-cell lymphoma. *N. Engl. J. Med.* **377**, 2531–2544 (2017).
7. N. N. Shah, T. J. Fry, Mechanisms of resistance to CAR T cell therapy. *Nat. Rev. Clin. Oncol.* **16**, 372–385 (2019).
8. S. Stoiber, L. B. Cadiha, M.-R. Bennebarek, S. Lesch, S. Endres, S. Kobold, Limitations in the design of chimeric antigen receptors for cancer therapy. *Cell* **8**, 472 (2019).
9. P. M. Sullivan, L. Argüedas-Jimenez, A. Johnson, J. Yokoyama, Y. Yuzefpolskiy, M. Jensen, V. Kalia, S. Sarkar, A novel preclinical immunocompetent CAR T cell mouse model for solid tumors. *J. Immunol.* **202**, 71.16 (2019).
10. L. Zitvogel, J. M. Pitt, R. Daillière, M. J. Smyth, G. Kroemer, Mouse models in oncoimmunology. *Nat. Rev. Cancer* **16**, 759–773 (2016).
11. C. H. Karches, M.-R. Bennebarek, M. L. Schmidbauer, M. Kurzay, R. Klaus, M. Geiger, F. Rataj, B. L. Cadiha, S. Lesch, C. Heise, R. Murr, J. vom Berg, M. Jastroch, D. Lamp, J. Ding, P. Duestel, G. Niederfellner, C. Sustmann, S. Endres, C. Klein, S. Kobold, Bispecific antibodies enable synthetic agonistic receptor-transduced T cells for tumor immunotherapy. *Clin. Cancer Res.* **25**, 5890–5900 (2019).
12. M. P. Avanzi, O. Yeku, X. Li, D. P. Wijewarnasuriya, D. G. van Leeuwen, K. Cheung, H. Park, T. J. Purdon, A. F. Daniyan, M. H. Spitzer, R. J. Brentjens, Engineered tumor-targeted T cells mediate enhanced anti-tumor efficacy both directly and through activation of the endogenous immune system. *Cell Rep.* **23**, 2130–2141 (2018).
13. S. Viaud, J. S. Y. Ma, I. R. Hardy, E. N. Hampton, B. Benish, L. Sherwood, V. Nunez, C. J. Ackerman, K. Khialeeva, M. Weglarz, S. C. Lee, A. K. Woods, T. S. Young, Switchable control over in vivo CAR T expansion, B cell depletion, and induction of memory. *Proc. Natl. Acad. Sci. U.S.A.* **115**, E10898–E10906 (2018).
14. W. A. Lim, C. H. June, The principles of engineering immune cells to treat cancer. *Cell* **168**, 724–740 (2017).
15. G. Pitas, C. Konopacki, K. Wu, P. D. Bos, M. Morrow, E. V. Putintseva, D. M. Chudakov, A. Y. Rudensky, Regulatory T cells exhibit distinct features in human breast cancer. *Immunity* **45**, 1122–1134 (2016).
16. Y. Barsheshet, G. Wildbaum, E. Levy, A. Vitenshtein, C. Akinseye, J. Griggs, S. A. Lira, N. Karin, CCR8<sup>hi</sup>FOXP3<sup>+</sup> Treg cells as master drivers of immune regulation. *Proc. Natl. Acad. Sci. U.S.A.* **114**, 6086–6091 (2017).
17. R. Wieser, L. Attisano, J. L. Wrana, J. Massagué, Signaling activity of transforming growth factor beta type II receptors lacking specific domains in the cytoplasmic region. *Mol. Cell. Biol.* **13**, 7239–7247 (1993).
18. C. C. Kloss, J. Lee, A. Zhang, F. Chen, J. J. Melenhorst, S. F. Lacey, M. V. Maus, J. A. Fraietta, Y. Zhao, C. H. June, Dominant-negative TGF- $\beta$  receptor enhances PSMA-targeted human CAR T cell proliferation and augments prostate cancer eradication. *Mol. Ther.* **26**, 1855–1866 (2018).
19. M. D. Miller, S. Hata, R. De Waal Malefyt, M. S. Krangel, A novel polypeptide secreted by activated human T lymphocytes. *J. Immunol.* **143**, 2907–2916 (1989).
20. M. D. Miller, M. S. Krangel, The human cytokine I-309 is a monocyte chemoattractant. *Proc. Natl. Acad. Sci. U.S.A.* **89**, 2950–2954 (1992).
21. T. J. Curiel, G. Coukos, L. Zou, X. Alvarez, P. Cheng, P. Mottram, M. Evdeomon-Hogan, J. R. Conejo-Garcia, L. Zhang, M. Burow, Y. Zhu, S. Wei, I. Kryczek, B. Daniel, A. Gordon, L. Myers, A. Lackner, M. L. Disis, K. L. Knutson, L. Chen, W. Zou, Specific recruitment of regulatory T cells in ovarian carcinoma fosters immune privilege and predicts reduced survival. *Nat. Med.* **10**, 942–949 (2004).
22. T. Brand, W. R. MacLellan, M. D. Schneider, A dominant-negative receptor for type beta transforming growth factors created by deletion of the kinase domain. *J. Biol. Chem.* **268**, 11500–11503 (1993).
23. C. M. Bolland, T. Tripic, C. R. Cruz, G. Dotti, S. Gottschalk, V. Torrono, O. Dakhova, G. Carrum, C. A. Ramos, H. Liu, M. F. Wu, A. N. Marcogliese, C. Barese, Y. Zu, Y. D. Lee, O. O'Connor, A. P. Gee, M. K. Brenner, H. E. Heslop, C. M. Rooney, Tumor-specific T-cells engineered to overcome tumor immune evasion induce clinical responses in patients with relapsed Hodgkin lymphoma. *J. Clin. Oncol.* **36**, 1128–1139 (2018).
24. P. S. Adusumilli, L. Cherkassky, J. Villena-Vargas, C. Colovos, E. Servais, J. Plotkin, D. R. Jones, M. Sadelain, Regional delivery of mesothelin-targeted CAR T cell therapy generates potent and long-lasting CD4-dependent tumor immunity. *Sci. Transl. Med.* **6**, 261ra151 (2014).
25. R. J. Brentjens, M. L. Davila, I. Riviere, J. Park, X. Wang, L. G. Cowell, S. Bartido, J. Stefanski, C. Taylor, M. Olszewska, O. Borquez-Ojeda, J. Qu, T. Wasielawska, Q. He, Y. Bernal, I. V. Rijo, C. Hedvat, R. Kobos, K. Curran, P. Steinhilber, J. Jurcic, T. Rosenblatt, P. Maslak, M. Frattini, M. Sadelain, CD19-targeted T cells rapidly induce molecular remissions in adults with chemotherapy-refractory acute lymphoblastic leukemia. *Sci. Transl. Med.* **5**, 177ra38 (2013).
26. A. Di Stasi, B. De Angelis, C. M. Rooney, L. Zhang, A. Mahendravada, A. E. Foster, H. E. Heslop, M. K. Brenner, G. Dotti, B. Savoldo, T lymphocytes coexpressing CCR4 and a chimeric antigen receptor targeting CD30 have improved homing and antitumor activity in a Hodgkin tumor model. *Blood* **113**, 6392–6402 (2009).
27. B. Molon, S. Ugel, F. Del Pozzo, C. Soldani, S. Zilio, D. Avela, A. De Palma, P. Mauri, A. Monegal, M. Rescigno, B. Savino, P. Colombo, N. Jonjić, S. Pecanica, L. Lazzarato, R. Fruttero, A. Gasco, V. Bronte, A. Viola, Chemokine nitration prevents intratumoral infiltration of antigen-specific T cells. *J. Exp. Med.* **208**, 1949–1962 (2011).
28. G. D'Amico, G. Frascaroli, G. Bianchi, P. Transidico, A. Doni, A. Vecchi, S. Sozzani, P. Allavena, A. Mantovani, Uncoupling of inflammatory chemokine receptors by IL-10: Generation of functional decoys. *Nat. Immunol.* **1**, 387–391 (2000).
29. M. H. Kershaw, G. Wang, J. A. Westwood, R. K. Pachynski, H. L. Tiffany, F. M. Marincola, E. Wang, H. A. Young, P. M. Murphy, P. Hwu, Redirecting migration of T cells to chemokine secreted from tumors by genetic modification with CXCR2. *Hum. Gene Ther.* **13**, 1971–1980 (2002).
30. J. A. Craddock, A. Lu, A. Bear, M. Pule, M. K. Brenner, C. M. Rooney, A. E. Foster, Enhanced tumor trafficking of GD2 chimeric antigen receptor T cells by expression of the chemokine receptor CCR2b. *J. Immunother.* **33**, 780–788 (2010).
31. I. Siddiqui, M. Erreni, M. van Brakel, R. Debets, P. Allavena, Enhanced recruitment of genetically modified CX3CR1-positive human T cells into Fractalkine/CX3CL1 expressing tumors: Importance of the chemokine gradient. *J. Immunother. Cancer* **4**, 21 (2016).
32. D. R. Principe, B. DeCant, E. Mascariñas, E. A. Wayne, A. M. Diaz, N. Diaz, R. Hwang, B. Pasche, D. W. Dawson, D. Fang, D. J. Bentrem, H. G. Munshi, B. Jung, P. J. Grippo, TGF $\beta$  signaling in the pancreatic tumor microenvironment promotes fibrosis and immune evasion to facilitate tumorigenesis. *Cancer Res.* **76**, 2525–2539 (2016).
33. L. Gorelik, R. A. Flavell, Transforming growth factor-beta in T-cell biology. *Nat. Rev. Immunol.* **2**, 46–53 (2002).
34. D. A. Thomas, J. Massagué, TGF- $\beta$  directly targets cytotoxic T cell functions during tumor evasion of immune surveillance. *Cancer Cell* **8**, 369–380 (2005).
35. G. A. Rabinovich, D. Gabrilovich, E. M. Sotomayor, Immunosuppressive strategies that are mediated by tumor cells. *Annu. Rev. Immunol.* **25**, 267–296 (2007).
36. J. Eyquem, J. Mansilla-Soto, T. Giavridis, S. J. van der Stegen, M. Hamieh, K. M. Cunanan, A. Odak, M. Gonen, M. Sadelain, Targeting a CAR to the TRAC locus with CRISPR/Cas9 enhances tumour rejection. *Nature* **543**, 113–117 (2017).
37. J. Feucht, J. Sun, J. Eyquem, Y. J. Ho, Z. Zhao, J. Leibold, A. Dobrin, A. Cabriolu, M. Hamieh, M. Sadelain, Calibration of CAR activation potential directs alternative T cell fates and therapeutic potency. *Nat. Med.* **25**, 82–88 (2019).
38. C. S. Hinrichs, N. P. Restifo, Reassessing target antigens for adoptive T-cell therapy. *Nat. Biotechnol.* **31**, 999–1008 (2013).
39. M. Rapp, S. Grassmann, M. Chaloupka, P. Layritz, S. Kruger, S. Ormanns, F. Rataj, K.-P. Janssen, S. Endres, D. Anz, S. Kobold, C-C chemokine receptor type-4 transduction of T cells enhances interaction with dendritic cells, tumor infiltration and therapeutic efficacy of adoptive T cell transfer. *Onco. Targets. Ther.* **5**, e1105428 (2015).
40. E. J. Cheadle, V. Sheard, D. G. Rothwell, J. S. Bridgeman, G. Ashton, V. Hanson, A. W. Mansoor, R. E. Hawkins, D. E. Gilham, Differential role of Th1 and Th2 cytokines in autotoxicity driven by CD19-specific second-generation chimeric antigen receptor T cells in a mouse model. *J. Immunol.* **192**, 3654–3665 (2014).
41. J. N. Brudno, J. N. Kochenderfer, Toxicities of chimeric antigen receptor T cells: Recognition and management. *Blood* **127**, 3321–3330 (2016).
42. L. Gorelik, R. A. Flavell, Abrogation of TGF $\beta$  signaling in T cells leads to spontaneous T cell differentiation and autoimmune disease. *Immunity* **12**, 171–181 (2000).
43. P. J. Lucas, S. J. Kim, S. J. Melby, R. E. Gress, Disruption of T cell homeostasis in mice expressing a T cell-specific dominant negative transforming growth factor  $\beta$  II receptor. *J. Exp. Med.* **191**, 1187–1196 (2000).
44. T. Kamada, Y. Togashi, C. Tay, D. Ha, A. Sasaki, Y. Nakamura, E. Sato, S. Fukuoka, Y. Tada, A. Tanaka, H. Morikawa, A. Kawazoe, T. Kinoshita, K. Shitara, S. Sakaguchi, H. Nishikawa, PD-1<sup>+</sup> regulatory T cells amplified by PD-1 blockade promote hyperprogression of cancer. *Proc. Natl. Acad. Sci. U.S.A.* **116**, 9999–10008 (2019).

## SCIENCE ADVANCES | RESEARCH ARTICLE

45. K. Ghani, X. Wang, P. O. de Campos-Lima, M. Olszewska, A. Kamen, I. Riviere, M. Caruso, Efficient human hematopoietic cell transduction using RD114- and GALV-pseudotyped retroviral vectors produced in suspension and serum-free media. *Hum. Gene Ther.* **20**, 966–974 (2009).
46. S. Kobold, S. Grassmann, M. Chaloupka, C. Lampert, S. Wenk, F. Kraus, M. Rapp, P. Duwell, Y. Zeng, J. C. Schmollinger, M. Schnurr, S. Endres, S. Rothenfußer, Impact of a new fusion receptor on PD-1-mediated immunosuppression in adoptive T cell therapy. *J. Natl. Cancer Inst.* **107**, djv146 (2015).
47. M.-R. Benmebarek, B. L. Cadilha, M. Herrmann, S. Lesch, S. Schmitt, S. Stoiber, A. Darwich, C. Augsburg, B. Brauchle, L. Rohrbacher, A. Oner, M. Seifert, M. Schwerdtfeger, A. Gottschlich, F. Rajat, N. C. Fenn, K. Klein, M. Subklewe, S. Endres, K.-P. Hopfner, S. Kobold, A modular and controllable T cell therapy platform for acute myeloid leukemia. *Leukemia*, 1–15 (2021).
48. S. A. Oh, A. Seki, S. Rutz, Ribonucleoprotein transfection for CRISPR/Cas9-mediated gene knockout in primary T cells. *Curr. Protoc. Immunol.* **124**, e69 (2019).
49. K. Labun, T. G. Montague, M. Krause, Y. N. Torres Cleuren, H. Tjeldnes, E. Valen, CHOPCHOP v3: Expanding the CRISPR web toolbox beyond genome editing. *Nucleic Acids Res.* **47**, W171–W174 (2019).
50. K. L. Heckman, L. R. Pease, Gene splicing and mutagenesis by PCR-driven overlap extension. *Nat. Protoc.* **2**, 924–932 (2007).
51. D. Sommermeyer, J. Neudorfer, M. Weinhold, M. Leisegang, B. Engels, E. Noessner, M. H. Heemskerck, J. Charo, D. J. Schendel, T. Blankenstein, H. Bernhard, W. Uckert, Designer T cells by T cell receptor replacement. *Eur. J. Immunol.* **36**, 3052–3059 (2006).
52. S. Das, E. Sarrou, S. Podgrabinska, M. Cassella, S. K. Mungamuri, N. Feirt, R. Gordon, C. S. Nagi, Y. Wang, D. Entenberg, J. Condeelis, M. Skobe, Tumor cell entry into the lymph node is controlled by CCL1 chemokine expressed by lymph node lymphatic sinuses. *J. Exp. Med.* **210**, 1509–1528 (2013).
53. C. A. Bauer, E. Y. Kim, F. Marangoni, E. Carrizosa, N. M. Claudio, T. R. Mempel, Dynamic Treg interactions with intratumoral APCs promote local CTL dysfunction. *J. Clin. Invest.* **124**, 2425–2440 (2014).
54. P. Jiang, S. Gu, D. Pan, J. Fu, A. Sahu, X. Hu, Z. Li, N. Traugh, X. Bu, B. Li, J. Liu, G. J. Freeman, M. A. Brown, K. W. Wucherpfennig, X. S. Liu, Signatures of T cell dysfunction and exclusion predict cancer immunotherapy response. *Nat. Med.* **24**, 1550–1558 (2018).
55. V. Thorsson, D. L. Gibbs, S. D. Brown, D. Wolf, D. S. Bortone, T. H. O. Yang, E. Porta-Pardo, G. F. Gao, C. L. Plaisier, J. A. Eddy, E. Ziv, A. C. Culhane, E. O. Paull, I. K. A. Sivakumar, A. J. Gentes, R. Malhotra, F. Farshidfar, A. Colaprico, J. S. Parker, L. E. Mose, N. S. Vo, J. Liu, Y. Liu, J. Rader, V. Dhankani, S. M. Reynolds, R. Bowlby, A. Califano, A. D. Cherniack, D. Anastassiou, D. Bedognetti, Y. Mokrab, A. M. Newman, A. Rao, K. Chen, A. Krasnitz, H. Hu, T. M. Malta, H. Noushmehr, C. S. Pedamallu, S. Bullman, A. I. Ojesina, A. Lamb, W. Zhou, H. Shen, T. K. Choueiri, J. N. Weinstein, J. Guinney, J. Saltz, R. A. Holt, C. S. Rabkin, A. J. Lazar, J. S. Serody, E. G. Demicco, M. L. Disis, B. G. Vincent, I. Shmulevich, The immune landscape of cancer. *Immunity* **48**, 812–830.e14 (2018).

**Acknowledgments:** We acknowledge the reviewers of this manuscript for critical input that strengthened the data herein presented. The results published here are in part based on data generated by the TCGA Research Network: <http://cancergenome.nih.gov/>. We acknowledge

Life Science Editors for editing assistance. We acknowledge the iFlow Core Facility of the LMU University Hospital for assistance with the generation of flow cytometry data. **Funding:** This study was supported by the International Doctoral Program I-Target: Immunotargeting of Cancer funded by the Elite Network of Bavaria (to S.K. and S.E.), by the Melanoma Research Alliance Grants 409510 (to S.K.), by the Marie-Sklodowska-Curie Program Training Network for the Immunotherapy of Cancer funded by the H2020 Program of the European Union (grant 641549 to S.E. and S.K.), by the Marie-Sklodowska-Curie Program Training Network for Optimizing Adoptive T Cell Therapy of Cancer funded by the H2020 Program of the European Union (grant 955575 to S.K.), by the Hector foundation (to S.K.), by the Else Kröner-Fresenius-Stiftung (to S.K.), by the German Cancer Aid (to S.K.), by the Ernst-Jung-Stiftung (to S.K.), by the LMU Munich's Institutional Strategy LMUexcellent within the framework of the German Excellence Initiative (to S.E. and S.K.), by the Bundesministerium für Bildung und Forschung Project Oncocontract (to S.E. and S.K.), by the European Research Council Grant 756017, ARMOR-T (to S.K.), by the German Research Foundation (DFG to S.K.), by the NIH grant AI123349 (to T.R.M.), by the Deutsche Gesellschaft für Immun- und Targeted-therapie (to B.L.C.), by the Fritz-Bender Foundation (to S.K.), by the European Research Council (ERC) under the European Union's Horizon 2020 research and innovation program (grant agreement no. 866411) (to C.M.), by the Volkswagen Foundation (project OntoTime) (to M.T.), and the José-Carreras Foundation (to S.K.). **Author contributions:** B.L.C. and M.-R.B. designed and performed experiments, analyzed the data, and wrote the manuscript; K.D., A.O., T.L., H.O., M.V., M.D.P., J.N.P., S.S., D.H., F.M., M.S., K.M., J.S.-G., and Y.Z. performed experiments and analyzed the data; S.L., C.H.K., A.G., M.T., C.M., J.Z., D.P., T.F., and M.S. provided technical and theoretical assistance; T.R.M. and S.E. supervised the project and designed experiments; S.K. conceived the study, supervised the project, designed experiments, and wrote the manuscript. **Competing interests:** Parts of this work have been performed for the thesis of B.L.C., K.D., and Y.Z. B.L.C., S.E., and S.K. are inventors on a patent application filed by Klinikum der Universität München (no. WO 2020/182681 A1, filed 6 March 2020, published 17 September 2020). S.E. and S.K. have received research support from TCR<sup>2</sup> Inc. and Arcus Biosciences for work unrelated to the present manuscript. S.K. has received honoraria from Novartis and TCR<sup>2</sup> Inc. The authors declare that they have no other competing interests. **Data and materials availability:** All data needed to evaluate the conclusions in the paper are present in the paper and/or the Supplementary Materials. Additional data related to this paper may be requested from the authors.

Submitted 17 March 2021

Accepted 21 April 2021

Published 9 June 2021

10.1126/sciadv.abi5781

**Citation:** B. L. Cadilha, M.-R. Benmebarek, K. Dorman, A. Oner, T. Lorenzini, H. Obeck, M. Vanttinen, M. Di Pilato, J. N. Pruessmann, S. Stoiber, D. Huynh, F. Märkl, M. Seifert, K. Manske, J. Suarez-Gosalvez, Y. Zeng, S. Lesch, C. H. Karches, C. Heise, A. Gottschlich, M. Thomas, C. Marr, J. Zhang, D. Pandey, T. Feuchtinger, M. Subklewe, T. R. Mempel, S. Endres, S. Kobold, Combined tumor-directed recruitment and protection from immune suppression enable CAR T cell efficacy in solid tumors. *Sci. Adv.* **7**, eabi5781 (2021).



## References

Anurathapan U, Chan RC, Hindi HF, Mucharla R, Bajgain P, Hayes BC, Fisher WE, Heslop HE, Rooney CM, Brenner MK, Leen AM, & Vera JF.

Kinetics of tumor destruction by chimeric antigen receptor-modified T cells.  
*Molecular Therapy* 2014; 22(3):623-633.

Asmamaw Dejenie T, Tiruneh GMM, Dessie Terefe G, Tadele Admasu F, Wale Tesega W, & Chekol Abebe E.

Current updates on generations, approvals, and clinical trials of CAR T-cell therapy.

*Human Vaccines & Immunotherapeutics* 2022; 18(6):2114254.

Barnes TA, & Amir E.

HYPE or HOPE: the prognostic value of infiltrating immune cells in cancer.

*British Journal of Cancer* 2018; 118(2):e5.

Benmeharek MR, Cadilha BL, Herrmann M, Lesch S, Schmitt S, Stoiber S, Darwich A, Augsberger C, Brauchle B, Rohrbacher L, Oner A, Seifert M, Schwerdtfeger M, Gottschlich A, Rataj F, Fenn NC, Klein C, Subklewe M, Endres S, Hopfner KP, & Kobold S.

A modular and controllable T cell therapy platform for acute myeloid leukemia.

*Leukemia* 2021; 35(8):2243-2257.

Bollard CM, Rossig C, Calonge MJ, Huls MH, Wagner HJ, Massague J, Brenner MK, Heslop HE, & Rooney CM.

Adapting a transforming growth factor beta-related tumor protection strategy to enhance antitumor immunity.

*Blood* 2002; 99(9):3179-3187.

Budhu S, Schaer DA, Li Y, Toledo-Crow R, Panageas K, Yang X, Zhong H, Houghton AN, Silverstein SC, Merghoub T, & Wolchok JD.

Blockade of surface-bound TGF-beta on regulatory T cells abrogates suppression of effector T cell function in the tumor microenvironment.

*Science Signaling* 2017; 10(494).

Burnet M.

Cancer; a biological approach. I. The processes of control.

*British Medical Journal* 1957; 1(5022):779-786.

Cadilha BL, Benmeharek MR, Dorman K, Oner A, Lorenzini T, Obeck H, Vanttinen M, Di Pilato M, Pruessmann JN, Stoiber S, Huynh D, Markl F, Seifert M, Manske K, Suarez-Gosalvez J, Zeng Y, Lesch S, Karches CH, Heise C, Gottschlich A, Thomas M, Marr C, Zhang J, Pandey D, Feuchtinger T, Subklewe M, Mempel TR, Endres S, & Kobold S.

Combined tumor-directed recruitment and protection from immune suppression enable CAR T cell efficacy in solid tumors.

*Science Advances* 2021; 7(24).

Chen K, Wang S, Qi D, Ma P, Fang Y, Jiang N, Wu E, & Li N.  
Clinical investigations of CAR-T cell therapy for solid tumors.  
*Frontiers in Immunology* 2022; 13(896685).

Cohen MH, Williams G, Johnson JR, Duan J, Gobburu J, Rahman A, Benson K, Leighton J, Kim SK, Wood R, Rothmann M, Chen G, U KM, Staten AM, & Pazdur R.

Approval summary for imatinib mesylate capsules in the treatment of chronic myelogenous leukemia.

*Clinical Cancer Research* 2002; 8(5):935-942.

Coley WB.

The treatment of malignant tumors by repeated inoculations of erysipelas. With a report of ten original cases.

*American Journal of the Medical Sciences* 1893; 487–511.

Dighe AS, Richards E, Old LJ, & Schreiber RD.

Enhanced in vivo growth and resistance to rejection of tumor cells expressing dominant negative IFN gamma receptors.

*Immunity* 1994; 1(6):447-456.

Dunn GP, Bruce AT, Ikeda H, Old LJ, & Schreiber RD.

Cancer immunoediting: from immunosurveillance to tumor escape.

*Nature Immunology* 2002; 3(11):991-998.

Dunn GP, Old LJ, & Schreiber RD.

The immunobiology of cancer immunosurveillance and immunoediting.

*Immunity* 2004a; 21(2):137-148.

Dunn GP, Old LJ, & Schreiber RD.

The three Es of cancer immunoediting.

*Annual Review of Immunology* 2004b; 22(329-360).

Durbin JE, Hackenmiller R, Simon MC, & Levy DE.

Targeted disruption of the mouse Stat1 gene results in compromised innate immunity to viral disease.

*Cell* 1996; 84(3):443-450.

Ehrlich P.

Über den jetzigen Stand der Karzinomforschung.

*Nederlands Tijdschrift voor Geneeskunde* 1909; 5(273–290).

Ellis GI, Sheppard NC, & Riley JL.

Genetic engineering of T cells for immunotherapy.

*Nature Reviews Genetics* 2021; 22(7):427-447.

- Galon J, & Bruni D.  
Tumor immunology and tumor evolution: Intertwined histories.  
*Immunity* 2020; 52(1):55-81.
- Gu T, Zhu M, Huang H, & Hu Y.  
Relapse after CAR-T cell therapy in B-cell malignancies: challenges and future approaches.  
*Journal of Zhejiang University-SCIENCE B* 2022; 23(10):793-811.
- Guedan S, Calderon H, Posey AD, Jr., & Maus MV.  
Engineering and design of chimeric antigen receptors.  
*Molecular Therapy—Methods & Clinical Development* 2019; 12(145-156).
- Guo F, & Cui J.  
CAR-T in solid tumors: Blazing a new trail through the brambles.  
*Life Sciences* 2020; 260(118300).
- Gupta P, Han SY, Holgado-Madruga M, Mitra SS, Li G, Nitta RT, & Wong AJ.  
Development of an EGFRvIII specific recombinant antibody.  
*BMC Biotechnology* 2010; 10(72).
- Hanahan D, & Coussens LM.  
Accessories to the crime: functions of cells recruited to the tumor microenvironment.  
*Cancer Cell* 2012; 21(3):309-322.
- Hanahan D, & Weinberg RA.  
The hallmarks of cancer.  
*Cell* 2000; 100(1):57-70.
- Harlin H, Meng Y, Peterson AC, Zha Y, Tretiakova M, Slingluff C, McKee M, & Gajewski TF.  
Chemokine expression in melanoma metastases associated with CD8+ T-cell recruitment.  
*Cancer Research* 2009; 69(7):3077-3085.
- Heiskala M, Leidenius M, Joensuu K, & Heikkilä P.  
High expression of CCL2 in tumor cells and abundant infiltration with CD14 positive macrophages predict early relapse in breast cancer.  
*Virchows Archiv* 2019; 474(1):3-12.
- Henze J, Tacke F, Hardt O, Alves F, & Al Rawashdeh W.  
Enhancing the efficacy of CAR T cells in the tumor microenvironment of pancreatic cancer.  
*Cancers* 2020; 12(6).

- Hirabayashi K, Du H, Xu Y, Shou P, Zhou X, Fuca G, Landoni E, Sun C, Chen Y, Savoldo B, & Dotti G.  
Dual targeting CAR-T cells with optimal costimulation and metabolic fitness enhance antitumor activity and prevent escape in solid tumors.  
*Nature Cancer* 2021; 2(9):904-918.
- Hogquist KA, & Jameson SC.  
The self-obsession of T cells: how TCR signaling thresholds affect fate 'decisions' and effector function.  
*Nature Immunology* 2014; 15(9):815-823.
- Hong M, Clubb JD, & Chen YY.  
Engineering CAR-T cells for next-generation cancer therapy.  
*Cancer Cell* 2020; 38(4):473-488.
- Huang J, Brameshuber M, Zeng X, Xie J, Li QJ, Chien YH, Valitutti S, & Davis MM.  
A single peptide-major histocompatibility complex ligand triggers digital cytokine secretion in CD4(+) T cells.  
*Immunity* 2013; 39(5):846-857.
- Huang J, Huang X, & Huang J.  
CAR-T cell therapy for hematological malignancies: Limitations and optimization strategies.  
*Frontiers in Immunology* 2022; 13(1019115).
- Iwai Y, Ishida M, Tanaka Y, Okazaki T, Honjo T, & Minato N.  
Involvement of PD-L1 on tumor cells in the escape from host immune system and tumor immunotherapy by PD-L1 blockade.  
*Proceedings of the National Academy of Sciences of the United States of America* 2002; 99(19):12293-12297.
- Johnson DB, Nebhan CA, Moslehi JJ, & Balko JM.  
Immune-checkpoint inhibitors: long-term implications of toxicity.  
*Nature Reviews: Clinical Oncology* 2022; 19(4):254-267.
- Karches CH, Benmebarek MR, Schmidbauer ML, Kurzay M, Klaus R, Geiger M, Rataj F, Cadilha BL, Lesch S, Heise C, Murr R, Vom Berg J, Jastroch M, Lamp D, Ding J, DUEWELL P, Niederfellner G, Sustmann C, Endres S, Klein C, & Kobold S.  
Bispecific antibodies enable synthetic agonistic receptor-transduced T cells for tumor immunotherapy.  
*Clinical Cancer Research* 2019; 25(19):5890-5900.
- Kershaw MH, Westwood JA, Parker LL, Wang G, Eshhar Z, Mavroukakis SA, White DE, Wunderlich JR, Canevari S, Rogers-Freezer L, Chen CC, Yang JC, Rosenberg SA, & Hwu P.

A phase I study on adoptive immunotherapy using gene-modified T cells for ovarian cancer.

*Clinical Cancer Research* 2006; 12(20 Pt 1):6106-6115.

Khong HT, Wang QJ, & Rosenberg SA.

Identification of multiple antigens recognized by tumor-infiltrating lymphocytes from a single patient: tumor escape by antigen loss and loss of MHC expression.

*Journal of Immunotherapy* 2004; 27(3):184-190.

Kloss CC, Lee J, Zhang A, Chen F, Melenhorst JJ, Lacey SF, Maus MV, Fraietta JA, Zhao Y, & June CH.

Dominant-negative TGF-beta receptor enhances PSMA-targeted human CAR T cell proliferation and augments prostate cancer eradication.

*Molecular Therapy* 2018; 26(7):1855-1866.

Kuehnemuth B, Piseddu I, Wiedemann GM, Lauseker M, Kuhn C, Hofmann S, Schmoeckel E, Endres S, Mayr D, Jeschke U, & Anz D.

CCL1 is a major regulatory T cell attracting factor in human breast cancer.

*BMC Cancer* 2018; 18(1):1278.

Leach DR, Krummel MF, & Allison JP.

Enhancement of antitumor immunity by CTLA-4 blockade.

*Science* 1996; 271(5256):1734-1736.

Lesch S, Blumenberg V, Stoiber S, Gottschlich A, Ogonek J, Cadilha BL, Dantes Z, Rataj F, Dorman K, Lutz J, Karches CH, Heise C, Kurzay M, Larimer BM, Grassmann S, Rapp M, Nottebrock A, Kruger S, Tokarew N, Metzger P, Hoerth C, Benmeharek MR, Dhoqina D, Grunmeier R, Seifert M, Oener A, Umut O, Joaquina S, Vimeux L, Tran T, Hank T, Baba T, Huynh D, Megens RTA, Janssen KP, Jastroch M, Lamp D, Ruehland S, Di Pilato M, Pruessmann JN, Thomas M, Marr C, Ormanns S, Reischer A, Hristov M, Tartour E, Donnadiou E, Rothenfusser S, Duewell P, Konig LM, Schnurr M, Subklewe M, Liss AS, Halama N, Reichert M, Mempel TR, Endres S, & Kobold S.

T cells armed with C-X-C chemokine receptor type 6 enhance adoptive cell therapy for pancreatic tumours.

*Nature Biomedical Engineering* 2021; 5(11):1246-1260.

Lohmueller JJ, Ham JD, Kvorjak M, & Finn OJ.

mSA2 affinity-enhanced biotin-binding CAR T cells for universal tumor targeting.

*Oncoimmunology* 2017; 7(1):e1368604.

Markl F, Huynh D, Endres S, & Kobold S.

Utilizing chemokines in cancer immunotherapy.

*Trends Cancer* 2022; 8(8):670-682.

Marofi F, Motavalli R, Safonov VA, Thangavelu L, Yumashev AV, Alexander M, Shomali N, Chartrand MS, Pathak Y, Jarahian M, Izadi S, Hassanzadeh A, Shirafkan N, Tahmasebi S, & Khiavi FM.

CAR T cells in solid tumors: challenges and opportunities.

*Stem Cell Research & Therapy* 2021; 12(1):81.

Martinez M, & Moon EK.

CAR T cells for solid tumors: New strategies for finding, infiltrating, and surviving in the tumor microenvironment.

*Frontiers in Immunology* 2019; 10(128).

Maude SL, Frey N, Shaw PA, Aplenc R, Barrett DM, Bunin NJ, Chew A, Gonzalez VE, Zheng Z, Lacey SF, Mahnke YD, Melenhorst JJ, Rheingold SR, Shen A, Teachey DT, Levine BL, June CH, Porter DL, & Grupp SA.

Chimeric antigen receptor T cells for sustained remissions in leukemia.

*New England Journal of Medicine* 2014; 371(16):1507-1517.

Maude SL, Laetsch TW, Buechner J, Rives S, Boyer M, Bittencourt H, Bader P, Verneris MR, Stefanski HE, Myers GD, Qayed M, De Moerloose B, Hiramatsu H, Schlis K, Davis KL, Martin PL, Nemecek ER, Yanik GA, Peters C, Baruchel A, Boissel N, Mechinaud F, Balduzzi A, Krueger J, June CH, Levine BL, Wood P, Taran T, Leung M, Mueller KT, Zhang Y, Sen K, Lebwohl D, Pulsipher MA, & Grupp SA.

Tisagenlecleucel in children and young adults with B-cell lymphoblastic leukemia.

*New England Journal of Medicine* 2018; 378(5):439-448.

Meraz MA, White JM, Sheehan KC, Bach EA, Rodig SJ, Dighe AS, Kaplan DH, Riley JK, Greenlund AC, Campbell D, Carver-Moore K, DuBois RN, Clark R, Aguet M, & Schreiber RD.

Targeted disruption of the Stat1 gene in mice reveals unexpected physiologic specificity in the JAK-STAT signaling pathway.

*Cell* 1996; 84(3):431-442.

Montano N, Cenci T, Martini M, D'Alessandris QG, Pelacchi F, Ricci-Vitiani L, Maira G, De Maria R, Larocca LM, & Pallini R.

Expression of EGFRvIII in glioblastoma: prognostic significance revisited.

*Neoplasia* 2011; 13(12):1113-1121.

Moon EK, Wang LS, Bekdache K, Lynn RC, Lo A, Thorne SH, & Albelda SM. Intra-tumoral delivery of CXCL11 via a vaccinia virus, but not by modified T cells, enhances the efficacy of adoptive T cell therapy and vaccines.

*Oncoimmunology* 2018; 7(3):e1395997.

Mulligan AM, Raitman I, Feeley L, Pinnaduwa D, Nguyen LT, O'Malley FP, Ohashi PS, & Andrulis IL.

Tumoral lymphocytic infiltration and expression of the chemokine CXCL10 in breast cancers from the Ontario Familial Breast Cancer Registry.  
*Clinical Cancer Research* 2013; 19(2):336-346.

Musha H, Ohtani H, Mizoi T, Kinouchi M, Nakayama T, Shiiba K, Miyagawa K, Nagura H, Yoshie O, & Sasaki I.  
Selective infiltration of CCR5(+)CXCR3(+) T lymphocytes in human colorectal carcinoma.  
*International Journal of Cancer* 2005; 116(6):949-956.

Nagarsheth N, Wicha MS, & Zou W.  
Chemokines in the cancer microenvironment and their relevance in cancer immunotherapy.  
*Nature Reviews: Immunology* 2017; 17(9):559-572.

Nakazawa T, Natsume A, Nishimura F, Morimoto T, Matsuda R, Nakamura M, Yamada S, Nakagawa I, Motoyama Y, Park YS, Tsujimura T, Wakabayashi T, & Nakase H.  
Effect of CRISPR/Cas9-mediated PD-1-disrupted primary human third-generation CAR-T cells targeting EGFRvIII on in vitro human glioblastoma cell growth.  
*Cells* 2020; 9(4).

Naran K, Nundalall T, Chetty S, & Barth S.  
Principles of immunotherapy: Implications for treatment strategies in cancer and infectious diseases.  
*Frontiers in Microbiology* 2018; 9(3158).

Nishimura H, Nose M, Hiai H, Minato N, & Honjo T.  
Development of lupus-like autoimmune diseases by disruption of the PD-1 gene encoding an ITIM motif-carrying immunoreceptor.  
*Immunity* 1999; 11(2):141-151.

Pak MG, Shin DH, Lee CH, & Lee MK.  
Significance of EpCAM and TROP2 expression in non-small cell lung cancer.  
*World Journal of Surgical Oncology* 2012; 10(53).

Pradeu T.  
Philosophy of immunology.  
*eLife* 2020; 8(47384).

Qian BZ, Li J, Zhang H, Kitamura T, Zhang J, Campion LR, Kaiser EA, Snyder LA, & Pollard JW.  
CCL2 recruits inflammatory monocytes to facilitate breast-tumour metastasis.  
*Nature* 2011; 475(7355):222-225.

Rohaan MW, Wilgenhof S, & Haanen J.

Adoptive cellular therapies: the current landscape.

*Virchows Archiv* 2019; 474(4):449-461.

Rosenberg SA, Packard BS, Aebersold PM, Solomon D, Topalian SL, Toy ST, Simon P, Lotze MT, Yang JC, Seipp CA, & et al.

Use of tumor-infiltrating lymphocytes and interleukin-2 in the immunotherapy of patients with metastatic melanoma. A preliminary report.

*New England Journal of Medicine* 1988; 319(25):1676-1680.

Schreiber RD, Old LJ, & Smyth MJ.

Cancer immunoediting: integrating immunity's roles in cancer suppression and promotion.

*Science* 2011; 331(6024):1565-1570.

Shafer P, Kelly LM, & Hoyos V.

Cancer therapy with TCR-engineered T cells: Current strategies, challenges, and prospects.

*Frontiers in Immunology* 2022; 13(835762).

Shankaran V, Ikeda H, Bruce AT, White JM, Swanson PE, Old LJ, & Schreiber RD.

IFN $\gamma$  and lymphocytes prevent primary tumour development and shape tumour immunogenicity.

*Nature* 2001; 410(6832):1107-1111.

Shou J, Zhang Z, Lai Y, Chen Z, & Huang J.

Worse outcome in breast cancer with higher tumor-infiltrating FOXP3+ Tregs : a systematic review and meta-analysis.

*BMC Cancer* 2016; 16(1):687.

Simon B, & Uslu U.

CAR-T cell therapy in melanoma: A future success story?

*Experimental Dermatology* 2018; 27(12):1315-1321.

Slaney CY, Kershaw MH, & Darcy PK.

Trafficking of T cells into tumors.

*Cancer Research* 2014; 74(24):7168-7174.

Song Y, Liu Q, Zuo T, Wei G, & Jiao S.

Combined antitumor effects of anti-EGFR variant III CAR-T cell therapy and PD-1 checkpoint blockade on glioblastoma in mouse model.

*Cellular Immunology* 2020; 352(104112).

Stock S, Benmeharek MR, Kluever AK, Darowski D, Jost C, Stubenrauch KG, Benz J, Freimoser-Grundschober A, Moessner E, Umana P, Subklewe M, Endres S, Klein C, & Kobold S.



Chimeric antigen receptor T cells engineered to recognize the P329G-mutated Fc part of effector-silenced tumor antigen-targeting human IgG1 antibodies enable modular targeting of solid tumors.

*Journal for ImmunoTherapy of Cancer* 2022; 10(7).

Subklewe M, von Bergwelt-Baildon M, & Humpe A.

Chimeric antigen receptor T cells: A race to revolutionize cancer therapy.

*Transfusion Medicine and Hemotherapy* 2019; 46(1):15-24.

Sykulev Y, Joo M, Vturina I, Tsomides TJ, & Eisen HN.

Evidence that a single peptide-MHC complex on a target cell can elicit a cytolytic T cell response.

*Immunity* 1996; 4(6):565-571.

Taylor BC, & Balko JM.

Mechanisms of MHC-I downregulation and role in immunotherapy response.

*Frontiers in Immunology* 2022; 13(844866).

Thomas ED, Lochte HL, Jr., Lu WC, & Ferrebee JW.

Intravenous infusion of bone marrow in patients receiving radiation and chemotherapy.

*New England Journal of Medicine* 1957; 257(11):491-496.

van den Broek ME, Kagi D, Ossendorp F, Toes R, Vamvakas S, Lutz WK, Melief CJ, Zinkernagel RM, & Hengartner H.

Decreased tumor surveillance in perforin-deficient mice.

*Journal of Experimental Medicine* 1996; 184(5):1781-1790.

Waterhouse P, Penninger JM, Timms E, Wakeham A, Shahinian A, Lee KP, Thompson CB, Griesser H, & Mak TW.

Lymphoproliferative disorders with early lethality in mice deficient in Ctla-4.

*Science* 1995; 270(5238):985-988.

Wieser R, Attisano L, Wrana JL, & Massague J.

Signaling activity of transforming growth factor beta type II receptors lacking specific domains in the cytoplasmic region.

*Molecular and Cellular Biology* 1993; 13(12):7239-7247.

Ying Z, He T, Wang X, Zheng W, Lin N, Tu M, Xie Y, Ping L, Zhang C, Liu W, Deng L, Qi F, Ding Y, Lu XA, Song Y, & Zhu J.

Parallel comparison of 4-1BB or CD28 co-stimulated CD19-targeted CAR-T cells for B cell non-Hodgkin's lymphoma.

*Molecular Therapy Oncolytics* 2019; 15(60-68).

Zhao Y, Deng J, Rao S, Guo S, Shen J, Du F, Wu X, Chen Y, Li M, Chen M, Li X, Li W, Gu L, Sun Y, Zhang Z, Wen Q, Xiao Z, & Li J.

Tumor infiltrating lymphocyte (TIL) therapy for solid tumor treatment: Progressions and challenges.  
*Cancers* 2022; 14(17).

Zhou J, Tang Z, Gao S, Li C, Feng Y, & Zhou X.  
Tumor-associated macrophages: Recent insights and therapies.  
*Frontiers in Oncology* 2020; 10(188).

The figures were created with BioRender on a paid license.

## Acknowledgements

Where to start with the acknowledgements? After 4.5 years here at the KlinPharm doing the PhD there are a lot of people to thank. My PhD would have not been possible without them.

I will start with Seb who gave me the chance to start my PhD here and provided everything a researcher needs to develop projects and to grow as a scientist: financing, experience, scientific rigor, and a lot of advice. It's incredible how he manages this large group, writes applications for new grants, is reachable at any time and still can spend time with his family. It is a demonstration how one can combine dedication, organizational skills and family obligations. I was happy I applied to this PhD position in 2018 and I still do not regret that decision for a second.

Then I come to Stefan who built and has shaped the KlinPharm over years better than anyone else could have done. He opens doors which do not seem to exist. He is a tremendous mentor to all students and post-docs who at some point in their life worked in the KlinPharm or were associated with i-Target. Stefan is a great example of how a real leader can push peoples' careers with full dedication and without wanting to get something back in return.

Duc, it was a pleasure working with you for more than four years. I am grateful that we started this journey as colleagues and finished it as friends. I am sure you will end up where you want to be "in the promised land", and I am also confident that I come along this way once in a while.

Reda and Bruno, you were great supervisors who started the PhD journey a little while before me. You made my start very smooth and helped with any lab-

related and personal questions I had. I really appreciate what you did for me, the group and the whole KlinPharm.

Katharina, you are the heart of the i-Target program and are one of the reasons why the i-Target program was such a success. You made the life for the students, for the PIs and for everyone else in the KlinPharm so much easier. Thank you very much.

All the other lab members, i-Target students, and collaborating researchers, you made this experience so joyful and a perfect place to do the PhD studies. Thank you very much.

To my family, in particular my parents, grandparents, and my brother, without you, this would have not been possible. You unconditionally supported me during all those years with your unwavering support, patience, and understanding throughout this challenging process.

To Franzi. You went through this entire journey together with me and I will always be grateful for your support, your belief in my abilities, and your endurance. I know it is just the beginning of our journey and I can't wait for what's to come.

